

**Unravelling the palaeobiology of the dinosaurian post crania and associated carnivore teeth from the Early Jurassic, Elliot Formation in the Eastern Cape.**



by

**Jessica Lee Logie**

*Department of Biological Sciences, University of Cape Town, Cape Town, South Africa*

DISSERTATION

*Presented for the degree of Master of Philosophy in the Department of Biological Sciences,  
University of Cape Town*

February 2025

SUPERVISOR: Prof. Anusuya Chinsamy-Turan

*Department of Biological Sciences, University of Cape Town, Cape Town*

CO-SUPERVISOR: Dr. Emil Krupandan

*Cenozoic Palaeontology, Iziko South African Museum, Cape Town*

The copyright of this thesis vests in the author. No quotation from it or information derived from it is to be published without full acknowledgement of the source. The thesis is to be used for private study or non-commercial research purposes only.

Published by the University of Cape Town (UCT) in terms of the non-exclusive license granted to UCT by the author.

PLAGIARISM DECLARATION

I understand the meaning of plagiarism and declare that all the work in the following dissertation, except for that which has been acknowledged to others, is my own.

Signed:

Signed by candidate

Jessica Logie  
LGXJES001

## TABLE OF CONTENTS

TABLE OF CONTENTS.....	ii
LIST OF TABLES.....	iv
LIST OF FIGURES.....	v
ACKNOWLEDGEMENTS .....	vii
ABSTRACT .....	viii
<b>CHAPTER 1 INTRODUCTION .....</b>	<b>1</b>
<b>1.1 Overview of Sauropodomorpha.....</b>	<b>1</b>
1.1.1 Sauropodomorpha of the Late Triassic - Early Jurassic of Gondwana.....	1
<b>1.2 The Elliot Formation.....</b>	<b>4</b>
1.2.1 Taxa of the Upper Elliot Formation of South Africa .....	5
1.2.2 Predators of the Elliot Formation.....	6
<b>1.3 Research Rationale.....</b>	<b>9</b>
1.3.1 Hypotheses.....	10
1.3.2 Research Aims and Objectives.....	11
<b>CHAPTER 2 MATERIALS AND METHODS .....</b>	<b>12</b>
<b>2.1 Specimen information.....</b>	<b>12</b>
<b>2.2 Research methodology .....</b>	<b>19</b>
2.2.1 Sauropodomorpha research methodology.....	19
2.2.2 Carnivore teeth research methodology .....	21
<b>2.3 Phylogenetic analysis .....</b>	<b>24</b>
<b>CHAPTER 3 RESULTS .....</b>	<b>25</b>
<b>3.1 Further exploration of the AM 6147 locality.....</b>	<b>25</b>
<b>3.2 Anatomical description of AM 6147 .....</b>	<b>27</b>
<b>3.3 Description of carnivore teeth .....</b>	<b>52</b>
<b>3.4 Phylogenetic position.....</b>	<b>57</b>
<b>CHAPTER 4 DISCUSSION .....</b>	<b>59</b>
<b>4.1 AM 6147 .....</b>	<b>59</b>
4.1.1 Stratigraphic position .....	59
4.1.1 Phylogenetic affinities.....	59
4.1.3 Autapomorphies.....	59
4.1.4 Overview of AM 6147.....	64
4.1.5 Pathology .....	65
<b>4.2 Associated carnivore teeth.....</b>	<b>65</b>
<b>CHAPTER 5 CONCLUSION.....</b>	<b>67</b>
<b>5.1 Outcome of the current study.....</b>	<b>67</b>

5.1.1 The taxonomic validity and phylogenetic affinity of AM 6147 .....	68
5.1.2 The taxonomic identification of the associated carnivore teeth .....	68
5.1.3 Synthesis of the findings .....	69
<b>5.2 Future work .....</b>	<b>69</b>
<b>5.3 Limitations .....</b>	<b>69</b>
<b>REFERENCES.....</b>	<b>71</b>
<b>APPENDIX A.....</b>	<b>79</b>
<b>APPENDIX B .....</b>	<b>83</b>
<b>APPENDIX C .....</b>	<b>89</b>

## LIST OF TABLES

<i>Table 1.1: The phylogenetic nomenclature for Sauropodomorpha taxa mentioned within the text are as follows.</i>	4
<i>Table 1.2: The phylogenetic nomenclature for predator taxa mentioned within the text are as follows.</i>	7
<i>Table 2.1: Description of the specimen blocks taken from the Albany Museum loan agreement.</i>	13
<i>Table 2.2: Sauropodomorph comparative taxa.</i>	19
<i>Table 2.3: Reviewed literature of sauropodomorph taxa included in the comparative study.</i>	21
<i>Table 2.4: Carnivore tooth comparative taxa.</i>	22
<i>Table 2.5: Reviewed literature of carnivore taxa included in the comparative study.</i>	23
<i>Table 3.1: The 22 pes elements of AM 6147.</i>	34
<i>Table 3.2: The calculated average length of the metatarsals of the six M. carinatus specimens compared to that of AM 6147.</i>	34
<i>Table 3.3: Measurements comparing AM 6147 and Glacialisaurus. Modified from Smith and Pol et al., (2007). Asterisks indicate incomplete measurements due to damage.</i>	35
<i>Table 3.4: Comparing Metatarsal I measurements for AM 6147, NMQR 1705, Blikanasaurus and M. carinatus. Modified from Yates (2008). Asterisk indicates approximate measurements due to incomplete bone elements.</i>	36
<i>Table A.1: Complete list of Late Triassic - Early Jurassic sauropodomorph pes elements available for study at the ESI collection.</i>	79
<i>Table A.2: Complete list of Late Triassic - Early Jurassic sauropodomorph pes elements available for study at the IZIKO collection.</i>	80
<i>Table A.3: Complete list of Late Triassic - Early Jurassic sauropodomorph vertebrae elements available for study at the ESI collection.</i>	81
<i>Table A.4: Complete list of Late Triassic - Early Jurassic sauropodomorph vertebrae elements available for study at the IZIKO collection.</i>	82
<i>Table A.5: Complete list of Late Triassic - Early Jurassic predator teeth available for study at the ESI collection.</i>	82
<i>Table A.6: Complete list of Late Triassic - Early Jurassic predator teeth available for study at the IZIKO collection.</i>	82
<i>Table B.1: Pes measurements of AM 6147. Table modified from Yates (2008). Asterisks indicates incomplete measurements.</i>	83
<i>Table B.2: Vertebrae and chevrons measurements (mm) for AM 6147.</i>	87

## LIST OF FIGURES

Figure 1.1: Phylogenetic tree for Sauropodomorpha of the Middle Triassic through Middle Jurassic from Apaldetti et al (2021).	3
Figure 1.2: Stratigraphic section showing UEF & CF genera found within the MRZ by Viglietti et al (2020).	8
Figure 2.1: Locality map for AM 6147 which was excavated along a road cutting from the upper Elliot Formation of Glenetive Farm, Khowa, Eastern Cape Province, South Africa. The red star indicates the excavated site. Inset shows the location of Eastern Cape Province within South Africa. Map image downloaded from GoogleEarth.	12
Figure 2.2: Caudal vertebrae in jacket AM 6147-I. Frame indicates position of the carnivore tooth. Scale bar = 10cm.	13
Figure 2.3: Carnivore tooth alongside chevron (framed in Figure 2.2) in jacket AM 6147-I. Scale bar = 1cm.	14
Figure 2.4: Vertebra and chevron fragments in jacket AM 6147-II. Scale bar = 5cm	14
Figure 2.5: Gastralria and rib fragments in jacket AM 6147-III. Scale bar = 5cm	15
Figure 2.6: Gastralria and rib fragments in jacket AM 6147-IV. Scale bar = 5cm	15
Figure 2.7: Dorsal view of the complete left pes of AM 6147-V. Scale bar = 5cm.	16
Figure 2.8: Ventral view of the complete left pes of AM 6147-V. Scale bar = 5cm.	17
Figure 2.9: Proximal view of the articulating metatarsals of AM 6147, right to left M1 – M5. Scale bar = 5cm.	17
Figure 2.10: Isolated carnivore tooth within the matrix, AM 6147-V (r). Scale bar = 0.3cm (3mm).	18
Figure 2.11: Isolated, fragmented carnivore tooth within the matrix, AM 6147-V (s). Scale bar = 0.5cm (5mm)	18
Figure 3.1: Excavation site of AM 6147. Large black dashes indicate the outer margin of the road cutting. Smaller black dashes indicate the 'transition' from the UEF to LCF. Red box A indicates the excavated location of jackets labelled AM 6147-I & II. Red box B indicates the excavated location of jackets labelled AM 6147-III, IV & V. See Table 2.1 for details regarding the elements of each block.	25
Figure 3.2: Anterior caudal vertebrae (CV 1-8) of AM 6147 in lateral view. Scale bar = 10cm.	28
Figure 3.3: Side by side illustration and image of anterior caudal vertebra (CV 5) of AM 6147 in lateral view. Red lines indicate fractures and breaks in the bone. ns, neural spine; poz, postzygapophyses; prz, prezygapophyses; tp, transverse process; cv, chevron. Arrow indicates dorsal direction. Scale bar = 10cm	29
Figure 3.4: The 'u'-shaped sulcus on the ventral side of the caudal centrum. Ventral sulcus, vs; bony bridge, bb; haemal arch, ha. Scale bar = 2cm	31
Figure 3.5: Closed y-shape haemal arch seen on all the chevrons. Bony bridge, bb; haemal arch, ha. Scale bar = 3cm	33
Figure 3.6: Metatarsal 1 in dorsal (left) and ventral (right) view. Phalanx 1 is attached to the distal end. Scale bar = 5cm	37
Figure 3.7: Metatarsal 2 in dorsal (left) and ventral (right) view. Scale bar = 5cm	38
Figure 3.8: Metatarsal 3 in dorsal (left) and ventral (right) view. Scale bar = 5cm	39
Figure 3.9: Metatarsal 4 in dorsal (left) and ventral (right) view. Scale bar = 5cm	40
Figure 3.10: Metatarsal 5 in dorsal (left) and ventral (right) view. Scale bar = 5cm	41
Figure 3.11: Phalanx 1 articulated with the proximal end of mt. 1 in dorsal (left) and ventral (right) view. Scale bar = 5cm	44
Figure 3.12: Ungual of mt. 1 in dorsal (left) and ventral (right) view. Scale bar = 5cm	44
Figure 3.13: Phalanx 1 of mt. 2 in dorsal (left) and ventral (right) view. Scale bar = 5cm	45
Figure 3.14: Phalanx 2 of mt. 2 in dorsal (left) and ventral (right) view. Scale bar = 5cm	45
Figure 3.15: Ungual of mt. 2 in dorsal (left) and ventral (right) view. Scale bar = 5cm	46
Figure 3.16: Phalanx 1 and 2 of mt. 3 in articulation in dorsal (left) and ventral (right) view. Scale bar = 5cm	46
Figure 3.17: Phalanx 3 of mt. 3 in dorsal (left) and ventral (right) view. Scale bar = 5cm	47
Figure 3.18: Ungual of mt. 3 in dorsal (left) and ventral (right) view. Scale bar = 5cm	47
Figure 3.19: Phalanx 1, 2 and 3 of mt. 4 in articulation in dorsal (left) and ventral (right) view. Scale bar = 5cm	48
Figure 3.20: Phalanx 4 and ungual of mt. 4 in articulation dorsal (left) and ventral (right) view. Scale bar = 5cm	49
Figure 3.21: Ungual of mt. 5 in lateral view. Scale bar = 2cm	49
Figure 3.22: Left astragalus of (AM 6147-V), (a) anterior and (b) posterior view, (c) dorsal and (d) ventral view, scale bar = 5cm, and (e) medial and (f) lateral view, scale bar = 3cm. ap, anterior process. Thick arrow indicates ventral direction.	50
Figure 3.23: Left calcaneum of AM 6147, (a) anterior and (b) posterior view, (c) dorsal and (d) ventral view, (e) medial and (f) lateral view. Scale bar = 5cm. Arrow indicates ventral direction.	51

Figure 3.24: Associated predator tooth with distal denticles alongside CV-1's chevron of AM 6147. Scale bar = 5mm.....	53
Figure 3.25: CT scan of the crown of AM 6147-V (r) in vertical cross section.....	54
Figure 3.26: CT scan of the crown of AM 6147-V (r) in transverse cross section oval in shape.....	54
Figure 3.27: Predator tooth AM 6147-V (r). en, enamel. Scale bar = 0.5cm (5mm).....	55
Figure 3.28: Close up of the exposed labial surface and preserved mesial denticles of AM 6147-V (s). Scale bar = 1mm.....	56
Figure 3.29: CT scan of the (left) mesial and (right) distal profile of AM 6147-V (s).....	56
Figure 3.30: AM 6147 is recovered among Massospondylidae in a reduced strict consensus summary. 21842 MPTs with a tree length of 1697 steps tree (CI of 0,29 and a RI of 0,67), after ten unstable taxa; Arcusaurus, Pradhania, Xixipiosaurus, Yizhousaurus, Camelotia, Isanosaurus, Amygdalodon, Volkheimeria, Barapasaurus and Patagosaurus were excluded from the consensus. The single digit numbers represent Bremer support values, and the double-digit numbers represent the Bootstrap support values. Only sauropodomorph taxa are shown (for the complete consensus tree, including all taxa, see Figure C.3.....	58
Figure 4.1: Left Metatarsal II of AM 6147 in dorsal view (a), lateroventral view (b), and ventral view (c). f, flange. Arrow indicates distal direction. Scale bar = 5cm.....	60
Figure 4.2: Left Metatarsal II of AM 6147 in proximal view. Emf, extended medioventral flange. Arrow indicates medial direction. Scale bar = 5cm.....	61
Figure 4.3: Left Metatarsal IV of AM 6147. Dorsal view (a), medial view (b), lateral view (c). f, flange; c, concave groove. Scale bar = 3cm.....	62
Figure 4.4: Dorsoposteriorly directed transverse process in dorsal view on the lateral side of the caudal centrum. Transverse process, tp; neural spine, ns. Arrow indicates the posterior direction. Scale bar = 4cm.....	63
Figure 4.5: Dorsoposteriorly directed transverse process in lateral view on the lateral side of the caudal centrum. Transverse process, tv; neural spine, ns. Arrow indicates the posterior direction. Scale bar = 4cm.....	63
Figure 4.6: Gastralia of AM 6147. ms, mid-section; p, process. Scale bar = 10cm.....	65
Figure B.1: Measurements (mm) of mt. 1 through mt. 5 of <i>M. carinatus</i> taken from Mukaddam et al (2021). .	88
Figure C.1: Bremer support values on the reduced Strict Consensus tree.....	89
Figure C.2: Bootstrap values on the reduced Strict Consensus tree.....	90
Figure C.3: AM 6147 is recovered among Massospondylidae in a reduced strict consensus summary. 21842 MPTs with a tree length of 1697 steps tree (CI of 0,29 and a RI of 0,67), after ten unstable taxa; Arcusaurus, Pradhania, Xixipiosaurus, Yizhousaurus, Camelotia, Isanosaurus, Amygdalodon, Volkheimeria, Barapasaurus and Patagosaurus were excluded from the consensus. Bremer support = 1, Bootstrap support = 60. ....	91
Figure C.4: AM 6147 is recovered among Massospondylidae in a reduced majority rule (50). 21842 MPTs with a tree length of 1697 steps tree (CI of 0,29 and a RI of 0,67), after ten unstable taxa; Arcusaurus, Pradhania, Xixipiosaurus, Yizhousaurus, Camelotia, Isanosaurus, Amygdalodon, Volkheimeria, Barapasaurus and Patagosaurus were excluded from the consensus. Bremer support = 1, Bootstrap support = 60. ....	92

## ACKNOWLEDGEMENTS

I would like to express my sincerest thanks to the following people and organisations for their support in the completion of my dissertation:

My supervisor, Prof. Anusuya Chinsamy-Turan for assisting with research funding and for providing constant guidance and an array of opportunities. I am grateful for all her support and advice throughout this project.

My co-supervisor, Dr. Emil Krupandan for his assistance with the phylogenetic research, vast knowledge of sauropodomorph dinosaurs and guidance throughout this project.

Dr. Rose Prevec (Albany Museum) for loaning the AM 6147 material to me for the duration of my study.

Claire Browning and Zaituna Skosan (Iziko South African Museum) for allowing me access to the Karoo Palaeontology Collection.

Dr. Bernhard Zipfel and Sifelani Jirah (Evolutionary Studies Institute) for providing access to the Palaeontology Collection.

Prof. Jonah Choiniere (Evolutionary Studies Institute) for his valuable insight and assistance in attaining the original notes on AM 6147's excavation.

My lab mates from the UCT Palaeobiology Research Group for their endless encouragement and friendship.

My parents, Malcolme & Gael, for their unwavering love and unparalleled support, without whom this journey would never have even started.

## ABSTRACT

The Elliot Formation of the Stormberg Group of South Africa ranges in age from the Late Triassic to the Early Jurassic. This stratigraphic unit bears a varied dinosaur assemblage, among which sauropodomorph dinosaurs are the most abundant. Sauropodomorpha are particularly well documented in the Upper Elliot Formation and are morphologically and taxonomically diverse. Specimen AM 6147, a large basal sauropodomorph, was excavated from the Barkley Pass, Eastern Cape, Elliot Formation of South Africa in 2013 by a joint team from the Albany Museum and the University of the Witwatersrand led by Dr Billy de Klerk. The specimen comprises post cranial material including ribs, gastralia, vertebrae of the mid-posterior section of the tail, and a complete left pes. Associated with the specimen are three teeth of contemporaneous carnivores.

Here, we describe the skeletal anatomy of AM 6147 and assess its phylogenetic affinities by scoring our findings in a phylogenetic data matrix. We also attempt to identify the carnivorous taxa to which the associated teeth may have belonged, and the nature of the relationship between them and AM 6147.

Our phylogenetic analyses reveal that this specimen belongs to the massospondylidae and that it is recovered as a new taxon, *Enkulusaura deklerki*, based on a unique combination of plesiomorphic and derived features. Our findings suggests that the three associated carnivore teeth could possibly belong to two different theropod dinosaur, while the third tooth is likely from a crocodylomorph.

In conclusion, this study of AM 6147 shows that it is a new large bodied Massospondylid from the Elliot Formation and provides a better understanding of the diversity of basal Sauropodomorpha in the Early Jurassic of South Africa. Furthermore, the associated teeth contribute insight into the ecological relationships between these contemporaneous taxa.

## Abbreviations

**UEF** - Upper Elliot Formation

**LEF** - Lower Elliot Formation

**CF** – Clarens Formation

**ESI** – Evolutionary Studies Institute

**IZIKO** - Iziko South African Museum

**ERZ** - “*Eusklesaurus*” Range Zone

**MRZ** – *Massospondylus* Range Zone

**TJB** – Triassic Jurassic Boundary

**Mt.** - Metatarsal

## Institutional Abbreviations

**BP** – Evolutionary Studies Institute, University of the Witwatersrand, Johannesburg, South Africa

**NM** - National Museum, Bloemfontein, South Africa

**SAM** - South African Museum, Iziko Museums, Cape Town, South Africa

**AM** - Albany Museum, Makhanda, South Africa

**QG** - Zimbabwe Museum of Human Sciences/Queen Victoria Museum, Harare, Zimbabwe

## CHAPTER 1 INTRODUCTION

### 1.1 Overview of Sauropodomorpha

From the Middle Triassic through to the Late Cretaceous, for approximately 160 million years during the Mesozoic, non-avian dinosaurs were some of the most diverse taxonomic groups globally (Nesbitt *et al.*, 2013a). This group of dinosaurs was further classified into Saurischia and Ornithischia through comparative analyses of the structure of their pelvic girdles (Seeley, 1888): The pelvic girdle of saurichians revealed a forward and downward facing ischium with a forward facing pubis, whereas the pelvic girdle of ornithischians revealed a backwards facing ilium and a backward facing pubis which sits parallel to the ischium

From the Middle Triassic through to the Late Jurassic, Sauropodomorpha fossils have been found in many formations across six continents, namely, the Elliot Formation of South Africa (McPhee *et al.*, 2018, Bordy *et al.*, 2020), Ischigualasto Formation of Argentina (Apaldetti *et al.*, 2011, Apaldetti *et al.*, 2013), Klettgau Formation of Switzerland (Rauhut *et al.*, 2020), Lufeng Formation of China (Young, 1940, Mao *et al.*, 2020), Morrison Formation of North America (Harris and Dodson, 2004), and the Hanson Formation of Antarctica (Smith *et al.*, 2007).

The Late Triassic diversification of basal saurischians to Sauropodomorpha (Langer *et al.*, 1999, Müller and García, 2020) and the evolution of the more derived Sauropodiformes and Gravisauria during the Early Jurassic (Otero *et al.*, 2020, Apaldetti *et al.*, 2021) provide valuable insight into the evolution and transition from basal Sauropodomorpha to the derived Sauropoda (Galton and van Heerden, 1998, Allain and Aquesbi, 2008).

#### 1.1.1 Sauropodomorpha of the Late Triassic - Early Jurassic of Gondwana

The oldest sauropodomorph specimens come from the Ischigualasto Formation of Argentina and the Santa María Formation of Brazil, and have been identified with an estimated age of ~231 Ma, placing them within the Early Late Triassic (Martinez *et al.*, 2011). *Saturnalia taijiqian* from the Santa María formation, has been recognised as the basal most Sauropodomorpha to date (Langer, 2003, Pol *et al.*, 2011), whereas a re-consideration of *Eoraptor lunensis*, from the Ischigualasto Formation, which was originally described as a theropod (Serenó, 1999, Ezcurra, 2010), is defined as a basal member of Sauropodomorpha, adding to the diversity of the basal sauropodomorphs of the Early Late Triassic (Martinez *et al.*, 2011, Sereno *et al.*, 2012, McPhee *et al.*, 2015b). Completing the Early Late Triassic (Carnian-early Norian) emergence of basal sauropodomorphs are, *Panphagia protos* and *Chromogisaurus novasi* of the Ischigualasto Formation (Martinez and Alcober, 2009, Ezcurra, 2010, Martínez *et al.*, 2012), and *Pampadromaeus barberani*, from Santa María Formation (Cabreira *et al.*, 2011, Langer *et al.*, 2019). These basal most forms of Sauropodomorpha can be distinguished from their more derived sauropodomorph relatives by their similarly small size, bipedal locomotion, distally recurved crowns of the teeth, elongated forelimbs, deep extensor pits on distal end of metacarpals 1-3, narrow metacarpal 4, narrow proximal width of metatarsal 5, relatively short cervical centra, two sacral vertebrae, partially open acetabulum, distinctively long postacetabular process of the ilium, and a femur which displays a short and curved shaft (Otero *et al.*, 2016).

In the Late Triassic sauropodomorphs greatly diversified and this divergence was reflected in many regions of the world.

As Otero *et al.* (2016) state: During the Norian-Rhaetian the next step in sauropodomorph evolution is described by the appearance of Sauropodomorpha such as the Argentinian Los Colorados Formation sauropodomorph *Coloradisaurus* (Apaldetti *et al.*, 2013) and sauropodiform *Lessemsaurus* (Pol and Powell, 2007), as well as the South African Lower Elliot Formation sauropodomorphs *Eucnemesaurus* (McPhee *et al.*, 2015a), *Plateosaurus* (Yates, 2003), *Sefapanosaurus* (Otero *et al.*, 2015), Lesotho's, *Melanorosaurus* (Barrett and Choiniere, 2024, Peyre de Fabrègues and Allain, 2016, Haughton, 1924), *Meroktenos* (Peyre de Fabrègues and Allain, 2016), and *Kholumolumo* (Peyre de Fabrègues and Allain, 2019). Within South Africa, the evolution diversifies Sauropodomorpha a step further with the appearance of sauropodiformes such as *Blikanasaurus* (Galton and van Heerden, 1998, Yates *et al.*, 2004) and *Antetonitrus* (McPhee *et al.*, 2014, Yates *et al.*, 2004).

Norian Sauropodomorphs can be distinguished from their Carnian relatives by several evolutionary traits, such as, a herbivorous diet, at least three sacral vertebrae, progression in quadrupedal locomotion, a femur with a straighter shaft, and a more robust manus (Otero *et al.*, 2016).

During the Early Jurassic, along with an increase in global sauropodomorph distribution, the massospondylids experienced a considerable diversification (Otero *et al.*, 2016). In Southern Gondwana, from Argentina, *Adeopapposaurus* of the Cañón del Colorado Formation (Martínez, 2009) and *Leyesaurus* of the Quebrada del Barro Formation (Apaldetti *et al.*, 2011), South Africa's Upper Elliot Formation's *Massospondylus* (Barrett, 2009, Yates and Barrett, 2010), and Antarctica's *Glacialisaurus* (Smith and Pol, 2007), and the basal sauropodiformes *Leoneosaurus* (Pol *et al.*, 2011) and *Mussaurus* (Otero and Pol, 2013) of Argentina and, from the Upper Elliot Formation of South Africa, *Aardonyx* (Yates *et al.*, 2010) are notably prolific. The anatomical diversification of sauropodomorphs in the Early Jurassic of Gondwana can be identified by the expression of graviportal quadrupedalism and fully herbivorous diets, refinements which can be tracked to the Late Triassic in *Lessemsaurus* and *Antetonitrus*, and into the Early Jurassic with *Blikanasaurus*, *Pulanesaura*, and *Vulcanodon* (Otero *et al.*, 2016).

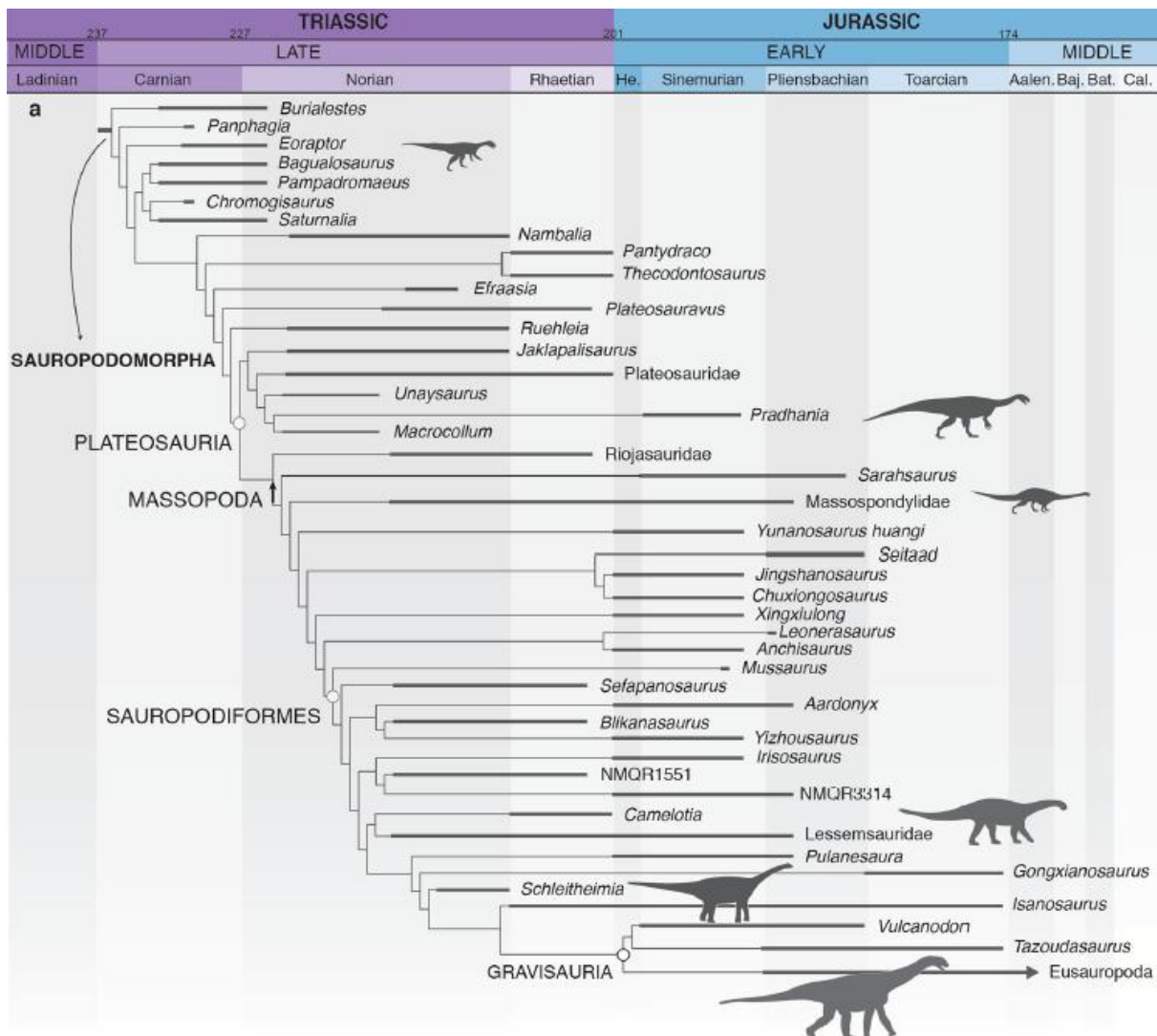


Figure 1.1: Phylogenetic tree for Sauropodomorpha of the Middle Triassic through Middle Jurassic from Apaldetti *et al* (2021).

As seen in Figure 1.1, after the Triassic Jurassic boundary (TJB), the global diversity of sauropodomorphs were thought to show a decline (Apaldetti *et al.*, 2021), however recent finds from the early Jurassic suggest continual high diversity levels, similar to the diversification seen in the Late Triassic (Mannion and Upchurch, 2010, Mannion *et al.*, 2011). Apaldetti *et al* (2021), suggest that these evolutionary changes across the TJB were a continual evolutionary divergence of pre-existing lineages (massospondylids and non-gravisaurian sauropodiformes) rather than a rise in new and different body plans.

The Late Triassic (middle-late Carnian) was restricted to only a few small species of sauropodomorphs that were characterised by low morphological disparity, however this smaller body plan was not restricted to the Carnian as many analogous features continued to occupy a similar region of the morphospace in the Norian and Rhaetian (Apaldetti *et al.*, 2021). The shift in body size accounts for approximately half of the diversification of the Sauropodomorph morphospace during the Carnian-Norian and is consistent with the rapid diversification of Sauropodomorpha during the Rhaetian (Apaldetti *et al.*, 2021). It is likely this change amidst the Sauropodomorph morphospace, in the Carnian-Norian, led to an increase in morphological evolutionary diversifications in body plans to fill new ecological

niches (McPhee *et al.*, 2017, Apaldetti *et al.*, 2021). The expansion and diversification at this time is when most of the early Sauropodomorpha (plateosaurids, riojasaurids, massospondylids, sauropodiformes) lineages appeared (McPhee *et al.*, 2017), the radiation seen during this time is evidenced by dietary changes, an increase in body plan which include the specialised characteristics of sauropods, a small head, elongated neck, three sacral vertebrae, columnar like limbs, and a modified first manual digit (McPhee *et al.*, 2017, Apaldetti *et al.*, 2021, Weishampel *et al.*, 2004, Sander and Lallensack, 2018).

Table 1.1: The phylogenetic nomenclature for Sauropodomorpha taxa mentioned within the text are as follows.

Clade	Definition	Reference
Sauropodomorpha	The most inclusive clade containing <i>Saltasaurus</i> but not <i>Passer</i> and <i>Triceratops</i> .	(Sereno, 2007)
Massopoda	The most inclusive clade containing <i>Saltasaurus loricatus</i> but not <i>Plateosaurus engelhardti</i> .	(Yates, 2007b)
Massospondylidae	All taxa more closely related to <i>Massospondylus carinatus</i> than to <i>Plateosaurus engelhardti</i> and <i>Saltasaurus loricatus</i> .	(Sereno, 1998)
Sauropodiformes	The least inclusive clade containing <i>Mussaurus</i> and <i>Saltasaurus</i> .	(Sereno, 2007)
Sauropoda	The most inclusive clade that contains <i>Saltasaurus loricatus</i> but not <i>Melanorosaurus readi</i> .	(Yates, 2007b, Yates, 2007a)
Gravisauria	The most recent common ancestor of <i>Tazoudasaurus</i> and <i>Saltasaurus</i> .	(Allain and Aquesbi, 2008)

## 1.2 The Elliot Formation

The Karoo Supergroup is a large inland basin that covers a vast majority of South Africa's terrestrial surface. It is divided into 5 subgroups: the Dwyka Group; the Ecca Group; the Beaufort Group; the Stormberg Group; and the Drakensberg Group basalts (Catuneanu *et al.*, 2005).

The Elliot Formation is found within the Stormberg group, between the Molteno and Clarens Formations. The formation represents the longest geological time span in the history of the Karoo Supergroup as the ages range from Late Triassic to the Early Jurassic (Bordy and Eriksson, 2015). The underlying features of the formation are a red-bed succession of mudstone, siltstones and fine-to-medium grained sandstone (Bordy and Eriksson, 2015), which is further divided into the Upper Elliot Formation and the Lower Elliot Formation (Bordy *et al.*, 2020).

The LEF is similarly fossiliferous but less taxonomically diverse when compared to the UEF, and is dominated by early branching basal sauropodomorph dinosaurs (Bordy *et al.*, 2020). Fossils within this horizon often present isolated skeletal remains, associated partial skeletons or disarticulated skeletons which are still closely associated (Kitching and Raath,

1984). Tridactyl theropod trace fossils (Sciscio *et al.*, 2017a) have also been identified within the LEF, however the only fossil evidence for theropods so far comes from isolated teeth (Ray and Chinsamy, 2002, Bordy *et al.*, 2020). Therapsids are also represented in the assemblages, as well as pseudosuchian archosaurs and non-crocodylomorph pseudosuchians (Tolchard *et al.*, 2019, Bordy *et al.*, 2020).

Toward the middle part of the Elliot Formation, where the LEF and UEF meet, the fossil yield begins to increase considerably, with several small basal sauropodomorphs making an appearance. While these basal sauropodomorphs first occur in the lower beds, their presence increases in the middle horizon alongside other genera such as ornithischian dinosaurs and protosuchians; this middle horizon has also revealed fragmentary remains of theropod dinosaurs (Kitching and Raath, 1984).

The UEF is fossiliferous with taxonomically diverse vertebrate assemblages (Bordy and Eriksson, 2015) and has some of the best preserved fossils, many of which are articulated partial skeletons (Kitching and Raath, 1984). The assemblages include, but are not limited to, Sauropodomorpha; Theropoda; Ornithischia; Pseudosuchia; and Crocodylomorpha (Bordy *et al.*, 2020). The UEF has also been recorded to show a body size variation amongst Sauropodomorpha, the smaller *Massospondylus* (Yates and Barrett, 2010) and the large *Ledumahadi* (McPhee *et al.*, 2018); as well as among the theropods, such as the smaller *Megapnosaurus* (Kitching and Raath, 1984, Raath *et al.*, 1990) and the large *Dracovenator* (Yates, 2005).

### **1.2.1 Taxa of the Upper Elliot Formation of South Africa**

In 1854 Owen named the first sauropodomorph, of the Elliot Formation, *Massospondylus*, which was then followed by "*Eusklesaurus*" which was named by Huxley in 1870 (Owen, 1854, Huxley, 1870). In the following century these aforementioned taxa were the focal point of discussions regarding the Elliot Formation's biostratigraphy. Haughton first noticed that the lower layers tended to preserve larger bodied specimens, such as "*Eusklesaurus*", while the upper layers were populated with smaller bodied massospondylids (Haughton, 1924, MCPhee *et al.*, 2017). The dichotomy of the layers was later formalised by Kitching and Raath in 1984, who described the biozonation of the Elliot Formation into the LEF "*Eusklesaurus*" Range Zone (ERZ) and the "middle" and UEF as the *Massospondylus* Range Zone (MRZ) due to the abundance of finds of each taxa in the respective layers (Kitching and Raath, 1984, MCPhee *et al.*, 2017). However, recent samplings and studies have indicated that suggested majority content of each of these ranges and layers is both taxonomically and stratigraphically inaccurate as, according to Yates (2003 & 2004), "*Eusklesaurus*" should be regarded as *nomen dubium* (Yates, 2003, Yates, 2004, MCPhee *et al.*, 2017).

*Massospondylus*'s validity is more certain due to the neotype of *Massospondylus carinatus* (BP/1/4934) being described, a necessary neotype as the holotype was destroyed during World War II (Yates and Barrett, 2010). As with the ERZ, recent studies and discoveries have shown the MRZ to be much more taxonomically diverse than was previously thought (MCPhee *et al.*, 2017).

The radiation of Sauropodomorpha is particularly well documented in the Elliot Formation of Southern Africa, the abundance and morphological variation within the Sauropodomorph morphospace indicates great diversity after the TJB (Bordy *et al.*, 2020, MCPhee *et al.*,

2017). A study conducted by McPhee *et al* in 2017 suggests that, firstly, the UEF sauropodomorph taxa are more morphologically disparate than the sauropodomorph of the LEF, secondly, the morphological disparity occupies a larger portion of the sauropodomorph morphospace within the first ~15 million years of the Jurassic as opposed to the final 15 million years of the Triassic (McPhee *et al.*, 2017).

The UEF bears taxonomically diverse Sauropodomorpha assemblages, it includes valid Sauropodomorpha taxon *Aardonyx* (Yates *et al.*, 2010), *Antetonitrus* (also noted in the LEF) (Yates and Kitching, 2003, McPhee *et al.*, 2014), *Arcusaurus* (Yates *et al.*, 2011), *Ledumahadi* (McPhee *et al.*, 2018), *Massospondylus* (Yates and Barrett, 2010, Barrett *et al.*, 2019, Viglietti *et al.*, 2020), NMQR 3314 (Viglietti *et al.*, 2020), *Pulanesaura* (McPhee *et al.*, 2015b), and *Ignavusaurus* (Knoll, 2010, Bodenham and Barrett, 2020, Viglietti *et al.*, 2020). *Ngwevu* has been described by Chappelle *et al* (2019) to have come from the UEF but Viglietti *et al* (2020) notes that *Ngwevu* is provenanced to the lower CF (Viglietti *et al.*, 2020).

### 1.2.2 Predators of the Elliot Formation

Theropoda, a lineage which first appeared in the Triassic period, was a name first proposed by Marsh in 1881 (Currie, 1997). A theropod is usually described as having slender long legs, bipedal in locomotion and capable of moving faster than most of the contemporary herbivorous dinosaurs. Most theropods had blade-like serrated ridged teeth and recurving claws, especially on the forearms (Currie, 1997). Most noticeably, unlike Ornithischia, they are known to have hollow limb bones, although this is not a trait exclusive to theropods (Currie, 1997).

Pseudosuchia is a clade of crocodylian-like archosaurs of the Triassic (Nesbitt, 2011). Pseudosuchia, as defined by Benton and Clark in 1988, include two archosaur families of Middle to Late Triassic, namely the stagonolepidids (aetosaurus) and the rausuchids. Stagonolepididae are described as being herbivorous armoured archosaurs, and Rausuchidae are described as large (2.5-5m long) carnivores that were the apex predators of their respective fauna (Benton and Clark, 1988).

Within the LEF Bordy *et al* (2020) state there are currently no recovered ornithischians. In terms of theropods, tridactyl trackways are well documented, however they are difficult to separately identify when compared to carnivorous pseudosuchians (Bordy *et al.*, 2020). In 2019, Tolchard *et al* identified two likely species of rausuchians from maxillary and dentary fragments, however the exact provenance of these fossils is unknown (Tolchard *et al.*, 2019).

The UEF and CF are more diverse than the LEF in terms of numbers of predator genera (Viglietti *et al.*, 2020). Theropods, represented by fragmentary remains, such as the small *Megapnosaurus rhodesiensis* (Kitching and Raath, 1984, Munyikwa and Raath, 1999, Raath *et al.*, 1990), previously referred to as *Syntarsus rhodesiensis* (Chinsamy-Turan, 2024) and the larger *Dracovenator regenti*, possibly related to the North America *Dilophosaurus* (Yates, 2005); crocodylomorphs such as *Sphenosuchus acutus* and *Litargosuchus leptorhynchus* (Walker, 1990, Clark and Sues, 2002); Crocodyliform taxa *Orthosuchus stormbergi*, *Notochampsa istedana* and *Protosuchus haughtoni* (Dollman *et al.*, 2019, Nash, 1975, Dollman *et al.*, 2021, Gow, 2000), are all identified within the formation (Viglietti *et al.*,

2020). It should be emphasized that based on a few common synapomorphies, Rauisuchia and other subgroups have been grouped together as they did not fit into the Dinosauria, Aetosauria, Phytosauria, or Crocodylomorpha genera (Nesbitt, 2011).

Table 1.2: The phylogenetic nomenclature for predator taxa mentioned within the text are as follows.

Clade	Definition	Reference
Crocodylomorpha	The most inclusive clade containing <i>Crocodylus niloticus</i> but not <i>Poposaurus gracilis</i> , <i>Gracilisuchus stipanicorum</i> Romer, <i>Prestosuchus chiniquensis</i> , or <i>Aetosaurus ferratus</i> .	(Sereno <i>et al.</i> , 2003)
Crocodyliform	A group including the traditional 'protosuchians', 'mesosuchians', and eusuchians.	(Clark, 1986, Benton and Clark, 1988)
Archosauria	A clade consisting of the last common ancestor of birds and crocodylians, and all its descendants.	(Cope, 1871, Benton, 2004, Benton and Clark, 1988)
Pseudosuchia	Most inclusive clade including <i>Crocodylus</i> but not <i>Passer</i> .	(Nesbitt, 2011)
Rauisuchia	A group of non-crocodylomorph pseudosuchian archosaurs.	(Nesbitt <i>et al.</i> , 2013b, Tolchard <i>et al.</i> , 2019)
Theropoda	A bipedal group of saurischian dinosaurs.	(Currie, 1997)

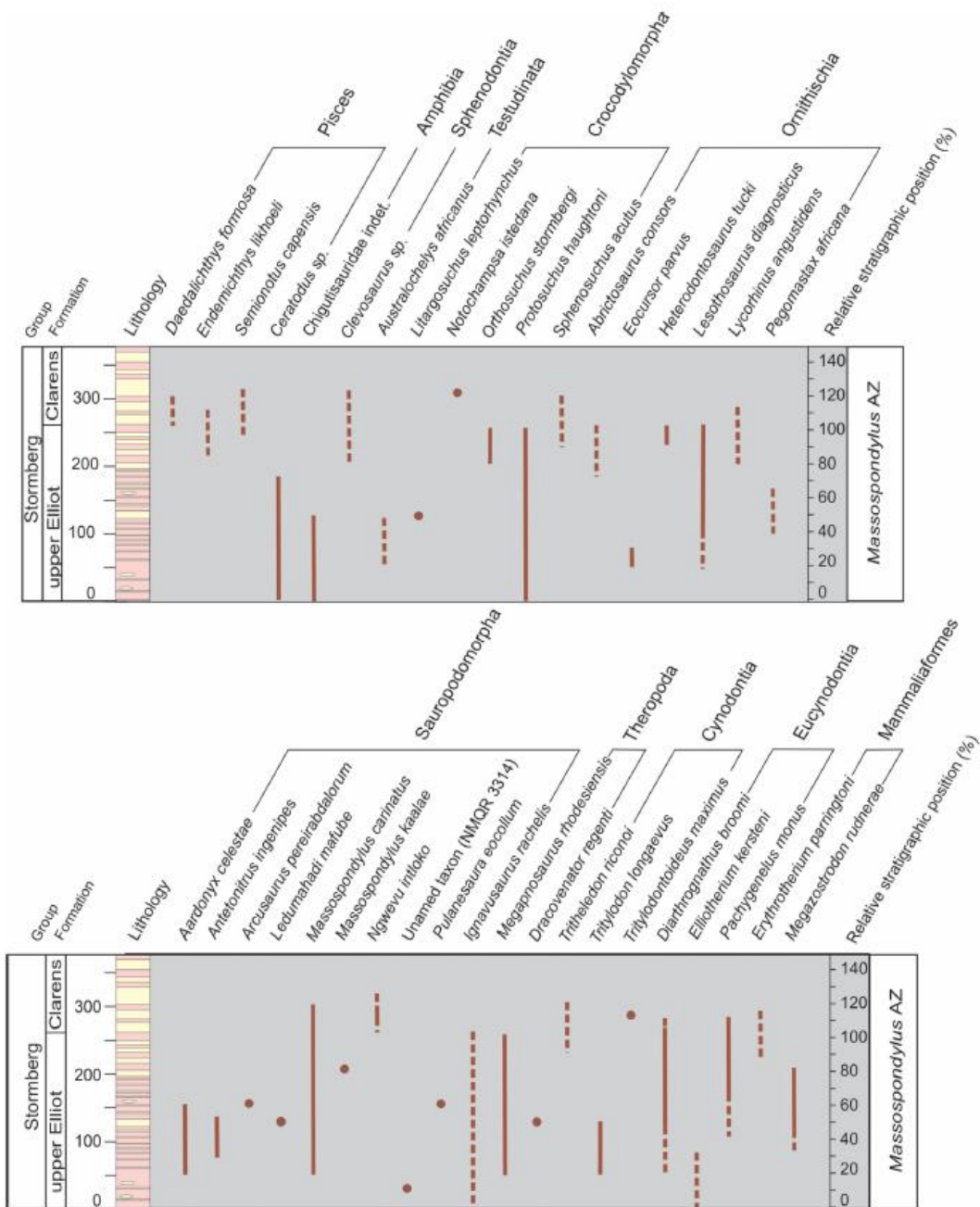


Figure 1.2: Stratigraphic section showing UEF & CF genera found within the MRZ by Viglietti et al (2020).

### 1.3 Research Rationale

Specimen AM 6147 was excavated from the Barkley Pass, Eastern Cape, South Africa in 2013. The remains appeared to be of a large sauropodomorph from the UEF. The excavation, led by the late Dr Billy de Klerk, was undertaken by a joint team from the Albany Museum and the University of the Witwatersrand. The specimen is housed in the Earth Sciences collection at the Albany Museum in Makhanda, Eastern Cape, South Africa.

Specimen AM 6147 comprises four jackets (I-IV) containing the post cranial material including ribs, gastralia, vertebrae of the mid-anterior section of the tail, and a fully prepared (V) complete left pes. Associated with the specimen are three teeth of contemporaneous carnivores, the largest of the teeth is embedded in the matrix alongside one of the chevrons in jacket AM 6147-I, the two smaller and similarly sized teeth were found in association with the pes. The latter are embedded in individual isolated blocks of matrix, AM 6147-V (r) and AM 6147-V (s).

Until now no taxonomic or phylogenetic analysis has been undertaken on AM 6147. This study will determine if AM 6147 belongs to a previously named sauropodomorph taxon of the UEF or if the material represents a new taxon. Thus, the study aims to fully describe the anatomy of the specimen and undertake a taxonomic assessment of AM 6147. The assessment will include anatomical descriptions of all the associated material including the ribs, gastralia, vertebrae of the mid-anterior section of the tail, and the left pes. It should however be noted that permission to fully prepare the ribs, gastralia and vertebrae was denied by the curator of the Albany Museum, as such the anatomy is described based on what is visible. Fortunately, the pes is fully prepared, and complete, allowing a full anatomical description. By comparing the anatomy of AM 6147 with other published data on sauropodomorphs of the Early Jurassic of Gondwana, information pertaining to AM 6147's phylogenetic relationship to other sauropodomorphs will be obtained.

A phylogenetic analysis of specimen AM 6147 will assist in a more thorough understanding of its phylogenetic relationships to other Early Jurassic Sauropodomorpha. Through the phylogenetic analysis AM 6147 will be compared to all other known and valid sauropodomorph taxa of the Early Jurassic. Should the specimen be recognised as an already existing taxon within sauropodomorphs the results of this study may increase our knowledge and phylogenetic data for the taxon. However, early inspection of the fossil elements indicates a large and robust dinosaur, larger than *M. carinatus*, the most abundant taxon of the UEF (Kitching and Raath, 1984, McPhee *et al.*, 2017). The size and robusticity of the pes elements appear like those of *Antetonitrus*, a large lessemsaurid of the UEF (Yates *et al.*, 2004, McPhee *et al.*, 2014). AM 6147 may represent a new Early Jurassic sauropodomorph, and if so, it would add to the diversity of known taxa from the UEF of South Africa.

The three associated carnivore teeth will be fully described. However, since permission to remove the teeth embedded in the matrix was denied by the curator of the Albany Museum, this study will describe the exposed parts of the teeth and where possible the serrations and curvature of the teeth will be described and compared to known carnivore taxon of the Early Jurassic and UEF to identify to which carnivore they belong.

Study of the contemporaneous carnivore teeth may provide insight into the nature of the predator and prey relationship of the extinct taxa. Since the teeth were found in close association with AM 6147 it is likely that the predators preyed and/or scavenged upon the sauropodomorph. The predator literature of the UEF largely focuses on small, early crocodylomorphs, and there is no published literature regarding ecological relationships, within the UEF. Identification of the associated carnivore teeth of AM 6147 may provide important insight into the ecological relationships of the UEF fauna.

### 1.3.1 Hypotheses

It is hypothesised that the Early Jurassic specimen AM 6147 will be recovered as an early branching sauropodomorph. Due to the large size of the specimen and the fact that it was recovered from the MZR of the UEF, a fossiliferous horizon abundant in sauropodomorph dinosaurs, it is expected that AM 6147 will be recovered as a Massospondylid.

**Hypothesis 1** - AM 6147 will be recovered as an early branching sauropodomorph.

**Hypothesis 2** - AM 6147 will be recovered as a massospondylid.

Based on the difference in the shape and serrations of the teeth associated with AM 6147 it is hypothesised they belong to archosauromorph and/or crocodylomorph taxa. Due to the close association of the teeth with AM 6147 it is expected that the associated carnivore teeth indicate a scavenging/predator-prey dynamic.

**Hypothesis 3** - The 3 carnivore teeth will belong to archosauromorph and/or crocodylomorph taxa.

**Hypothesis 4** - The associated carnivore teeth will indicate a scavenging/predator-prey dynamic.

If these hypotheses are correct, it is predicted that:

- I. Comparisons between early branching sauropodomorph taxa and AM 6147 will reveal taxonomic and morphological similarities.
- II. The specimen will show anatomical similarities to other UEF Massospondylidae.
- III. A phylogenetic analysis will recover AM 6147 as a *Massospondylid*.
- IV. The carnivore teeth will belong to two different genera: As the two smaller teeth are similar in shape and serration expression, it is anticipated that they belong to the same carnivore taxon. Because the shape and serrations are much larger on the larger third tooth, it is anticipated to belong to a different taxon.
- V. There will be serrations and/or puncture marks on the bones of the AM 6147 that will correspond with the serration patterns and size of the associated teeth.

### 1.3.2 Research Aims and Objectives

The aim of this study is to describe the anatomy and assess the taxonomy of AM 6147 and identify to which taxa the carnivore teeth belong. The results of these analyses will be compared to already published literature on Early Jurassic sauropodomorphs and carnivores of Gondwana. A phylogenetic assessment will assist in understanding AM 6147's relationship with Early Jurassic sauropodomorphs of the UEF. The identification of AM 6147 will increase our knowledge of sauropodomorphs nationally, as well as globally.

Research objectives:

- 1) Describe the anatomy of the remains of AM 6147.
- 2) Compare the anatomy of AM6147 to other Late Triassic – Early Jurassic sauropodomorphs to identify any synapomorphies and/or autapomorphies.
- 3) Undertake a phylogenetic assessment of AM 6147 to determine the specimen's phylogenetic placement amongst sauropodomorphs.
- 4) Describe the predator teeth associated with AM 6147 and identify to which taxa they belong.
- 5) Assess the bones of AM 6147 to identify if there is any damage caused by the teeth of the carnivores.

## CHAPTER 2 MATERIALS AND METHODS

### 2.1 Specimen information

#### Locality and Stratigraphy

Specimen AM 6147 was excavated in November 2013 from UEF on Glenetive Farm, Khowa, Eastern Cape, by Dr William de Klerk and a joint team from the Albany Museum and University of the Witswatersrand. The site coordinates are 31°06'58"S and 27°52'32"E.

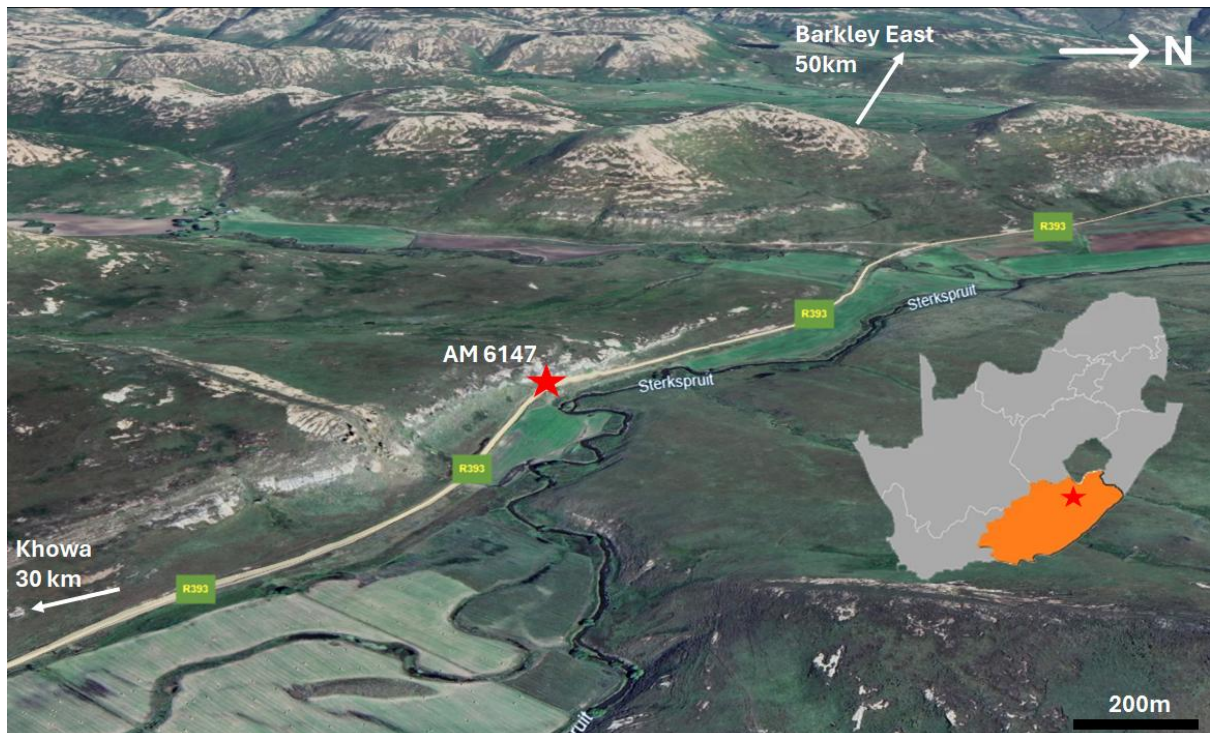


Figure 2.1: Locality map for AM 6147 which was excavated along a road cutting from the upper Elliot Formation of Glenetive Farm, Khowa, Eastern Cape Province, South Africa. The red star indicates the excavated site. Inset shows the location of Eastern Cape Province within South Africa. Map image downloaded from GoogleEarth.

The postcranial remains of specimen AM 6147 is found within 5 jackets, as indicated below in Table 2.1. Of the three carnivore teeth, the largest is associated with jacket AM 6147-I, and the two smaller teeth, each isolated in their own block of matrix, are associated with the pes.

The Albany Museum specimen accession card describes the specimen as follows: "Prosauropod dinosaur; most of mid-hindquarters (vertebrae, ribs, gastralta) and base of tail, and a large, complete pes. Several theropod teeth found in association, presumably from scavengers. Affectionately known as 'Selby'."

Table 2.1: Description of the specimen blocks taken from the Albany Museum loan agreement.

Jacket number	Contents of the jacket
AM 6147-I (SV-13-12 E)	Block containing 8 articulated (mostly complete) proximal caudal vertebrae and ribs. Associated theropod tooth.
AM 6147-II (SC-13-12 D)	Block containing 1 incomplete vertebra and 4 incomplete ribs.
AM 6147-III (SC-13-12 A)	Block containing 14 gastralia or fragments thereof. A rib fragment from top of block III prior to jacket removal, labelled in a separate bag (SV-13-13).
AM 6147-IV (SC-13-12 B)	Block containing 8 gastralia or fragments thereof.
AM 6147-V (SC-13-12 C)	Full prepared pes, 16 pieces, 21 bones (a-p); 3 theropod teeth on separate slabs (q, r, s).



Figure 2.2: Caudal vertebrae in jacket AM 6147-I. Frame indicates position of the carnivore tooth. Scale bar = 10cm.



*Figure 2.3: Carnivore tooth alongside chevron (framed in Figure 2.2) in jacket AM 6147-I. Scale bar = 1cm.*



*Figure 2.4: Vertebra and chevron fragments in jacket AM 6147-II. Scale bar = 5cm*



*Figure 2.5: Gastralium and rib fragments in jacket AM 6147-III. Scale bar = 5cm*



*Figure 2.6: Gastralium and rib fragments in jacket AM 6147-IV. Scale bar = 5cm*



*Figure 2.7: Dorsal view of the complete left pes of AM 6147-V. Scale bar = 5cm.*



Figure 2.8: Ventral view of the complete left pes of AM 6147-V. Scale bar = 5cm.



Figure 2.9: Proximal view of the articulating metatarsals of AM 6147, right to left M1 – M5. Scale bar = 5cm



Figure 2.10: Isolated carnivore tooth within the matrix, AM 6147-V (r). Scale bar = 0.3cm (3mm)



Figure 2.11: Isolated, fragmented carnivore tooth within the matrix, AM 6147-V (s). Scale bar = 0.5cm (5mm)

## 2.2 Research methodology

Anatomical terminology herein is based on the traditional or “Romerian” directional terms (Wilson, 2006). Regarding the carnivore teeth, the anatomical terminology used is based on Hendrickx et al (2015).

Photography is done by Jessica Logie with Canon EOS 1300D and EOS 250D digital cameras. Post processing is done in Adobe Photoshop 2017. The standard measurements taken are in millimetres (mm), unless otherwise stated, using digital callipers.

Nomenclatural Acts: This study follows the nomenclatural terminology and definitions regarding types as set out in the Fourth Edition of the International Code of Zoological Nomenclature (ICZN) (W.D.L. Ride *et al.*, 2000).

The comparative study included museum visits to the Evolutionary Studies Institute (ESI) collection at the University of Witwatersrand and the Karoo Palaeontology Collection at the IZIKO South African Museum, and a literature comparison which assisted with the identification of the fossil elements and orientation of the metatarsals (mt.), phalanxes, and other pes elements of specimen AM 6147, as well as the identification of the associated carnivore teeth. Photographs and measurements were taken of all the AM 6147 pes elements, the caudal series and of the associated carnivore teeth. Unique features were noted and compared to those of other Late Triassic – Early Jurassic sauropodomorphs and sauropodiformes and contemporaneous carnivores.

### 2.2.1 Sauropodomorpha research methodology

Amongst the two collections, the most observed pedal material belonged to *Aardonyx*, *Massospondylus* and *Antetonitrus*. There was little available in terms of comparative caudal vertebrae at the time of the visits to the collections. The two available caudal vertebrae for comparison belonged to *Melanorosaurus* and *Ledumahadi*. Published literature was also consulted during the comparison.

The Sauropodomorpha specimens examined at ESI and IZIKO are listed in Table A.1, Table A.2, Table A.3 & Table A.4.

Table 2.2: *Sauropodomorph comparative taxa.*

Taxa
<i>Aardonyx celestae</i>
<i>Antetonitrus ingenipes</i>
<i>Blikanasaurus cromptoni</i>
<i>Ledumahadi mafube</i>
<i>Massospondylus carinatus</i>
<i>Melanorosaurus readi</i>

These specimens were all recovered from the LEF-UEF and were therefore from a similar period (Late Triassic – Early Jurassic) to AM 6147. Below is a brief description of each of the taxa.

*Aardonyx celestae*, as described by Yates *et al* (2010), is a sauropodomorph from the Early Jurassic of the UEF. It is found within the closest known sister group to the definitive obligatory quadrupedal, if not habitual bipedal, sauropodomorph clade- a clade of basal sauropodomorph – sauropod transition (Yates *et al.*, 2010). The comparable elements for study comprised of pes elements, mt. 1, mt. 2, mt. 3, mt. 4, multiple individual phalanges and an ungual.

*Antetonitrus ingenipes* was originally described by Yates and Kitching in 2003 as a basal sauropod, and later as a sauropodiform by McPhee *et al* (2014). It is found in both the LEF and the UEF. *Antetonitrus* shows adaptations for graviportal quadrupedalism and is the oldest known definitive sauropod (Yates and Kitching, 2003). McPhee *et al.*, (2014) however suggested that *Antetonitrus* still retained an intermediary form of bipedal locomotion. The comparable elements for study comprised of pes elements, mt. 1, mt. 2, mt. 3, phalanges and unguals, as well as the complete pes of NMQR 1705.

*Blikanasaurus*, of the LEF, was described as a ‘prosauropod’ by Galton and Heerden in 1985, but later redescribed as a basal sauropod (Yates, 2008). With a similarly stout first metatarsal to that of *Antetonitrus*, *Blikanasaurus* seemed to follow the transition toward quadrupedalism. With this transition a trend of increased body size followed, however with *Blikanasaurus* an autapomorphic reversal of the trend towards an increase in size was evident (Yates, 2008, McPhee *et al.*, 2018). The comparable elements for study comprised of pes elements, a complete left pes, mt. 1 and a phalanx.

*Ledumahadi* is a gigantic non-sauropodan sauropodiform, of the UEF described by McPhee *et al* (2018), which represents an independent origin of sauropod-like body size in non-sauropodians. *Ledumahadi* expresses several autapomorphies not observed in any other sauropodomorph and is recovered as a sister taxon to *Antetonitrus* (McPhee *et al.*, 2018). The comparable elements for study comprised of a single caudal vertebra and a single ungual.

*Massospondylus* named and described by Owen, 1854, is one of the earliest described dinosaurs of Gondwana. *Massospondylus* is a non-sauropod sauropodomorph of the Late Triassic – Early Jurassic UEF, the multiple finds makes *Massospondylus* the best represented early dinosaur (Barrett *et al.*, 2019). This taxon forms the basis for extensive palaeobiological reference and is the nominal taxon of the MRZ (Yates and Barrett, 2010). The comparable elements for study comprised of three complete pedes, a partial mt. 4 and a partial pes.

*Melanorosaurus* was named in 1924 by Haughton. In 2016 the type specimen of Haughton’s *Melanorosaurus* was reclassified as *Meroktenos* by Peyre de Fabrègues and Allain as new material classified to *Melanorosaurus* was described (Peyre de Fabrègues and Allain, 2016). *Melanorosaurus* is noted to have come from the LEF placing it within the Late Triassic (Peyre de Fabrègues and Allain, 2016) and is defined as a sauropodiform (Barrett and Choiniere, 2024). The comparable elements for study comprised of a partial M4 and a caudal vertebra.

In addition to the visits to the ESI and IZIKO collections to examine sauropodomorph taxa, published literature was also consulted to consolidate the comparisons.

Table 2.3: Reviewed literature of sauropodomorph taxa included in the comparative study.

<b>Taxon</b>	<b>Author(s)</b>
<i>Coloradisaurus</i>	(Apaldetti <i>et al.</i> , 2013)
<i>Lessemsaurus</i>	(Pol and Powell, 2007)
<i>Lufengosaurus</i>	(Young, 1940, Mao <i>et al.</i> , 2020, Peyre De FabrÈGues <i>et al.</i> , 2021)
<i>Eucnemesaurus</i>	(McPhee <i>et al.</i> , 2015a)
<i>Sefapanosaurus</i>	(Otero <i>et al.</i> , 2015)
<i>Melanorosaurus</i>	(Houghton, 1924, Barrett and Choiniere, 2024, Peyre de Fabrègues and Allain, 2016, Yates, 2007a)
<i>Meroktenos</i>	(Peyre de Fabrègues and Allain, 2016)
<i>Kholumolumo</i>	(Peyre de Fabrègues and Allain, 2019)
<i>Antetonitrus</i>	(McPhee <i>et al.</i> , 2014, Yates <i>et al.</i> , 2004)
<i>Blikanasaurus</i>	(Galton and van Heerden, 1998, Galton and Van Heerden, 1985, Yates, 2008, Yates <i>et al.</i> , 2004)
<i>Adeopapposaurus</i>	(Martínez, 2009)
<i>Leyesaurus</i>	(Apaldetti <i>et al.</i> , 2011)
<i>Ignavusaurus</i>	(Bodenham and Barrett, 2020, Knoll, 2010)
<i>Sarhsaurus</i>	(Marsh and Rowe, 2018)
<i>Yunnanosaurus</i>	(Lü, 2007, Wang <i>et al.</i> , 2017)
<i>Massospondylus</i>	(Barrett, 2009, Barrett <i>et al.</i> , 2019, Viglietti <i>et al.</i> , 2020, Yates and Barrett, 2010, Yates <i>et al.</i> , 2004)
<i>Ngwevu</i>	(Chapelle <i>et al.</i> , 2019)
<i>Glacialisaurus</i>	(Smith and Pol, 2007)
<i>Leoneriasaurus</i>	(Pol <i>et al.</i> , 2011)
<i>Mussaurus</i>	(Otero and Pol, 2013)
<i>Aardonyx</i>	(Yates <i>et al.</i> , 2010)
<i>Pulanesaura</i>	(McPhee <i>et al.</i> , 2015b, McPhee and Choiniere, 2017)

### 2.2.2 Carnivore teeth research methodology

Although the study was restricted as permission to fully prepare the teeth was denied by the curator of the Albany Museum, the teeth were able to be described with various details from the exposed surfaces. Permission to further prepare the associated teeth was granted on condition they were not removed entirely from the matrix. The visible details were then compared to the teeth of other contemporaneous carnivores of the LEF and UEF in the comparative collections. Published literature was also consulted during the comparison. It is necessary to point out that the two smaller teeth AM 6147-V (r) and (s) were small enough to be put under a CT scanner.

CT scanning was performed by X-Sight X-ray Services CC in Somerset West, Cape Town,

using 190 kV (voltage); 550  $\mu$ A (current) and 74  $\mu$ m (resolution). The data was then saved to an output format – VG Project. Upon receiving the VG Project file, using MyVGL, we were able to view two of the teeth AM 6147-V (r) and (s) in full 3D view.

The teeth of the contemporaneous carnivore specimens examined at ESI and IZIKO are listed in Table A.5 & Table A.6.

Table 2.4: Carnivore tooth comparative taxa.

Taxa
<i>Notochampsia istedana</i>
<i>Orthosuchus stormbergi</i>
<i>Protosuchus haughtoni</i>
Rauisuchids
<i>Sphenosuchus acutus</i>
<i>Megapnosaurus rhodesiensis</i>
<i>Dracovenator regenti</i>

These teeth are from the same formation (LEF-UEF), and therefore from a similar period (Late Triassic – Early Jurassic), and would have been contemporaneous with AM 6147.

*Notochampsia istedana* originally described by Broom in 1904 is an early-branching crocodylomorph from the Lower Jurassic of the UEF and lower CF (Broom, 1904, Dollman *et al.*, 2019). Four early short publications by Broom (1904 and 1927), Haughton (1924) and von Huene (1925) all had differing anatomical interpretations, especially of the poorly preserved skull, which caused uncertainty with regards to the taxonomic validity and phylogenetic position of *Notochampsia* (Dollman *et al.*, 2021). *Notochampsia* has been recovered as a sister taxon to *Orthosuchus stormbergi* (Dollman *et al.*, 2021). The comparable elements for study comprised of the skull of holotype (SAM-PK-4013), however the dentition is poorly preserved.

*Orthosuchus stormbergi* described by Nash in 1968, is a crocodylomorph from the UEF of the Lower Jurassic (Dollman *et al.*, 2019, Nash, 1975). Earlier publications recovered *Orthosuchus* just outside of Protosuchidae (Dollman *et al.*, 2019), however Dollman *et al.* 2021 recovered *Notochampsia istedana* as *Orthosuchus*' sister taxon within Notochampsoidae (Dollman *et al.*, 2021). The comparable elements for study comprised of the skull of holotype (SAM-PK-K409) and dentary teeth.

*Protosuchus haughtoni* belongs to the well-defined clade of small basal Crocodyliformes of the Early Jurassic, UEF (Gow, 2000). Originally described by only the braincase in 1984 by Busbey and Gow, in later years Gow further examined *Protosuchus haughtoni* in order to establish a more comprehensive comparison with other *Protosuchus* species from other parts of the world (Gow, 2000). There were three specimens with dental remains available for comparison, SAM-PK-K01321, SAM-PK-K01323 and SAM-PK-K08026.

Rauisuchia, a group first recognised in 1942 by Huene are non-crocodylomorph pseudosuchians of the Late Triassic (Gower, 2000). In South America, East Africa and

Laurasia there have been an abundance of finds for this group, yet there was no fossil record from South Africa, however in 2019 several fragmentary archosaurian remains, likely that of *Rauisuchia* were recovered (Tolchard *et al.*, 2019). The last recorded appearance of *rauisuchid* fossils in South Africa is documented in the LEF, the end of the Triassic (Tolchard *et al.*, 2019, Tolchard *et al.*, 2023). Multiple individual teeth were available for comparison, BP/1/6062, BP/1/6894, BP/1/6598, BP/1/6508, BP/1/5730 and SAM-PK-K383.

*Sphenosuchus acutus*, first described by Haughton in 1915, is described as a slender-limbed cursorial carnivore that was small to moderate in size yet one of the largest early-crocodylomorphs from the UEF of the Late Triassic – Early Jurassic (Haughton, 1924, Walker, 1990). The type specimen SAM-PK-003014 which included the skull and dentition was available for study.

*Megapnosaurus rhodesiensis*, an early Jurassic theropod, originally named *Syntarsus* by Raath (1969) is, commonly found in the Forest Sandstone Formation of Zimbabwe, a formation equivalent to the UEF of South Africa. *Megapnosaurus*, was a small, lightly built, bipedal carnivore of coelurid affinities (Raath *et al.*, 1990). A further two fossils have been recovered from the EF (Munyikwa and Raath, 1999) and are reported to belong to the same taxon as the Zimbabwean material. No teeth were available in the ESI or IZIKO collections at the time of the visits, but comparisons were made against publications, Raath *et al.*, (1990), Munyikwa and Raath (1999), Chinsamy-Turan (2024) and Hendrickx *et al.*, (2015).

*Dracovenator regenti*, an Early Jurassic theropod of the UEF, was described by Yates (2005) as a medium-sized theropod that closely resembles *Dilophosaurus wetherilli*. The comparable elements for study comprised of an articulated set of premaxillae, maxillae, nasals and dentaries belonging to the type specimen BP/1/5243. Within the published 2005 paper, Yates also identifies a possible juvenile of the species (BP/1/5278). Personal communication with the ESI collections confirms this specimen was stolen.

In addition to the visits to the ESI and IZIKO collections to examine contemporaneous carnivore taxa, published literature was also consulted to consolidate the comparisons.

Table 2.5: Reviewed literature of carnivore taxa included in the comparative study.

Taxon	Author(s)
<i>Megapnosaurus</i>	(Kitching and Raath, 1984, Munyikwa and Raath, 1999, Raath <i>et al.</i> , 1990)
<i>Dracovenator</i>	(Yates, 2005)
<i>Sphenosuchus</i>	(Walker, 1990)
<i>Litargosuchus</i>	(Clark and Sues, 2002)
<i>Orthosuchus</i>	(Dollman <i>et al.</i> , 2019, Nash, 1975)
<i>Notochampsia</i>	(Dollman <i>et al.</i> , 2021)
<i>Protosuchus</i>	(Gow, 2000)
<i>Rauisuchia</i>	(Gower, 2000, Nesbitt <i>et al.</i> , 2013b, Tolchard <i>et al.</i> , 2019, Tolchard <i>et al.</i> , 2023)

<i>Ceolophysis</i>	(Buckley, 2009, Jasinski, 2011)
<i>Redondavenator</i>	(Nesbitt <i>et al.</i> , 2005)
<i>Dilophosaurus</i>	(Serrano-Martínez <i>et al.</i> , 2015)

### 2.3 Phylogenetic analysis

Characters on the pes and vertebrae elements of AM 6147 were added to and analysed using the Ezcurra *et al.* (2024) character matrix (See APPENDIX C for the full character list used in this study). This character list includes the characters listed by Yates 2007 a & b, the characters added by Smith & Pol (2007), those added by Martínez *et al.* (2012), Otero & Pol (2013), Otero *et al.* (2015) and Cerda *et al.* (2017). The matrix includes all the valid taxon species of Sauropodomorpha from the Late Triassic and the Early Jurassic.

The data matrix included 89 taxa scored across a total of 421 characters. The following multistate characters were treated as ordered, summing to a total of 37: 8, 13, 19, 23, 40, 57, 69, 92, 102, 108, 117, 121, 134, 144, 147, 149, 150, 157, 167, 170, 171, 177, 205, 207, 222, 227, 242, 251, 254, 277, 294, 299, 336, 342, 349, 353, and 370. In total 421 characters are included in the matrix, for AM 6147, 39 characters across the pes and caudal vertebrae were recorded.

For the pes 26 characters were recorded: 331 332 333 334 335 337 338  
339 340 341 342 343 344 345 346 347 348 349 350  
351 352 354 357 358 359 361

For the vertebrae 13 characters were recorded: 161 165 184 185 187 189  
190 191 192 193 195 196 197

The 39 characters were added to the matrix using Mesquite 3.70 (Maddison and Maddison, 2018).

The matrix was analysed using TNT v.1.6 (Goloboff and Morales, 2023) with the most parsimonious trees recovered via a traditional search of 1000 replicates of Wagner trees with TBR algorithm with 10 trees saved per replication.

Applying the IterPCR procedure (Pol and Escapa, 2009) to identify unstable taxa, a majority rule 50 and strict consensus tree(s) were run to exclude the unstable taxa from the analysis *a posteriori*. Bremer support and Bootstrapping support analyses were run on both strict and reduced strict consensus trees to compare their values.

Results taken from the TNT analysis were run through Figtree 1.4.4 (Rambaut, 2006), a graphical viewer for phylogenetic trees and program for producing publication-ready figures, to finalise the structure of the cladogram. Any labelling, inserting of values and colourisation took place during this final step.

## CHAPTER 3 RESULTS

### 3.1 Further exploration of the AM 6147 locality

The site has not been further excavated since 2013; however, during a brief prospecting on the site in early 2024 further caudal vertebrae and other vertebra fragments were found *in situ*. The site sits along the southwest side of a road reserve cutting on the Barkley East Pass, which passes through Glenetive Farm. The material is exposed on a  $\sim 45^\circ$  slope angled toward the road. The location where the original vertebral series (AM 6147 – I) was excavated from is little less than a metre and a half from the gravel road cutting. The northeast side of the road cutting slopes steeply into a flowing stream.

The 2013 field notes by field member, Jonah Choiniere, suggests that the site appears to be right at the transition to the Lower Clarens Formation (LCF). This was confirmed during the site visit in February 2024, where the contact between the UEF to LCF is roughly a metre above the location of the excavated material. Assuming horizontality, AM 6147 sits within the red-bed fine sandstones of the UEF close to the transition to the pale-coloured fine sandstones of the LCF, which is late Early Jurassic in age (Bordy *et al.*, 2020). As AM 6147 lies within the upper part of the UEF it is regarded as earliest Jurassic in age.

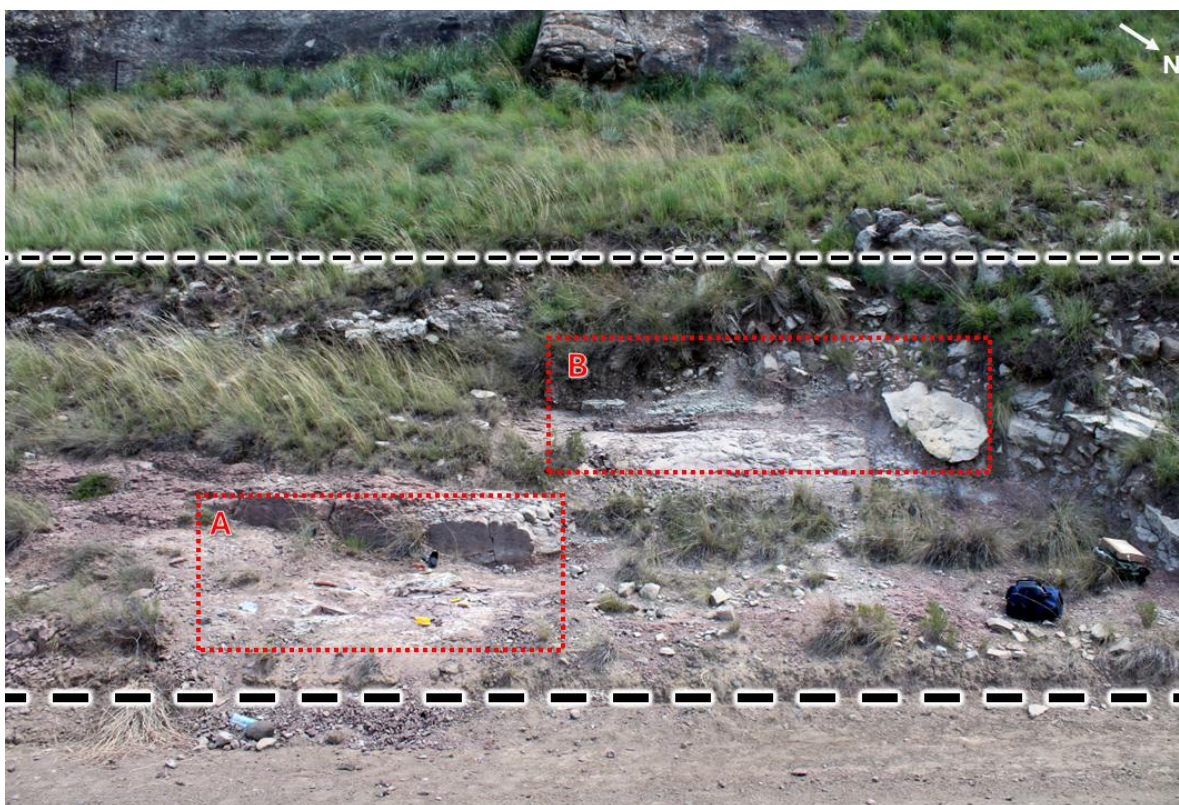


Figure 3.1: Excavation site of AM 6147. Large black dashes indicate the outer margin of the road cutting. Smaller black dashes indicate the 'transition' from the UEF to LCF. Red box A indicates the excavated location of jackets labelled AM 6147-I & II. Red box B indicates the excavated location of jackets labelled AM 6147-III, IV & V. See Table 2.1 for details regarding the elements of each block.

## Systematic Palaeontology

Dinosauria, Owen, 1842  
 Saurischia, Seeley, 1888  
 Sauropodomorpha, von Huene, 1932  
 Massopoda, Yates, 2007

**Massospondylidae** von Huene, 1914 (sensu Sereno 1998)

**Definition.** The clade Massospondylidae is defined here by Sereno (1998) as all taxa more closely related to *Massospondylus carinatus* (Owen, 1854) than to *Plateosaurus engelhardti* and *Saltasaurus loricatus*.

**Comments:** In 1999 Sereno was the first to undertake a formal phylogenetic analysis of the Massospondylid clade which included *Massospondylus* and *Yunnanosaurus* (Sereno, 1999). Recently many other phylogenetic analyses have identified a monophyletic Massospondylidae that includes *M. carinatus*, *Coloradisaurus* and *Lufengosaurus* amongst other taxa (Barrett *et al.*, 2019), however many publications misattribute the current definition of Massospondylidae to either Yates (2003b) or Yates (2007b).

*Enkulusaura deklerki*, gen. et sp. nov.

### Etymology.

*Enkulusaura* from the isiXhosa *enkulu*, meaning 'big' or 'large', and the Latin *saura*, feminine, meaning 'lizard'. The name refers to the significant size of this taxon relative to other Early Jurassic Massospondylidae found in southern Gondwana. The specific epithet, *deklerki*, honours Dr William de Klerk who led the excavation of the dinosaur in 2013.

### Holotype

AM6147, a partial complete skeleton including gastralia fragments, rib fragments, articulated mid-anterior caudal vertebrae with chevrons, and a complete left pes.

### Locality and Horizon

Specimen AM 6147 was excavated from a road reserve cutting on the Barkley East Pass in the Eastern Cape, South Africa. The site coordinates are S 31° 07.012' and E 27° 53.140'. Uppermost part of the Elliot Formation, Stormberg Group (Hettangian–Sinemurian) (Sciscio *et al.*, 2017b).

### Diagnosis

A non-eusauropod sauropodomorph that can be distinguished from other sauropodomorphs by the presence of the following autapomorphies and unique combination of features (autapomorphies marked by \*):

\*A small flange on the dorsolateral surface of the shaft of Metatarsal 2. \*A deeply concave medial profile and \*robust ventromedial flange on the proximal articulating surface of Metatarsal 2. \*A concave groove running the length of the dorsal surface of Metatarsal 4. \*A dorsomedial flange on the shaft of Metatarsal 4. \*The extended dorsoposterior curve and dorsoposterior direction of the anterior caudal transverse processes.

### 3.2 Anatomical description of AM 6147

A detailed anatomical description was undertaken of the skeletal elements of jacket AM 6147-I containing the 8 articulated caudal vertebrae and one of the associated predator teeth (Figure 2.2 & Figure 2.3), the complete left pes (Figure 2.7) and its two associated teeth (Figure 2.10 & Figure 2.11). The description of the material in the jackets containing the fragmentary gastralia, ribs and chevrons are done at a surface level as these elements provide no insightful anatomical information to the study. Note that permission was not granted by the Albany Museum to fully prepare out all the elements from the matrix. As such the anatomical descriptions are based on the exposed parts of the skeletal elements. Permission was obtained to further prepare blocks AM 6147 – I and AM 6147 – V (r) in order to further expose the fossil elements. This was done by fossil preparator Tiffany van Zyl of Pushing Up Daisies.

#### **Caudal vertebrae and chevrons (AM 6147-I)**

Figure 3.2 contains 4 complete and 4 incomplete caudal vertebrae, 9 chevrons or fragments thereof and 1 predator tooth.

Of the 8 vertebrae, all preserve their centrum or part thereof, 7 preserve the articulated chevron, 5 preserve the neural spines, and 4 preserve complete transverse processes. Five of the vertebrae preserve the prezygapophyses and 4 preserve the postzygapophyses. For a comprehensive list of measurements see Table B.2.

The vertebrae all represent anterior caudal vertebrae as their centra are somewhat laterally compressed (based on the first visible centrum). The length of the transverse processes and the height of the neural spine decrease in the posterior vertebrae, and further posteriorly, the extension of the postzygapophyses lessens. The chevrons associated with the anterior caudal vertebra either present straight or curved shafts.

As there are only 8 recovered vertebra it is not possible to identify their exact number within the caudal series and thus they are numbered in this study as CV 1–8 for convenience.



*Figure 3.2: Anterior caudal vertebrae (CV 1-8) of AM 6147 in lateral view. Scale bar = 10cm.*

The vertebrae and chevron elements are described and measured in anatomical position. The remains are preserved in series within the matrix in a dorsoventral orientation, with the left lateral surfaces exposed.

CV 5, and CV 4, are the best-preserved anterior caudal vertebra in the sequence (Figure 3.3). Both vertebrae are almost complete with just small fragments missing along the base of the transverse processes and prezygapophyses, a small amount of weathering on the border of the distal articulation surface of the centrum and a few cracks across the neural spines and chevrons.

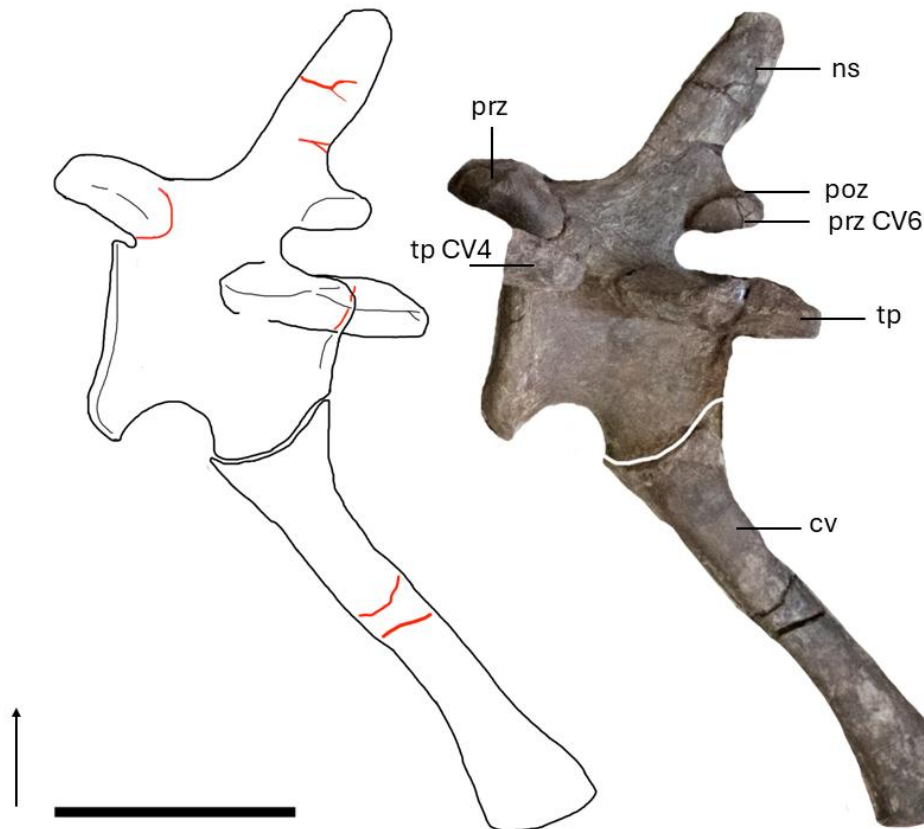


Figure 3.3: Side by side illustration and image of anterior caudal vertebra (CV 5) of AM 6147 in lateral view. Red lines indicate fractures and breaks in the bone. ns, neural spine; poz, postzygapophyses; prz, prezygapophyses; tp, transverse process; cv, chevron. Arrow indicates dorsal direction. Scale bar = 10cm

The best-preserved complete chevron belongs to CV2; however, the haemal arch is not visible on this chevron as it is covered by the matrix. Haemal arches are visible on the chevrons of CV2-6. The distal ends of the chevrons of CV 4-7 are incomplete and/or damaged. CV8 is missing its distal surface as well as its chevron as they were cut off during extraction.

### Caudal series

The caudal vertebrae elements of AM 6147 are proportionally longer and larger than those of massospondylids *Massospondylus* (Barrett et al., 2019), *Coloradisaurus* (Apaldetti et al., 2013), *Ignavusaurus* (Knoll, 2010) and *Adeopapposaurus* (Martínez, 2009). In AM 6147 the anteroposterior length of centrum is 1,2 times longer than the dorsoventral height of the anterior articulating surfaces, whereas, according to Apaldetti et al (2013) the anteroposterior length of *Coloradisaurus's* centrum is 0,87 times shorter than the dorsoventral height of the articulating surfaces. AM 6147's transverse process is measured at 0.77 times the total length of the centrum, whereas *Coloradisaurus's* transverse process is only 0.45 times the total length of the centrum (Apaldetti et al., 2013).

### Neural arch & spines

As in most sauropodomorphs, the neural arch is saddle shaped. The form of the anterior surface of the neural arch reveals a simple centroprezygapophyseal ridge. The length of the base of the neural spine is greater than half the length of the neural arch, this is dissimilar to

other Massospondylids in which the length is less than; viz. *Coloradisaurus* (Apaldetti *et al.*, 2013), *Lufengosaurus* (Young, 1941), *Massospondylus* (Yates and Barrett, 2010), *Adeopapposaurus* (Martínez, 2009) and *Leyesaurus* (Apaldetti *et al.*, 2011). The neural spine slopes posterodorsally (Figure 3.3), similarly seen in *Adeopapposaurus*, with the spinous process extending past the posterior margin of the centrum, this extension lessens the more distal the vertebrae become. The anterior and posterior margin of the neural spine is straight in its posterior slope. The spinous process measures dorsoventrally 23.71mm at the tip and 34.13mm at the base and is anteroposteriorly narrow unlike the sister taxon *Coloradisaurus* where the neural spine is very broad anteroposteriorly. The base of the neural spine is broad and stretches the full distance between the prezygapophyses and the postzygapophyses. As the vertebra is still embedded in the matrix, it cannot be fully described mediolaterally.

### **Centra**

All the centra are proximodistally compressed, the dorsal margin is straight, similar to *M. carinatus*, but only slightly concave. The anteroposterior length of the centrum is 1.1 times longer than the dorsoventral height of the anterior articulating surface, whereas in *Coloradisaurus* the anteroposterior is 0.75 times shorter than the dorsoventral height of the anterior articulating surface (Apaldetti *et al.*, 2013). The length of the mid-caudal centra is greater than twice the height of their anterior faces, similarly, seen in *Massospondylus* and *Adeopapposaurus*. The shape of the anterior and posterior faces of the centra are oval with rounded lateral and ventral sides. The ventral surface of the centrum is strongly concave producing a distinct waist while the articulating faces are weakly amphicoelous. The ventral surface of CV1-7 presents a longitudinal ventral sulcus; it is well defined and 'u'-shaped, a feature also present in *Massospondylus* and *Adeopapposaurus* but absent in sister taxon *Coloradisaurus* and *Lufengosaurus* (Young, 1941). The sulcus is not visible on CV 8 as the matrix covers the ventral surface. A cross-section shape of the distal caudal centra is oval with rounded lateral and ventral sides, a feature AM 6147 shares with *Coloradisaurus* and *Lufengosaurus*. The neural canal cannot be described as the vertebrae are too deeply embedded in the matrix.

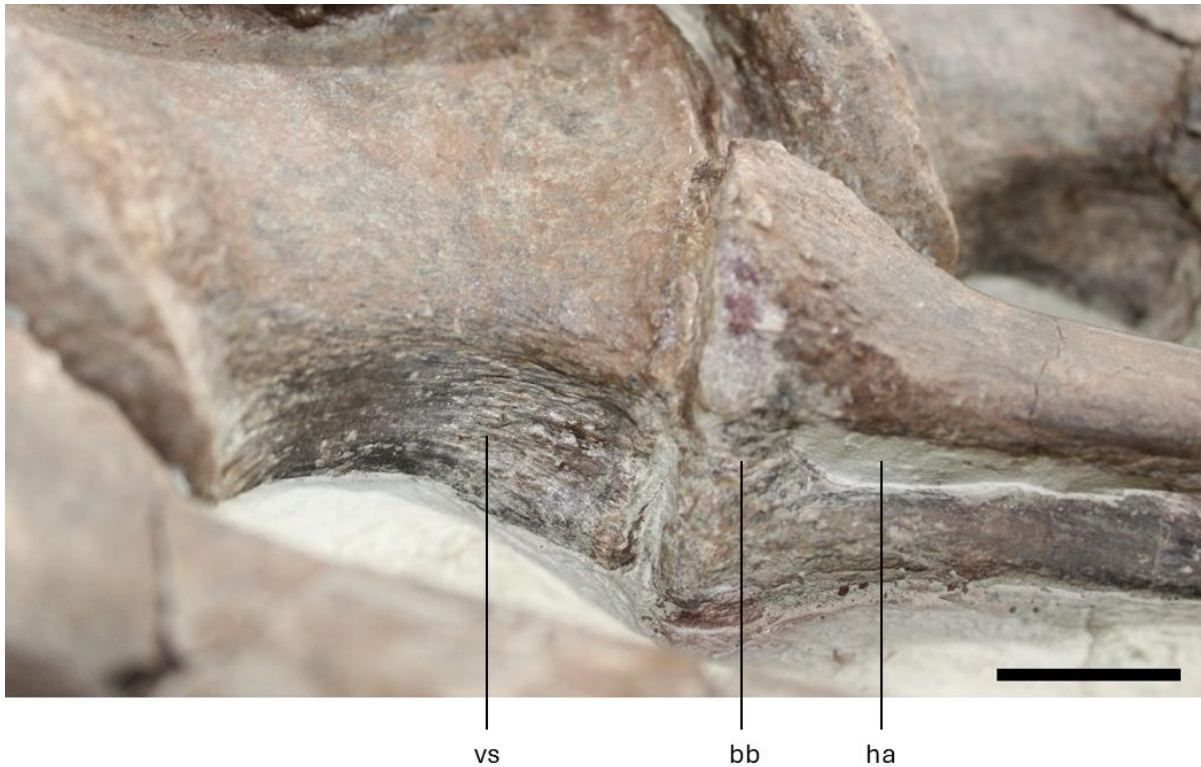


Figure 3.4: The 'u'-shaped sulcus on the ventral side of the caudal centrum. Ventral sulcus, vs; bony bridge, bb; haemal arch, ha. Scale bar = 2cm

### Zygapophyses

The prezygapophyses extend anteriorly beyond the anterior margin of the centrum while the postzygapophyses extend posteriorly only slightly beyond the posterior margin. The length of the prezygapophyses measure 38.85mm and overlap the preceding centrum by half their length. The prezygapophyses project anteriorly in lateral view and the articular facets face dorsomedially. In *M. carinatus* the facets also face dorsomedially but they project almost vertically (Barrett *et al.*, 2019). Both the prezygapophyses and postzygapophyses have an oval cross-sectional shape in the medial plane, which is dissimilar to *M. carinatus* but more like that of *Coloradisaurus*. The postzygapophyses project posteriorly in lateral view, and the articular facets face latero-ventrally, as in *Coloradisaurus*. The interpostzygapophyseal notches are visible in dorsal view.

### Transverse process

The transverse processes are completely fused to the centrum and extended laterally at the anteroposterior midpoint of the neural arch. The base of the transverse processes are broad and are restricted to the dorsal surface of the centrum, similar to *Sefapanosaurus* (Otero *et al.*, 2015), *Leyesaurus* and *Adeopapposaurus* but unlike *Coloradisaurus* where they are placed entirely on the neural arch. The base of the transverse process is a rounded ratio of 1:2 to the length of the centrum. The transverse processes are slightly dorsoventrally flattened while expanding posterior-laterally from the base so that the dorsal surface is concave, and the ventral surface is convex. The transverse processes of AM 6147 are dorsoposteriorly directed, similar to *Adeopapposaurus*. The lateral tip curves further dorsally and posteriorly (Figure 4.4 & Figure 4.5). The antero-posterior length of the transverse process is 78% of the total length of the centrum. The transverse process is oval in cross-section.

### **Incomplete caudal vertebra and chevron fragments (AM 6147-II):**

AM 6147-II (Figure 2.4) contains four chevron fragments, still mostly embedded in the matrix, and one exposed vertebral fragment with an articulated proximal head of a caudal chevron. The fragments include part of the shaft and their distal ends. The distal ends are present on only two of the chevron fragments.

The fragments (from left to right): The first two fragments include part of a chevron's distal shaft including distal end, the next two include part of a chevron's distal shaft with the distal and proximal ends missing, and the last fragment comprises of a vertebra fragment accompanied by an articulated proximal chevron head.

The fragments are identified as chevron fragments as there are visible concave grooves on the anterior surface of the element which corresponds with the haemal arches on the other known chevron elements.

The vertebra preserved is too fragmentary to further study; however, it is likely to be a caudal vertebra as it is associated with the caudal fragments, and it shows an articulation with a proximal head of a chevron.

### **Chevrons**

CV2-6 preserve a laterally straight closed Y-shape morphotype on the haemal arch with two proximal rami on either side of the haemal canal with an additional bony 'bridge' connecting the two dorsal rami. Distally the canal is compressed laterally. This canal runs the proximodistal length of the blade and amounts to 64% of the length on anterior surface, this percentage falls well within the typical 50-75% recorded for Y-shaped haemal arches in sauropods. The haemal arch is straight in lateral view. Closed Y-shape haemal arches are commonly seen in other Early Jurassic early diverging sauropodomorphs, sauropods, and eusauropods, as well as theropod dinosaurs (Otero *et al.*, 2012). The proximal head of the chevron is articulated with its preceding vertebra and the distal end, partially visible in lateral view, is rounded in shape. The chevron shaft sits posterior-ventrally at a 52° angle relative to the antero-posterior plane of the vertebrae. The bone surface of the chevron is partially weathered at the distal end. The chevrons are greater than twice the length of the preceding centrum, this is unlike *Coloradisaurus*, *Plateosaurus*, *Massospondylus*, *Adeopapposaurus* and *Leyesaurus* which are less than twice the length of the preceding centrum. The distal ends of the chevrons are rounded and medio-laterally flattened, and an anteroventral process on the distal chevrons is absent. The proximal articulating surface of the proximal most vertebrae (CV1) is slightly weathered, although the articulating face reveals a shallow concave surface and raised exterior ridges. The shape of the proximal articulating surface is subcircular and the dorsoventral height to the mediolateral width has a ratio of 42:47. The mid-caudal chevrons present a haemal arch unlike relatives *Coloradisaurus*, *Lufengosaurus*, *Massospondylus*, *Adeopapposaurus* and *Leyesaurus* who do not present any.



Figure 3.5: Closed y-shape haemal arch seen on all the chevrons. Bony bridge, bb; haemal arch, ha. Scale bar = 3cm

#### **Gastralia and rib fragment (AM 6147-III & AM 6147-IV):**

The excavated block AM 6147-III comprises gastralia and loose rib fragment (Figure 2.5). More precisely, the jacket contains 14 gastralia and fragments thereof, as well as rib fragments from the top of block III prior to jacket removal. The rib fragment is stored separately in a labelled plastic bag. The fragment is too incomplete and small to provide any anatomical data. Six of the larger fragments lie parallel to each other with the rest of the smaller fragments scattered throughout the rest of the matrix.

AM 6147-IV (Figure 2.6) comprises of 8 gastralia or fragments thereof. The 6 gastralia lie parallel to each other. Gastralia 4-6 have a slight 'S' shape curve (Figure 4.6). The largest 'S' shaped gastralia (6) has a thickened mid-section and is much more robust than the other gastralia. From this thickened mid-section, a new process extends and follows a similar curve to the rest of the gastralia. This shape and process is not known in other sauropodomorphs and may be pathological.

#### **Complete left pes (AM 6147-V (a-p)):**

AM 6147-V (Figure 2.7) comprises of a fully prepared, 22-piece pes that makes up a complete left foot. The pes was found in articulation *in situ*. Mt. 1 is still joined to its articulated phalanx; mt. 3's proximal phalanx, mt. 4's proximal phalanx, and mt. 5's distal phalanx and ungual are also articulated to each other.

According to the 2013 excavation fieldnotes by field member Jonah Choiniere, Jacket C, AM 6147-V (SV-13-12C), contained a partial femur, tibia, fibula and the pes. Through personal communication with Jonah Choiniere (2023) and the Albany Museum, at the time of this study only the pes is available as the femur is said to have been stolen during excavation, whereas the tibia and fibula could not be found in the Albany Museum's collection.

Table 3.1: The 22 pes elements of AM 6147.

Digit 1	Digit 2	Digit 3	Digit 4	Digit 5
Metatarsal 1	Metatarsal 2	Metatarsal 3	Metatarsal 4	Metatarsal 5
Phalanx 1	Phalanx 1	Phalanx 1	Phalanx 1	Ungual
Ungual	Phalanx 2	Phalanx 2	Phalanx 2	
	Ungual	Phalanx 3	Phalanx 3	
		Ungual	Phalanx 4	
			Ungual	

For a comprehensive list of the measurements for the pes elements see Table B.1. These measurements include the midshaft width percentage of the total length of the bone, total length, minimum anterior-posterior depth of shaft, minimum mediolateral shaft width, maximum width of proximal articular surface mediolateral, maximum depth of proximal surface anterior-posterior, mediolateral width of distal articular surface and anterior-posterior depth of distal articular surface.

Two other bone elements associated with the pes are the astragalus and the calcaneum.

### Metatarsals

Within Massospondylidae, the metatarsals of AM 6147 are proportionally much larger than *Massospondylus* (Mukaddam et al., 2021), *Coloradisaurus* (Apaldetti et al., 2013), *Ignavusaurus* (Knoll, 2010), *Adeopapposaurus* (Martínez, 2009) and *Leyesaurus* (Apaldetti et al., 2011), but more alike *Glacialisaurus* in size and robusticity (Smith and Pol, 2007).

The difference in pes size of AM 6147 and its, geographically, closest relative, *M. carinatus*, is very apparent. Mukaddam et al (2021) measures mt. 1 through mt. 5 across six *M. carinatus* specimens (QG1159 (R), BP/1/5241 (R), BP/1/4779 (R), SAMPK 1304 (R), SAMPK 388 (R) and SAMPK 388 (L)) (Figure B.1). The comparison of the calculated data from these specimens against the measurements of AM 6147 reveals that AM 6147's metatarsals are 45% larger (Table 3.2).

Table 3.2: The calculated average length of the metatarsals of the six *M. carinatus* specimens compared to that of AM 6147.

Metatarsal	<i>M. carinatus</i> on average	AM 6147
Mt. 1	69.08	165.10
Mt. 2	11.30	173.08
Mt. 3	121.11	300.48
Mt. 4	115.39	271.14
Mt. 5	53.41	135.64

\*Average calculated from the specimens in Figure B.1.

AM 6147 exhibits a size that is similar to, and/or slightly smaller than, that of *Glacialisaurus*, based on the few measurements that have been published in Smith and Pol (2007) (Table 3.3).

Table 3.3: Measurements comparing AM 6147 and *Glacialisaurus*. Modified from Smith and Pol et al., (2007). Asterisks indicate incomplete measurements due to damage.

	AM 6147	<i>Glacialisaurus</i> (Pol et al., 2007)
Mt.1		
Total Length (mm)	165.1	163
Minimum mediolateral shaft width	58.11	62
Mt.2		
Total Length (mm)	173	218
Minimum mediolateral shaft width	52	62
Mt. 3		
Total Length (mm)	301	*105
Minimum mediolateral shaft width	60	66
Mt. 4		
Total Length (mm)	271	*91
Minimum mediolateral shaft width	55	*59

The prominent size of the metatarsals in AM 6147 suggested a possible affiliation with larger sauropodiformes, thereby warranting a comparison with more derived Sauropodomorpha found in South Africa. Further comparative measurements of mt. 1 can be seen for AM 6147, NMQR 1705, *Antetonitrus*, *Melanorosaurus* and *Blikanasaurus* in Table 3.4.

Table 3.4: Comparing Metatarsal I measurements for AM 6147, NMQR 1705, *Blikanasaurus* and *M. carinatus*. Modified from Yates (2008). Asterisk indicates approximate measurements due to incomplete bone elements.

	<i>E. deklerki</i> AM 6147	NMQR 1705	<i>Melanorosaurus</i> NM 1551 (Yates 2008)	<i>Antetonitrus</i> BP/1/4952 (Yates 2008)	<i>Blikanasaurus</i> BP/1/5271 (Yates 2008)	<i>Blikanasaurus</i> SAM-PK-K 403 (Yates 2008)
Metatarsal 1						
The midshaft width % of the total length of the bone	36%	40%	39%	54%	55%	53%
Total Length (mm)	165,1	152.7	119	120	70	76
Minimum anteroposterior depth of shaft	28.14	35.48	23	31.1	21	31
Minimum mediolateral shaft width	58.11	60.8	47	63	36.5	41
Maximum width of proximal articular surface mediolateral	80.92	49.99	69	93.5	56.4	76.5
Maximum depth of proximal surface anteroposterior	*35.63	70.91	33	59	36.5	36.5
Mediolateral width of distal articular surface	83.78	42.87	67	88.36	45	54
Anteroposterior depth of distal articular surface	x	55.25	37	43.7	23	38

Mt. 1 is attached to its proximal phalange. The proximal end and articulating surface of mt. 1 are lacking the bone surface, as such it is unknown how much weathering may have occurred. The proximal articular surface is rectangular in shape, this is dissimilar to *M. carinatus* which has a sub-triangular outline and *Coloradisaurus* which has a subvoid outline but it is more similar to the subelliptical outline of *Sarhsaurus* (Marsh and Rowe, 2018). The orientation slopes proximolaterally relative to the long axis of the bone, this is dissimilar to all other Massospondylidae except *Sarhsaurus* (Marsh and Rowe, 2018). The element is dorsoventrally flattened, wider than it is deep. The proximal width of mt. 1 is less than the width of mt. 2, as seen in *Massospondylus*, *Adeopapposaurus* and *Coloradisaurus* and other early diverging sauropodomorphs. The dorsal surface is flat with a noticeable rounded ridge on the proximal ventrolateral surface of the tarsal. The medial and lateral side of the distal head have robust condyles with deep collateral fossae. The lateral fossa is more robust.



Figure 3.6: Metatarsal 1 in dorsal (left) and ventral (right) view. Phalanx 1 is attached to the distal end. Scale bar = 5cm

The proximal end of mt. 2 has an hourglass shape, commonly seen in other sauropodomorphs. The proximal medial surface is deeply concave - this exaggerated concave surface may have been induced by weathering; however, the relatively smooth and even surface of this margin suggests that this is not the case. The concave medial surface is present in many sauropodomorphs, but the exaggerated degree of the concavity of AM 6147 is distinctive. A large ventromedial flange and a slightly weaker concave proximal lateral surface present articulation surface for mt. 1 and mt. 3. As noted by Cooper (1984) and Yates (2003), *Vulcanodon* and basal eusauropods lack this lateral concave surface. This ventromedial flange is present in other early diverging sauropodomorphs, and although *Tazoudasaurus* presents an extended flange, there are no descriptions of such a hyper

elongation as seen in AM 6147 (Figure 4.2). The anterior ventral margin of the proximal face is slightly convex while the anterior dorsal is straight mediolaterally. The proximal end is trapezoidal in shape with the ventral surface extending wider than the dorsal surface. Distally, the shaft narrows mediolaterally and dorsoventrally. The dorsal surface of the shaft is flat, aside from a slight concave slope on the dorsal proximal surface and a small lateral lip. At the midpoint on the lateral dorsal surface of the shaft a small flange is visible. The ventral surface curves upward slightly in the centre. The proximal ventral surface is slightly concave while the lateral and medial margins reveal robust ridges. The dorsal surface slopes distally. A small flange is present on the medial dorsal surface midway down the shaft (Figure 4.1). The condyles and fossae on the distal head are weathered and worn down, the lateral condyle is severely worn down and presents a small fossa, the medial condyle is much more robust, but its fossa is nearly completely weathered. The proximal articulating surface slopes posteromedially, this slope may have been exaggerated slightly by weathering.



Figure 3.7: Metatarsal 2 in dorsal (left) and ventral (right) view. Scale bar = 5cm

Mt. 3 is the longest of the metatarsus and is dorsoventrally wider and flatter than it is deep. The proximal end is slightly distorted and damaged but reveals a subtriangular shape with a rounded posterior border, similar to *Massospondylus*, *Lufengosaurus* and *Adeopapposaurus* – however the articulating surface is too damaged to describe. The distal end of mt. 3 deflects slightly medially along its proximodistal axis, similarly, seen in other early diverging sauropodomorphs such as *Massospondylus*, *Adeopapposaurus* and *Lessemsaurus*. The shaft is relatively straight and flat on both the dorsal and ventral side, a slight concave groove is present on the distal ventral end. The distal head's condyles are relatively shallow with deep set fossae. The distal articulation surface is rectangular in shape in distal view with the ventral and dorsal margins being similar in their length. The dorsal margin slopes slightly laterally, the articulation surface reveals an intercondylar groove.



Figure 3.8: Metatarsal 3 in dorsal (left) and ventral (right) view. Scale bar = 5cm

The proximal end of mt. 4 is acutely triangular, the articulating surface is narrow with a slight concave midpoint. As seen in all non-eusauropod sauropodomorphs, the proximal end of mt. 4 is broader than the distal end and is subtriangular in outline. The dorsal margin reveals a short ridge that runs distally along the proximomedial side of the shaft where it meets a well-defined flange at the mid-point on the medial surface (Figure 4.3). This flange is considered as an autapomorphy for *Tazoudasaurus* (Allain and Aquesbi, 2008). The flange measures 2.9cm in length and 0.4cm high. The medial surface of the proximal end slopes at a 45-degree angle medially. The lateral surface of the proximal end is nearly planar dorsally and slightly concave ventrally as it articulates with the dorsomedial margin of mt. 5. The shaft is dorsoventrally flattened, wider than it is deep, and it is wider proximally than distally. The dorsal surface of the shaft reveals a prominent concave groove (Figure 4.3) which extends proximodistally stopping just before the distal head, this can be seen in lateral view. The distal articulation surface is trapezoidal in shape with the ventral margin wider than the dorsal margin, it is lateromedially broader than it is dorsoventrally high. The transverse width of the distal end of mt. 4 is narrower than that of mt. 3. The lateral condyle on the distal head is largely worn away while the medial condyle is intact. The intercondylar fossae are shallow on both the lateral and medial condyles.



Figure 3.9: Metatarsal 4 in dorsal (left) and ventral (right) view. Scale bar = 5cm

Mt. 5 is obtusely triangular and flat in shape, a shape seen in all early diverging sauropodomorphs. The medial surface extends medially as it articulates with the ventrolateral surface of mt. 4. The proximal end is obtusely triangular, the medial side is lowly sloped and extends for two-thirds of the width of the proximal end. The angle formed is acute, a feature dissimilar to most sauropodomorphs but similar to *Yunnanosaurus* (Lü, 2007), *Blikanasaurus* (Galton and van Heerden, 1998) and *Mussaurus* (Otero and Pol, 2013). The lateral side is steeply sloped and is one-third of the width of the proximal end. On the dorsal margin a ridge runs proximodistally to the midpoint of the shaft. The ventral surface of the distal end is largely concave in shape. The shaft's dorsal surface curves upward slightly toward the distal end. The ventral surface of the shaft is largely convex which follows through into an upturned distal end. The distal end is rounded.



Figure 3.10: Metatarsal 5 in dorsal (left) and ventral (right) view. Scale bar = 5cm

### Phalanges

The phalangeal formula of the pes is 2-3-4-5-1, this formula is seen in other early diverging sauropodomorphs. The phalanges have similar morphology to *Saturnalia*, *Lufengosaurus*, *Massospondylus*, *Adeopapposaurus*, and *Leyesaurus* where they are proximo-distally longer than transversely wide with a midpoint constriction to the shaft, however some of the distal phalanges are as wide as long. All the phalanges have an expanded ventral surface that are wider than the dorsal surface.

The first phalanx (Figure 3.11) of mt. 1, mt. 1.1 is roundly robust in its shape and proximodistally longer than it is mediolaterally wide. It is the longest of the phalanges as in *Lufengosaurus*. The proximal end is lateromedially wider than the distal end with a midpoint constriction, as with *Coloradisaurus*, *Adeopapposaurus*. The dorsal surface is relatively flat

while the ventral surface is concave distally. The distal articulation surface is trapezoidal in shape with the ventral margin wider than the dorsal margin. The condyles are well developed with deep collateral fossae.

The proximal phalanx mt. 2.1 (Figure 3.13) is missing most of the original bone surface due to weathering. It is dorsoventrally flattened in shape and proximodistally longer than it is mediolaterally wide, with a midpoint constriction. The proximal articulating surface is weathered, the surface is concave, and no intercondylar groove is present. The distal head is weathered and mildly distorted, the articulation surface is trapezoidal in shape with the ventral margin wider than the dorsal margin. The fossae are barely visible on what remains of the condyles. Mt. 2.2 (Figure 3.14) is not as elongated as the first phalanx and is narrower, a morphology also seen in *Coloradisaurus* but not in *Adeopapposaurus*. The proximal articulation surface is missing part of the bone surface and is weathered to a point that the shape of the articulation surface is mildly distorted. The proximal face is slightly rectangular in shape and is as broad as the distal end with a ventral and dorsal intercondylar process. The dorsal surface presents a proximal dorsal lappet, also present in *Adeopapposaurus*, and slopes downward distally. The ventral surface has a concave groove running the length of the phalanx. The distal articulation surface is trapezoidal in shape with the ventral margin wider than the dorsal margin. The condyles are well developed with deep collateral fossae and are more rounded in their shape, similar to *Coloradisaurus* but unlike the acute shapes seen in *Massospondylus* and *Adeopapposaurus*.

The proximal and subsequent phalanx mt. 3.1 and mt. 3.2 are co-joined in articulation (Figure 3.16). Mt. 3.1 is proximodistally longer than it is mediolaterally wide, with a midpoint constriction. The proximal end of mt. 3.1 is round with a shallow articulating surface; and no intercondylar ridge is present. The dorsal surface is flat and slopes distally and the ventral surface is concave. The distal end reveals robust condyles with weathered collateral fossae. Mt. 3.2 is proximodistally shorter in comparison to earlier phalanges; and the midpoint constriction is tighter on this element. The dorsal surface is flat and slopes distally and the ventral surface is strongly concave. The distal articulation surface is trapezoidal in shape with the ventral margin wider than the dorsal margin. The condyles are well developed with deep collateral fossae, in *Adeopapposaurus* the collateral fossae are less deep. The distal phalanx mt. 3.3 (Figure 3.17) is a stout and robust element with a tight midpoint constriction. The proximal end is slightly rounded in shape, a dorsal intercondylar process is present as well as an intercondylar ridge on the articulating surface. The dorsal surface is flat and slopes distally and the ventral surface has a concave groove running the length of the phalanx. This is unlike *Coloradisaurus* in which the third phalanx of mt. 3 and 4 are dorsoventrally low. The distal articulation surface is trapezoidal in shape with the ventral margin wider than the dorsal margin. The condyles are rounded, robust and well developed with visible collateral fossae. As in *Adeopapposaurus*, the lateral condyle is more developed than the medial condyle. Both mt. 3.2 and mt. 3.3 present dorsal lappets.

Mt. 4 has a phalanx count of 5, 4 non-terminal phalanges and an ungual, which is common in other early deriving sauropodomorphs. Three of the four phalanges (mt. 4.1, mt. 4.2, mt. 4.3) are co-joined in articulation (Figure 3.19). Mt. 4.1 is proximodistally longer than it is mediolaterally wide, with a weak midpoint constriction. The proximal end of mt. 4.1 is sub circular in shape, similar to *Adeopapposaurus* but unlike *Coloradisaurus* where it is subvoid

in shape. Its articulating surface is weathered with no intercondylar ridge present. On the proximal dorsal surface there are several shallow grooves created during fossil preparation. The dorsal surface is flat and slopes distally, the ventral surface is concave. The distal end presents two condyles and fossae. Mt. 4.2 is square in shape with a weak midpoint constriction. The distal articulating surface has a dorsal intercondylar process. The dorsal surface of the phalanx is relatively flat, the ventral surface is slightly concave. The distal head condyles are small with shallow intercondylar fossae. Mt. 4.3 is square in shape with a midpoint constriction. The distal articulating surface has a dorsal intercondylar process. The dorsal surface of the phalanx is relatively flat, like *Coloradisaurus*, while the ventral surface is slightly concave. The distal articulating surface is rectangular in shape in distal view with the ventral and dorsal margins being similar in their length. The articulation surface reveals an intercondylar groove. The distal condyles are small with shallow intercondylar fossae. Mt. 4.2 and mt. 4.3 and mt. 4.4 present dorsal lappets. The distal phalanx (mt. 4.4) and ungual (mt. 4.U) are co-joined in articulation (Figure 3.20). Mt. 4.4 is square in shape. The proximal articulating surface of mt. 4.4 is slightly concave with an intercondylar ridge present. A missing fragment on the dorsal ridge of the articulating surface suggests that there was a dorsal intercondylar process. The dorsal surface of the phalanx is relatively flat. The distal articulation surface is trapezoidal in shape with the ventral margin wider than the dorsal margin, the condyles are small with shallow intercondylar fossae, unlike *Adeopapposaurus* where the fossae are deep.

### **Ungual**

Mt. 1.U (Figure 3.12) is the largest and most robust of the pes. Mt. 2.U (Figure 3.15) and 3.U (Figure 3.18) are similar in size but markedly smaller than mt. 1.U. This is unlike *Coloradisaurus*, *Adeopapposaurus* and *Massospondylus* where mt. 3.U is notably smaller than those of digit 1 and 2. The unguals of mt. 1 – mt. 4 are all proximodistally longer than mediolaterally wide and have a sub-ovate outline in proximal view. The proximal articulating surfaces are deep with a noticeable intercondylar groove and an intercondylar dorsal lappet present. There are distinct concave ridges visible on the sides of the ungual sheath of mt. 1.U, mt. 2.U and mt. 4.U, these ridges are also seen in *Coloradisaurus*, *Adeopapposaurus* and *Massospondylus*. The distal tip of mt. 2.U and mt. 3.U is broken.

The ungual mt. 5 (Figure 3.21), as in most early sauropodomorphs, is a rounded kidney-bean shape, the dorsal surface curves ventrally while the ventral surface has a sharp concave midpoint.



*Figure 3.11: Phalanx 1 articulated with the proximal end of mt. 1 in dorsal (left) and ventral (right) view. Scale bar = 5cm*



*Figure 3.12: Ungual of mt. 1 in dorsal (left) and ventral (right) view. Scale bar = 5cm*



Figure 3.13: Phalanx 1 of mt. 2 in dorsal (left) and ventral (right) view. Scale bar = 5cm



Figure 3.14: Phalanx 2 of mt. 2 in dorsal (left) and ventral (right) view. Scale bar = 5cm

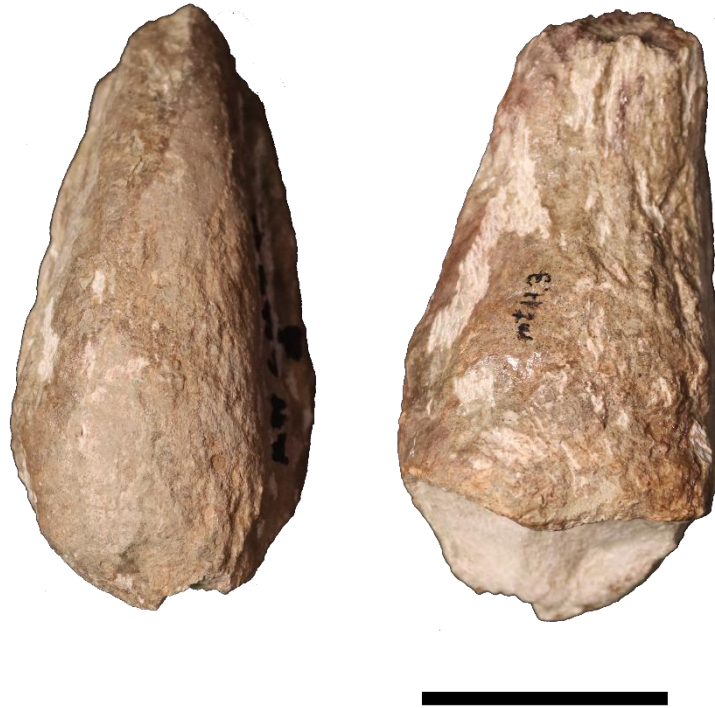


Figure 3.15: Ungual of mt. 2 in dorsal (left) and ventral (right) view. Scale bar = 5cm



Figure 3.16: Phalanx 1 and 2 of mt. 3 in articulation in dorsal (left) and ventral (right) view. Scale bar = 5cm



Figure 3.17: Phalanx 3 of mt. 3 in dorsal (left) and ventral (right) view. Scale bar = 5cm



Figure 3.18: Ungual of mt. 3 in dorsal (left) and ventral (right) view. Scale bar = 5cm



Figure 3.19: Phalanx 1, 2 and 3 of mt. 4 in articulation in dorsal (left) and ventral (right) view. Scale bar = 5cm



*Figure 3.20: Phalanx 4 and ungual of mt. 4 in articulation dorsal (left) and ventral (right) view. Scale bar = 5cm*



*Figure 3.21: Ungual of mt. 5 in lateral view. Scale bar = 2cm*

**Left astragalus (AM 6147-V (q)):**

An element originally labelled as 'presenting a predator tooth' is identified as a well preserved astragalus. There is no associated tooth with the element. The basic shape of the astragalus is plesiomorphic for early sauropodomorphs. The anterior outline is subtrapezoidal, the lateral margin is shorter than the medial. It is dorsoventrally thick, especially at the anteromedial corner. The dorsal surface has a raised portion in the anteromedial area extending upwards dorsally, this ascending process articulates with the tibia. The anteromedial process rises dorsally and is nearly double the height of the anterolateral corner, similar to *Adeopapposaurus*. The dorsal surface slopes posteroventrally from the anteromedial process, while the ventral surface is smooth and flat. The medial articulating surface is posteriorly sloped and has two slightly concave areas with a defined mid ridge. The ventral concavity of this surface is deeper than the dorsal concave surface. The lateral surface is rounded.

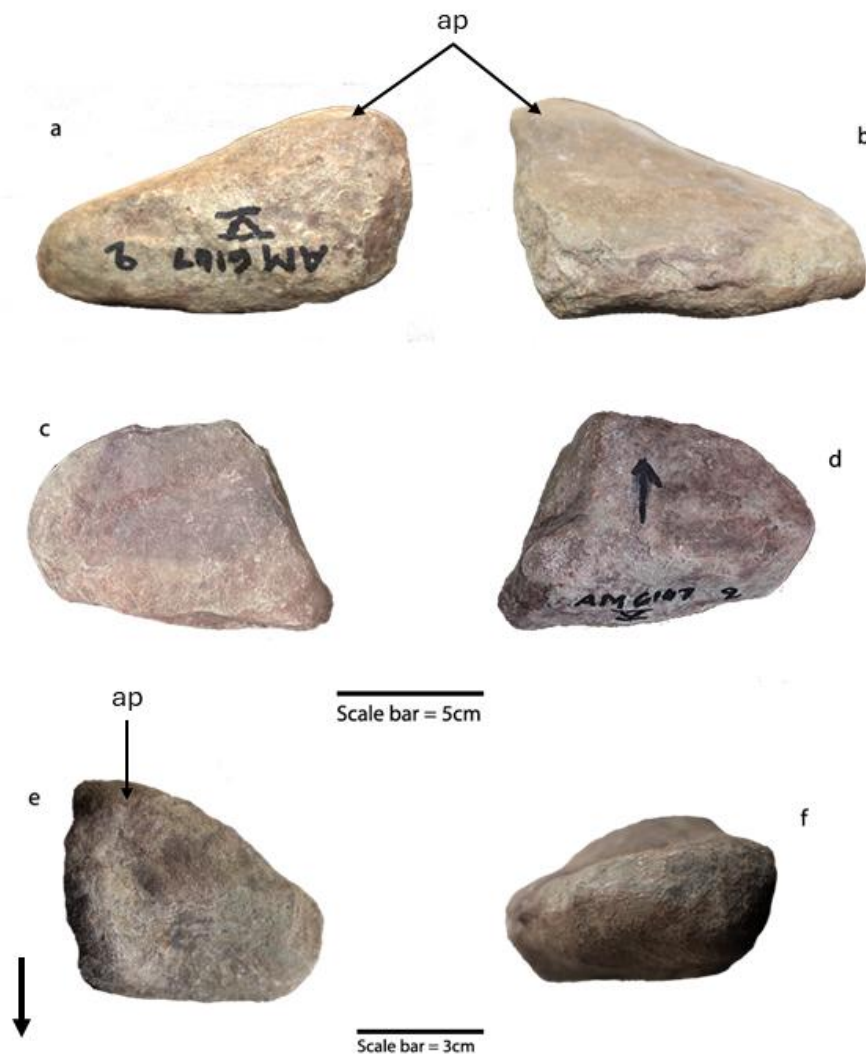


Figure 3.22: Left astragalus of (AM 6147-V), (a) anterior and (b) posterior view, (c) dorsal and (d) ventral view, scale bar = 5cm, and (e) medial and (f) lateral view, scale bar = 3cm. ap, anterior process. Thick arrow indicates ventral direction.

**Left calcaneum (AM 1647-V (c)):**

AM 6147-V (c) is identified as a very weathered calcaneum. It is subtriangular in shape and articulates tightly with the ventromedial face of the astragalus with a simple concave-convex joint. The posterior surface is largely misshapen leaving a very uneven and worn surface. The ventral and lateral surfaces are worn and slightly eroded. The dorsal surface has a slight concavity to it. The medial articulating face is relatively flat while the lateral face is rounded. The anterior surface is convex. As the element is heavily weathered, most identifiable features are not preserved.

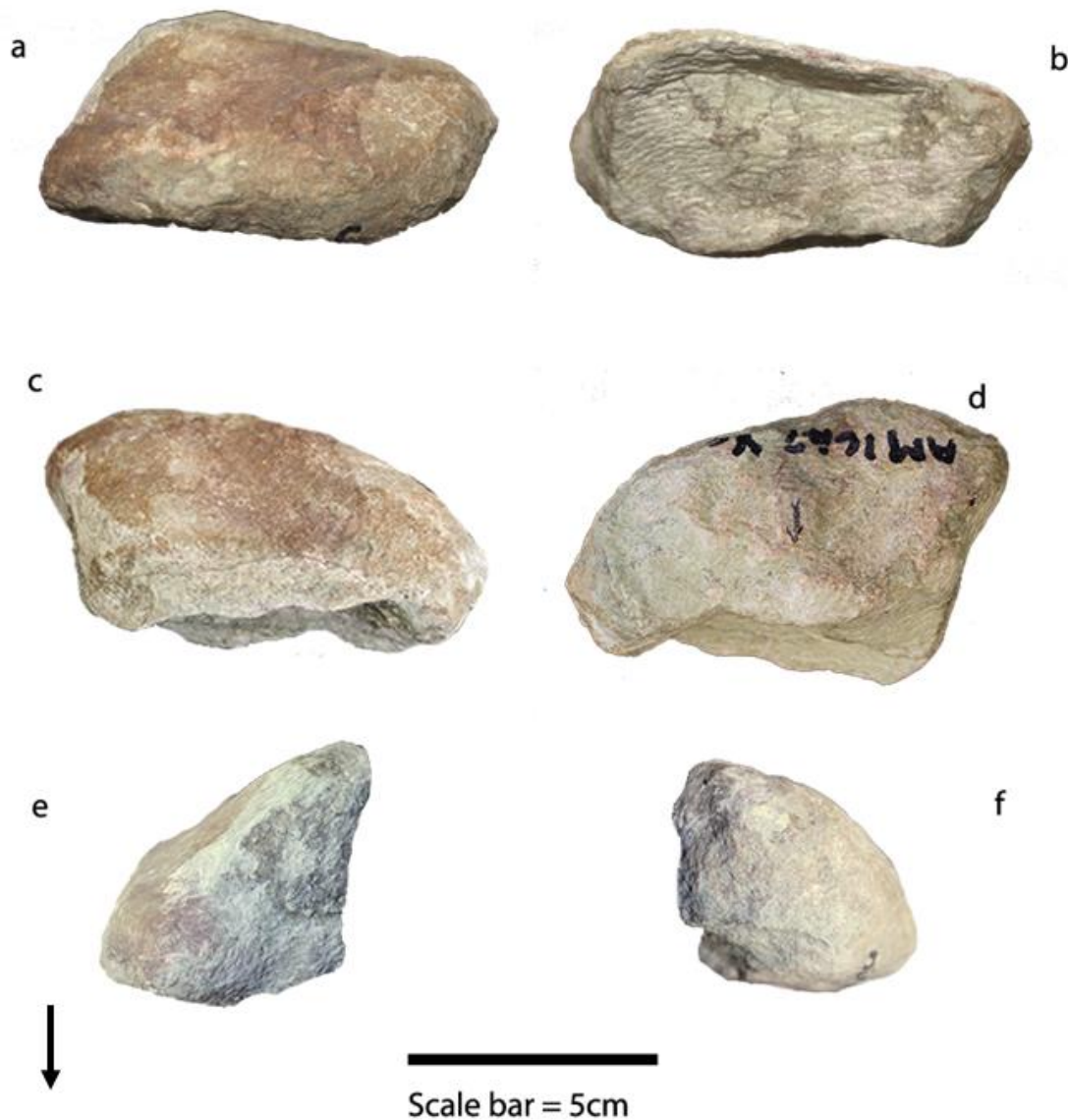


Figure 3.23: Left calcaneum of AM 6147, (a) anterior and (b) posterior view, (c) dorsal and (d) ventral view, (e) medial and (f) lateral view. Scale bar = 5cm. Arrow indicates ventral direction.

### 3.3 Description of carnivore teeth

#### **Carnivore tooth associated with the caudal series (AM 6147-I):**

The associated tooth is exposed lingually (Figure 2.3 & Figure 3.24). The crown measures 31.5mm in length and 14mm at its widest. This is similar in size to the third tooth of the premaxilla of *Dracovenator regenti* (Yates, 2005). The thickness and width of the tooth cannot be measured as the element sits within the matrix and is flush against a chevron. The crown is ziphodont in its shape. From what is visible of the shape of the tooth the mesial profile is slightly convex. The distal profile is slightly concave and gently curves distally along its length, and the tooth presents a weak basal depression, on the lingual surface – these descriptions are noted for most theropod teeth.

It is difficult to identify whether the tooth is a mesial or lateral tooth as it cannot be determined how broad the tooth is, nor can the mesial margin be described. The enamel can be seen to extend symmetrically on the mesial-distal margins of the crown.

The tooth possesses denticulate carinae, a morphology common in non-neotheropod Theropoda, Coelophysoidea, Dilophosauridae, Ceratosauria, non-spinosaurid Megalosauoidea, Allosauoidea, non-tyrannosaurid Tyrannosauoidea, Compsognathidae, and Dromaeosauridae (Hendrickx *et al.*, 2015). The carina begins at the base of the crown and extends along the entire distal margin. The carina margin is centrally positioned on the distal margin, the basal mesial margin sits underneath the chevron and is not visible. The apical region is gently curved and has serrated carinae on both the mesial and distal profiles.

The denticles are subrectangular in shape with the length shortening in a smooth transition into a square shape closer to the cap of the tooth. The denticle count is 11 per 5mm, this is 4 less than in the recovered *Dracovenator's* premaxillary teeth. The interdenticular sulci for the distal profile are straight in curvature and incline horizontally, the space between each serration is both shallow and narrow.

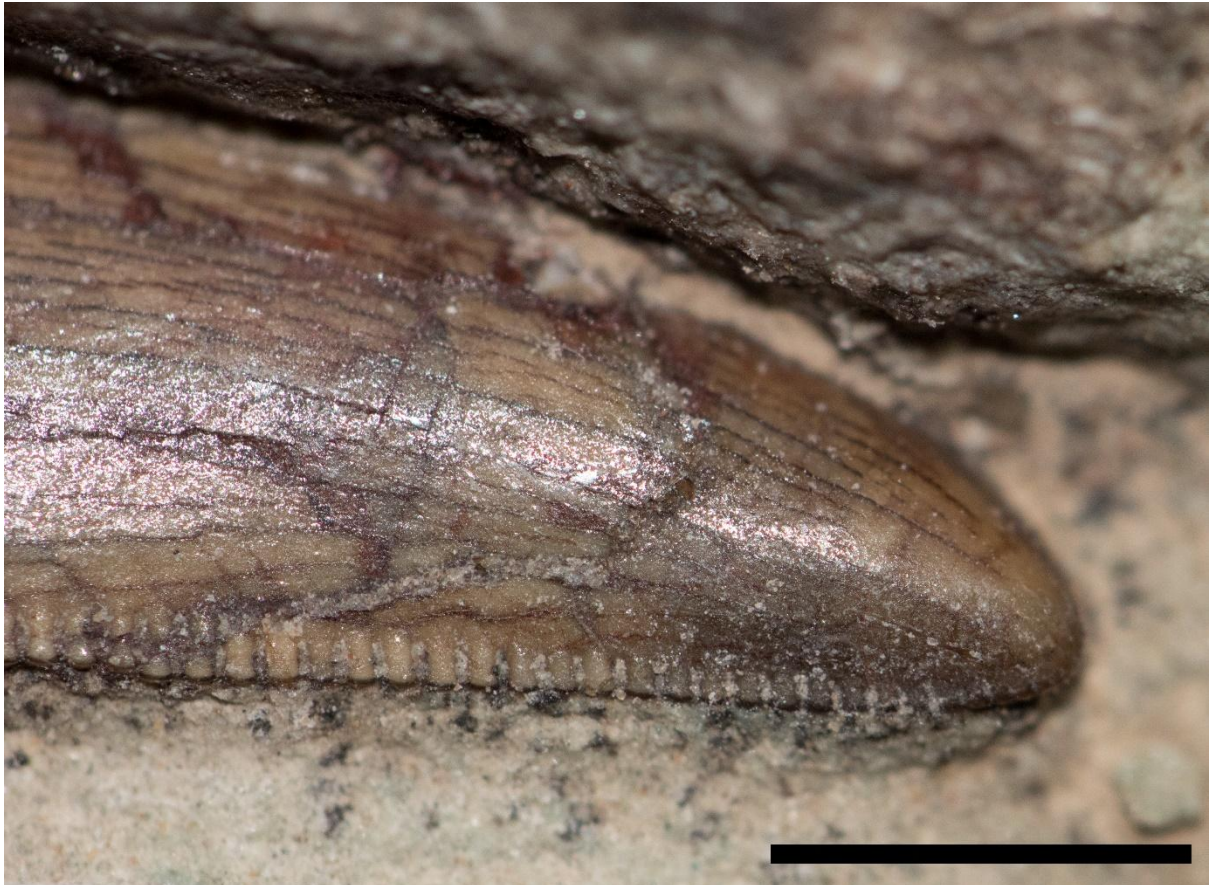


*Figure 3.24: Associated predator tooth with distal denticles alongside CV-1's chevron of AM 6147. Scale bar = 5mm.*

**Isolated well preserved predator tooth (AM 6147-V (r))**

The tooth is isolated in its own small matrix block (Figure 2.10). It was found in association with the gastralia of AM 6147-III (Choiniere, 2013). A CT scan reveals the crown to be conodont in shape. The cross-section outline of the crown base is oval in shape.

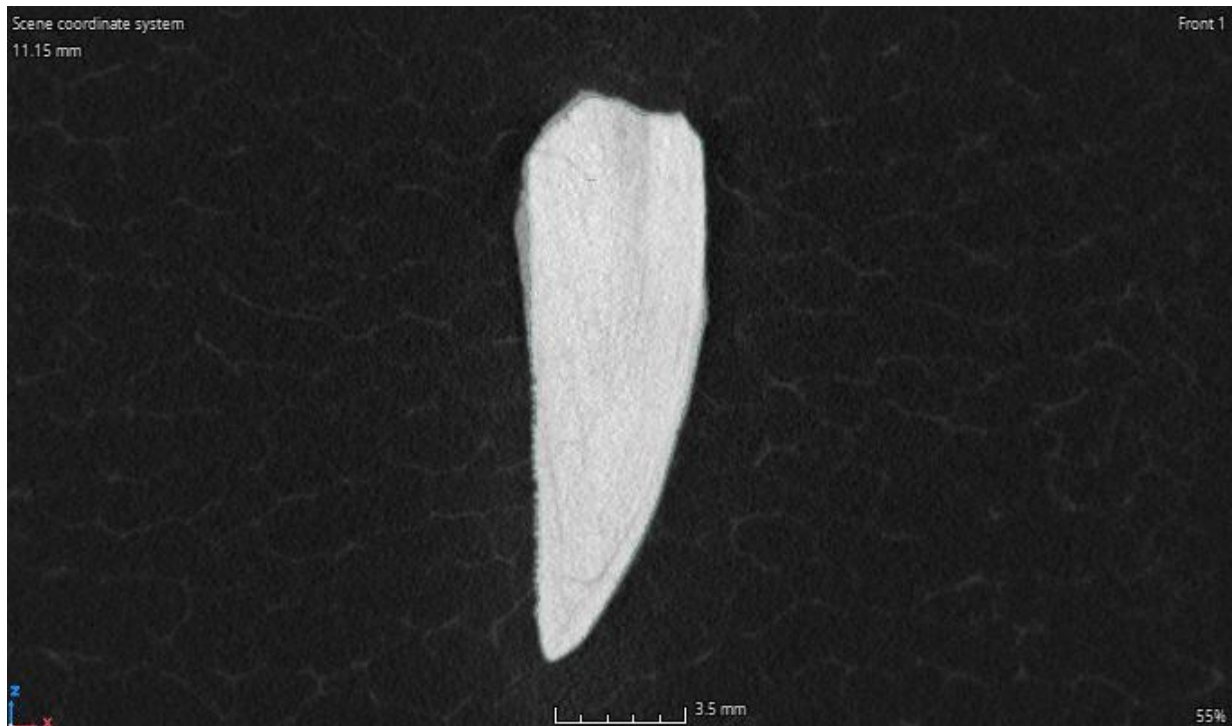


Figure 3.25: CT scan of the crown of AM 6147-V (r) in vertical cross section.

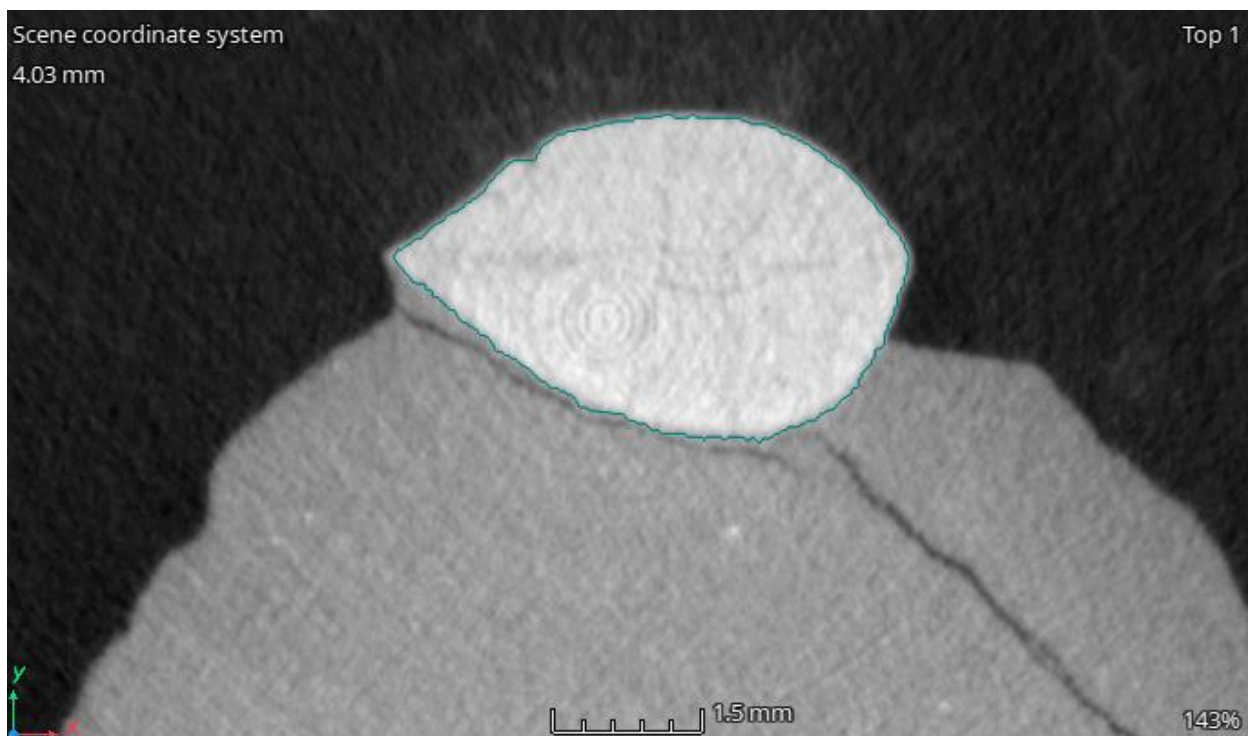


Figure 3.26: CT scan of the crown of AM 6147-V (r) in transverse cross section oval in shape.

The mesial profile is slightly concave while the distal profile is almost planar in its curvature. The tooth has a slight recurve. The tooth presents a weak basal depression on the lingual/labial surface. The enamel can be seen to extend symmetrically on the crown (Figure 3.27) while the carinae is centrally positioned on the distal and mesial margin. The denticles are in a straight orientation and are positioned on the entire length of the distal margin but only seen partially along the mesial margin. The inconsistent serrations on the mesial profile of the tooth may be due to weathering. Denticles can be seen on the apical portion of the mesial profile, further up the mesial profile marks from weathered/lost denticles are visible, this extends basally up the profile until regular, but weathered, denticles are visible closer to the cervix. This ziphodont dentition is also present in basal archosaurs (Hendrickx *et al.*, 2015). The denticles present are square in shape.



Figure 3.27: Predator tooth AM 6147-V (r). en, enamel. Scale bar = 0.5cm (5mm).

The tooth measures 16mm in length and is 5.2mm at its widest region. The denticle count is 19 per 5mm, this count is 9 more than *Sphenosuchus acutus*, but only 1 less than *Redondavenater* (Nesbitt *et al.*, 2005). The interdenticular sulci for the distal profile are straight in curvature and incline horizontally, the space between each serration is both deep and large.

The tooth is recovered as belonging to Crocodylomorpha.

**Isolated poorly preserved predator tooth (AM 6147-V (s)):**

The tooth is isolated in its own small matrix block, it is very weathered and poorly preserved (Figure 2.11). As with the tooth above, it was also found in association with the gastralia of AM 6147 III (Choiniere field notes, 2013). A CT scan suggests the crown is ziphodont in shape, however the labial side of the tooth, within the matrix, is very poorly preserved, this makes accurately describing the tooth's shape unattainable. The exposed tooth is very weathered, the enamel is flaky and only a small number of denticles from the mesial profile of the tooth are preserved and are square in shape. The tooth measures approximately 9.3mm in length and 4.2mm at its widest region. The denticle count is 5 per 1mm, this is 3-4 less than *Coelophys bauri* (Buckley, 2009).



Figure 3.28: Close up of the exposed labial surface and preserved mesial denticles of AM 6147-V (s). Scale bar = 1mm.

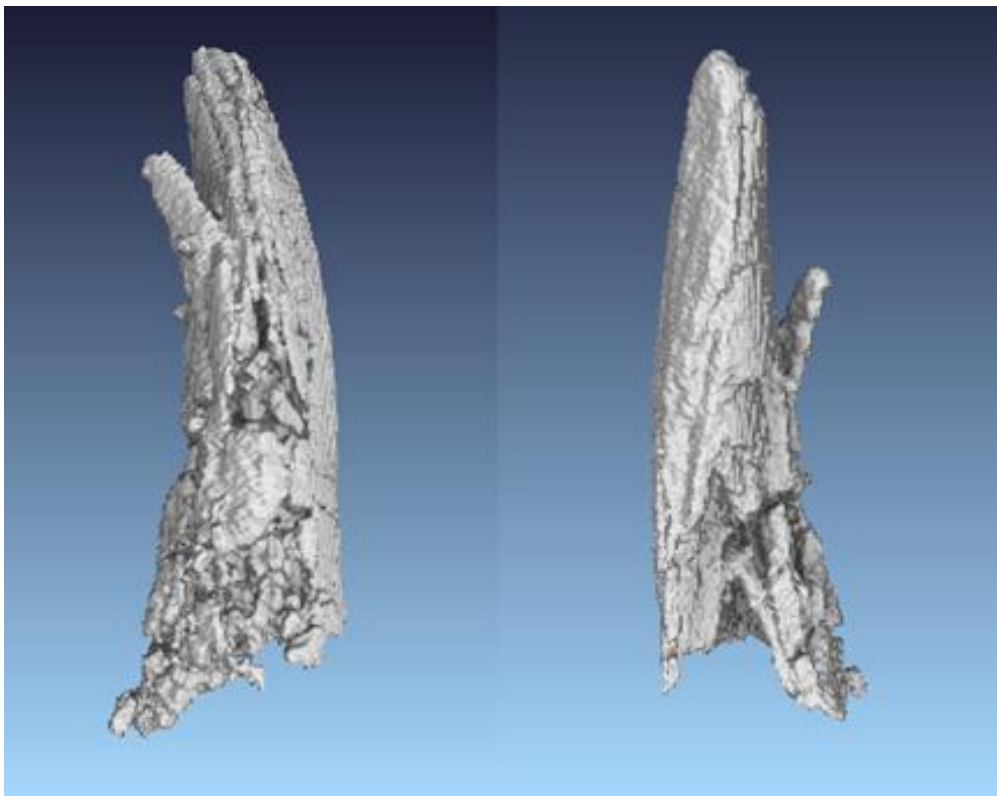


Figure 3.29: CT scan of the (left) mesial and (right) distal profile of AM 6147-V (s)

Due to the degraded state of the tooth it cannot be confidently assigned to a genus.

### 3.4 Phylogenetic position

The Ezcurra *et al* (2024) matrix included a total of 89 taxa and 421 characters. Of these characters 39 were identifiable for AM 6147: 13 were identified on the anterior vertebrae and 26 on the pes.

The initial heuristic search resulted in 70 most parsimonious trees (MPTs) of 1532 steps found in 8 out of 1000 replicates. A further round of TBR branch swapping of these 70 trees resulted in 3 744 MPTs of the same tree length (CI=0.307, RI= 0.671). Nodes within Sauropodomorpha generally have a Bremer support value no higher than 3, GC Bootstrap values are extremely low and rarely >50 (Figure C.1 & Figure C.2).

The strict consensus has large polytomies in the basal nodes of Sauropodomorpha, this was due to the instability of ten taxa due to character conflict and missing data identified using the IterPCR procedure (Pol and Escapa, 2009). Applying the IterPCR procedure implemented in TNT 1.6 (Goloboff *et al.*, 2008, Goloboff and Morales, 2023): the following taxa (10) are unstable and collapse nodes in the strict consensus: *Arcusaurus*, *Pradhania*, *Xixipiosaurus*, *Yizhousaurus*, *Camelotia*, *Isanosaurus*, *Amygdalodon*, *Volkheimeria*, *Barapasaurus* and *Patagosaurus*. These taxa were excluded *a posteriori* in a reduced strict consensus.

When the above-mentioned unstable taxa were excluded from the consensus *a posteriori*, a reduced strict consensus analysis recovered AM 6147 as the sister taxon to *Coloradisaurus*, *Glacialisaurus* and *Lufengosaurus*, within Massospondylidae (Figure 3.30).

The following taxa form polytomies in which all descendants are unstable: Node 130 of the strict consensus [*Anchisaurus* + *Lampughsauro* + *Mussaurus* (*Sefapanosaurus* + *Aardonyx*)]. These taxa were not excluded as it did not affect the resolution of the taxon under study and comprised far more derived Sauropodiforme taxa.

The position of AM 6147 corroborates with the results found in both the reduced strict consensus (Figure 3.30) and the majority rule 50 consensus (Figure C.4). In both of the consensuses AM 6147 is recovered as a sister taxon to *Coloradisaurus*, *Glacialisaurus* and *Lufengosaurus*.

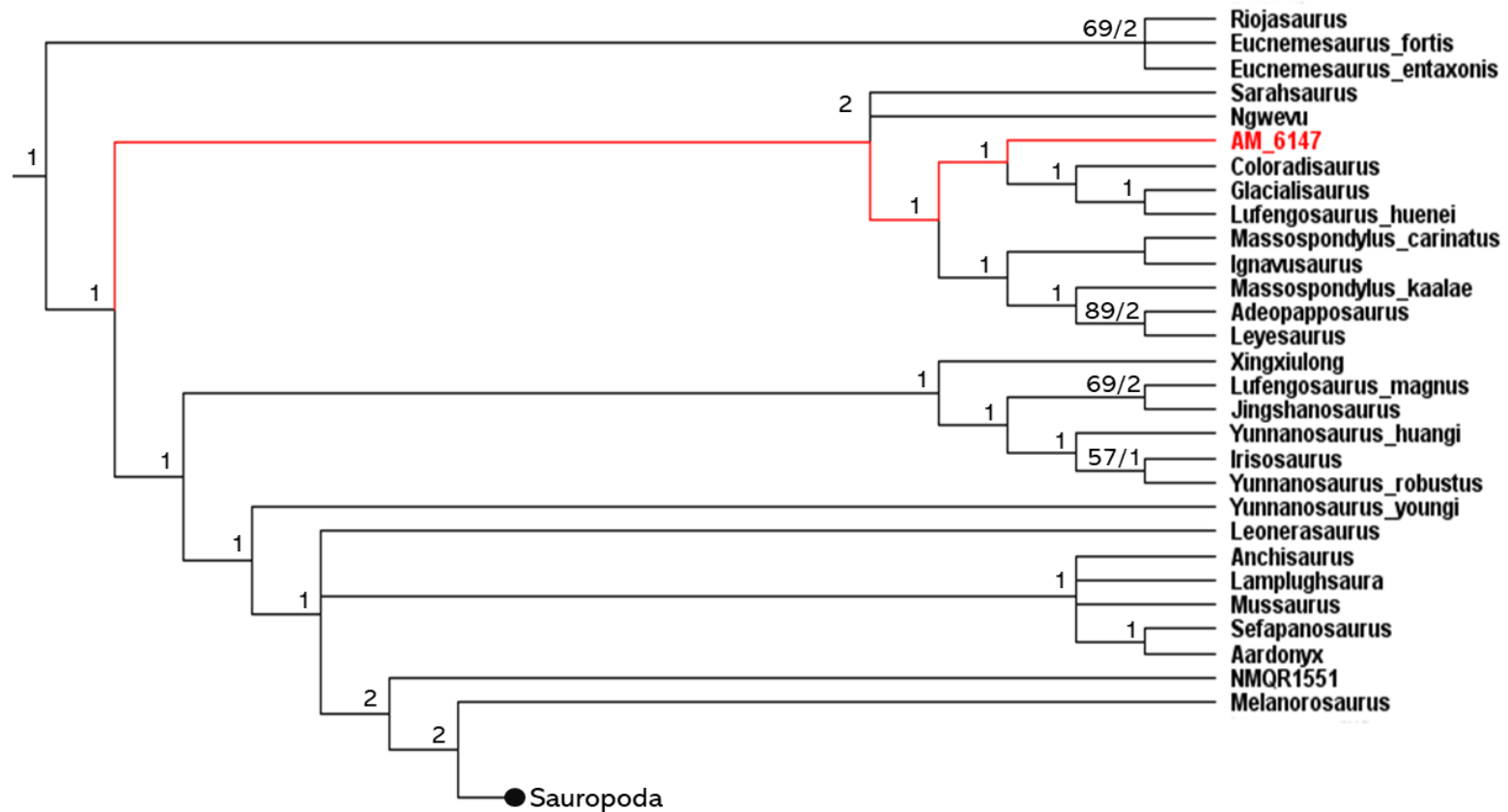


Figure 3.30: AM 6147 is recovered among Massospondylidae in a reduced strict consensus summary. 21842 MPTs with a tree length of 1697 steps tree (CI of 0,29 and a RI of 0,67), after ten unstable taxa; Arcusaurus, Pradhania, Xixipiosaurus, Yizhousaurus, Camelotia, Isanosaurus, Amygdalodon, Volkheimeria, Barapasaurus and Patagosaurus were excluded from the consensus. The single digit numbers represent Bremer support values, and the double-digit numbers represent the Bootstrap support values. Only sauropodomorph taxa are shown (for the complete consensus tree, including all taxa, see Figure C.3

## CHAPTER 4

## DISCUSSION

### 4.1 AM 6147

#### 4.1.1 Stratigraphic position

AM 6147 is among the stratigraphically highest, and thus youngest, sauropodomorphs of the Upper Elliot Formation, originating within the uppermost portion of the UEF approximately a metre below the overlying Clarens Formation. The UEF is dated to 201 Ma to 190 Ma, and includes the Hettangian and Sinemurian stages (Bordy *et al.*, 2020), with the Sinemurian being the last stage of the UEF before the recording of the CF. This indicates that AM 6147 would have lived during the Sinemurian, along with *Aardonyx*, *Massospondylus*, *Pulanesaura*, *Sefapanosaurus* and *Ledumahadi*, and was contemporary to the Antarctic *Glacialisaurus*, and Argentinian *Adeopapposaurus* and *Leoneosaurus* (Pol *et al.*, 2011). Of these previously described sauropodomorph taxa that share a similar stratigraphic position only the South African *Massospondylus*, the Antarctic *Glacialisaurus* and the Argentinian *Adeopapposaurus* belong to the same family.

#### 4.1.1 Phylogenetic affinities

The phylogenetic analyses recovers AM 6147 as a unique early diverging sauropodomorph within Massospondylidae (Figure 3.30). This diagnosis is based on a total of 39 characters across the pes and caudal vertebrae. Many synapomorphies are present in AM 6147 including; the dorsoposteriorly directed transverse processes on the caudal vertebrae, great length of the caudal neural spines, presence of a sulcus on the ventral surface of the caudal vertebrae, sloping orientation of the proximal head of mt. 1, some of the distal phalanges being as wide as long, the presence of a dorsomedial flange on mt. 4, and the acute angle of the anterior and anteromedial border of mt. 4. These mentioned features are considered as synapomorphies present in more derived sauropodiformes and even some Sauropoda such as *Pulanesaura* and *Tazoudasaurus*. As AM 6147 is recovered as an early deriving sauropodomorph the presence of this collection of derived features raises the question about the point at which these features become established. Thus, while AM 6147 is recovered as a massospondylid, it presents a unique combination of early diverging and several derived synapomorphies.

#### 4.1.3 Autapomorphies

AM 6147 displays a unique combination of synapomorphic and autapomorphic characters and presents five features that distinguishes it from all other known basal sauropodomorphs. Presented below is a list of the autapomorphic characteristics evident in AM 6147:

##### Metatarsal II

- 1- A small but distinct flange is present on the lateral dorsal surface midway down the shaft (Figure 4.1). This flange is not seen in any other sauropodomorphs.



Figure 4.1: Left Metatarsal II of AM 6147 in dorsal view (a), lateroventral view (b), and ventral view (c). f, flange. Arrow indicates distal direction. Scale bar = 5cm

- 2- The proximal medial surface of M2 is deeply concave (Figure 4.2), this exaggerated concavity is not seen in other Massospondylidae. This characteristic still adheres to the typical hourglass shape that is often observed in sauropodomorphs; however, this concavity is not as pronounced in other Massospondylidae as it is in AM 6147.
- 3- The very large ventromedial flange (Figure 4.2) is much more robust than the flange present in other Massospondylidae such as *Lufengosaurus*, *Massospondylus*, *Glacialisaurus*, *Adeopapposaurus* and *Coloradisaurus*.



Figure 4.2: Left Metatarsal II of AM 6147 in proximal view. Emf, extended medioventral flange. Arrow indicates medial direction. Scale bar = 5cm.

#### Metatarsal IV

- 4- The shaft reveals a prominent concave groove on the dorsal surface (Figure 4.3). The feature is proximally mediolaterally wide and extends proximodistally before narrowing distally and stopping just before the distal head. This concave groove is not seen in any other sauropodomorphs.



Figure 4.3: Left Metatarsal IV of AM 6147. Dorsal view (a), medial view (b), lateral view (c). f, flange; c, concave groove. Scale bar = 3cm.

## Transverse process

- 5- The dorsoposterior directed transverse process of AM 6147 is not commonly seen in sauropodomorphs (besides *Adeopapposaurus*) and is rather recorded as a possible autapomorphy in later branching sauropodomorphs such as *Pulanesaura* (Moopen *et al.*, 2023). The lateral tip curves further dorsally and posteriorly (Figure 4.4 & Figure 4.5), this exaggerated curvature is not seen in other sauropodomorphs.



Figure 4.4: Dorsoposteriorly directed transverse process in dorsal view on the lateral side of the caudal centrum. Transverse process, tp; neural spine, ns. Arrow indicates the posterior direction. Scale bar = 4cm

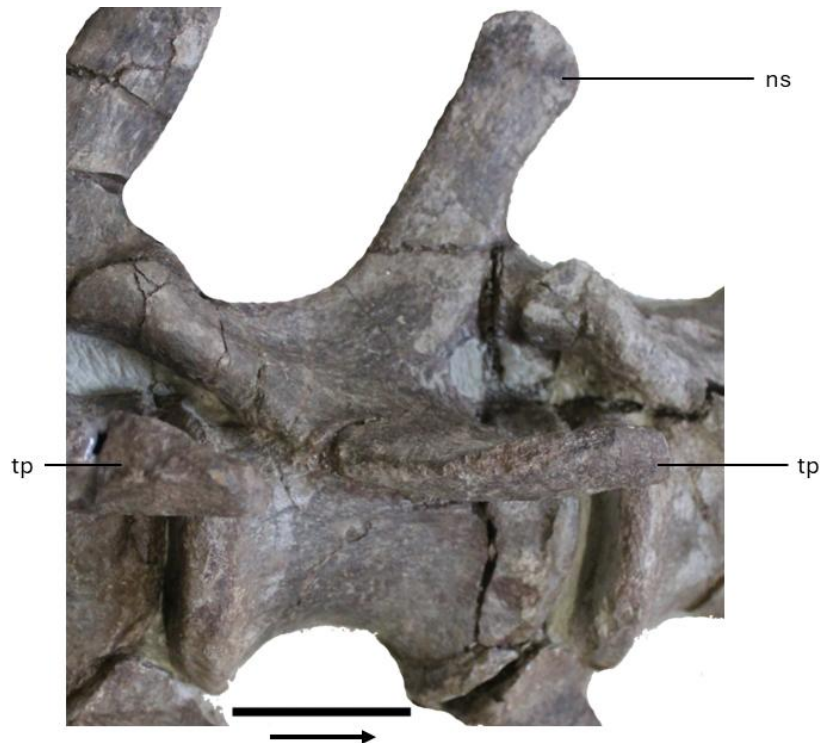


Figure 4.5: Dorsoposteriorly directed transverse process in lateral view on the lateral side of the caudal centrum. Transverse process, tv; neural spine, ns. Arrow indicates the posterior direction. Scale bar = 4cm

Although the phylogenetic analysis recovers AM 6147 as a massospondylid the specimen reveals further synapomorphies which have been described in much more derived sauropodomorphs. Thus, it is evident that AM 6147 cannot be referred to any previously mentioned genera as the specimen can be readily differentiated from other UEF taxa by a series of autapomorphies and a unique combination of characters.

#### **4.1.4 Overview of AM 6147**

The well-worn articular surfaces and well-developed condyles of the metatarsals and the fusion of neural arches of vertebrae to their centra suggest that AM 6147 was a mature dinosaur rather than a juvenile.

AM 6147 is much larger than the South African massospondylid *Massospondylus*, as seen by the pes comparisons in Table 3.2 & Figure B.1. The specimen is also larger than most other Early Jurassic massospondylids in both caudal vertebrae and metatarsals measurements, except for *Glacialisaurus*. Unfortunately, there is a lack of published data regarding the vertebral elements of *Glacialisaurus*, which limits the comparison to the pes. Furthermore, the pes material is also incomplete due to incomplete bone elements. AM 6147 has similar, and/or somewhat smaller, metatarsal measurements when compared to *Glacialisaurus* (Table 3.3), however given that the measurements suggest a resemblance in size, AM 6147 can be considered a large bodied massospondylid of the Early Jurassic.

The comparison of AM 6147's metatarsals to other, more derived Sauropodomorpha (Table 3.4) indicated that AM 6147 did indeed exhibit a large body size. Within this comparison, AM 6147 is most comparable in size to NMQR 1705 and *Antetonitrus*; however, it surpasses both specimens in the measurement of the total length of mt. 1, indicating that AM 6147 can be regarded as large even among sauropodiformes.

A thorough examination of the comparative size data pertaining to the metatarsals and caudal vertebrae of various Early Jurassic Sauropodomorpha indicates that AM 6147 is markedly larger than most other members of the Massospondylidae family, as well as some sauropodiformes. The considerably large size of AM 6147 provides a compelling justification for its nomenclature, *Enkulusaura*, from the isiXhosa word meaning 'big' or 'large' (see Etymology on page 26).

### 4.1.5 Pathology

#### Gastralia

The gastralia of AM 6147 have an unusual 'S' shape and have extended processes: this shape and process are not seen in other sauropodomorphs. As gastralia are generally not noted as having any distinguishing features, the odd shape of gastralia 5 and the thickened mid-section and extended process of gastralia 6 (Figure 4.6) could possibly be pathological. Further analysis (possibly using CT scanning) and histological analyses could help resolve whether this is indeed a unique characteristic of AM 61247 or pathological.

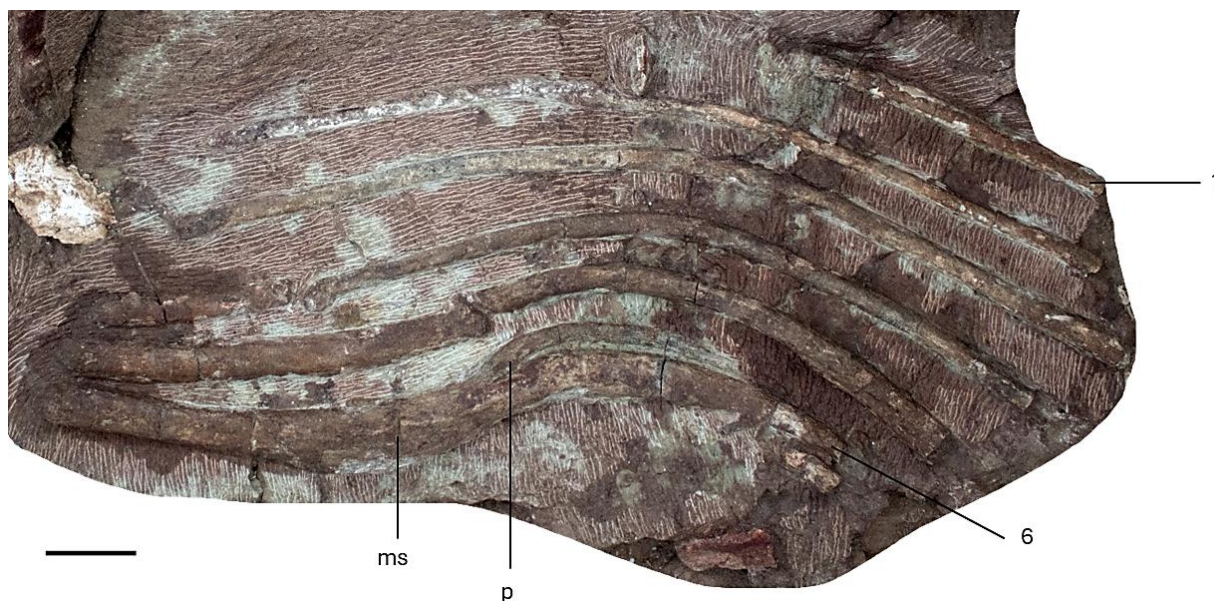


Figure 4.6: Gastralia of AM 6147. *ms*, mid-section; *p*, process. Scale bar = 10cm

### 4.2 Associated carnivore teeth

Within the stratigraphic layer of the UEF there are described Theropoda including *Megapnosaurus* and *Dracovenator*, and Crocodylomorpha including *Sphenosuchus*, *Litargosuchus*, *Orthosuchus*, *Notochampsia* and *Protosuchus*.

The morphological features present in the associated teeth suggests that they belong to different archosaurians, most likely Theropoda and Crocodylomorpha. The larger of the teeth is likely to be from a theropod, whilst one of the smaller teeth (*r*) is likely from a crocodylomorph. The third tooth (*s*) is poorly preserved and could either belong to a theropod or a crocodylomorph.

#### AM 6147-I (associated tooth):

The ziphodont shape of the tooth indicates that the tooth (Figure 2.3 & Figure 3.24) is likely from a theropod dinosaur. However, the denticle count of 11 per 5m does not match any of the known theropods of the UEF. The tooth shape and size resemble that of *Dracovenator* but differs from it in terms of its denticle count. Since the tooth is neither like *Megapnosaurus* nor identical to *Dracovenator*, it is possible that the tooth may represent an undescribed theropod from the UEF.

**AM 6147-V (r):**

The conodont shape of the tooth (Figure 2.10) suggests that it possibly belongs to a crocodylomorph. The tooth does not match any of the known crocodylomorphs or theropods of the UEF, however the denticle count is similar to sphenosuchian *Redondavenater*, while the tooth shape and size resembles that of *Sphenosuchus acutus*.

**AM 6147-V (s):**

The poor preservation of the tooth (Figure 2.11 & Figure 3.29) hinders its taxonomic identification. The suggested ziphodont shape of the tooth may indicate that it belonged to a small theropod. The shape and size of the tooth is similar to theropods such as, *Megapnosaurus rhodesiensis* and *Coelophysis bauri*. The features on this tooth suggest that it could belong to either a small crocodylomorph or to a small theropod.

## CHAPTER 5 CONCLUSION

### 5.1 Outcome of the current study

*Enkulusaura deklerki* is recovered as a new early branching sauropodomorph, within Massospondylidae, from the later Sinemurian of the UEF of South Africa.

Taxonomic and morphological comparisons between early branching sauropodomorph taxa and *E. deklerki* reveals many anatomical similarities to other Massospondylidae of the UEF. However, *E. deklerki* is much larger and more robust than *Massospondylus*, its sister taxa and many other Massospondylidae - as well as some Early Jurassic sauropodiformes. It is evident that *E. deklerki* has autapomorphic features that suggest it is a unique taxon. This mixture of synapomorphies of early and later deriving sauropodomorphs suggests that much like *Pulanesaura*, *E. deklerki* was a transitional sauropodomorph. As many of the so called “derived” features, are present in what is recovered an early diverging sauropodomorph, this suggests that some of these characteristics are in fact more basal in their origin and in the evolution of sauropodomorphs. This suggestion of feature appearance and evolution being more basal and continuous challenges some of the clear-cut diverging versus diverged synapomorphies mentioned in Galton and van Heerden (1998), Allain and Aquesbi (2008), Otero et al (2016 & 2020) and Apaldetti et al (2021).

It may imply that ‘derived features’ began to appear in sauropodomorphs much earlier than previously understood and may have been incentivised by the trajectory towards increased body size and quadrupedality seen in the Jurassic among Sauropodomorpha. It is also important to acknowledge that early diverging branches evolved into their own distinct families and unique genera, and that the “derived” Sauropoda clade does not signify a teleological endpoint, instead it constitutes a further stage in the persistent evolutionary process and divergence of sauropodomorphs.

*E. deklerki*'s placement amongst Massospondylidae is further consolidated by the phylogenetic analysis which recovered it as a sister taxon to 3 known massospondylid taxa; *Coloradisaurus*, *Glacialisaurus* and *Lufengosaurus*.

In summary, no known UEF sauropodomorph taxon has identical anatomical features to *E. deklerki*. Thus, *E. deklerki* is considered to represent a previously unknown and new genus and species, until additional morphological and phylogenetical information is recovered.

The three associated carnivore teeth in association with *E. deklerki* provides some understanding of the ecology of the UEF. Until now, there has been no fossilised evidence that these carnivores scavenged or had an ecological relationship with the contemporaneous sauropodomorph dinosaurs. Interestingly, although the teeth are directly associated with *E. deklerki*, there are no serrations and/or puncture marks visible on the skeletal remains, this might suggest that the carnivores were more flesh eaters than bone crunchers. However, due to the intimate association of the teeth to the dinosaur remains, it is highly likely that they had an ecological relationship: either as scavengers or as active predators.

### 5.1.1 The taxonomic validity and phylogenetic affinity of AM 6147

*Hypotheses tested in this study (see Hypotheses on page 10):*

**Hypothesis 1** - AM 6147 will be recovered as an early branching sauropodomorph.

**Hypothesis 2** - AM 6147 will be recovered as a massospondylid.

Comparisons between early branching sauropodomorph taxa and AM 6147 reveal taxonomic and morphological similarities. The phylogenetic analysis finds that AM 6147 is recovered as an early branching sauropodomorph.

Thus, **Hypothesis 1** is valid.

The specimen shows anatomical similarities to other Massospondylidae. Phylogenetic analysis recovers AM 6147 within Massospondylidae as the sister taxon to *Coloradisaurus*, *Glacialisaurus* and *Lufengosaurus*.

Thus, **Hypothesis 2** is valid.

### 5.1.2 The taxonomic identification of the associated carnivore teeth

*Hypotheses tested in this study (see Hypotheses on page 10):*

**Hypothesis 3** - The 3 carnivore teeth will belong to archosauromorph and/or crocodylomorph taxa.

**Hypothesis 4** - The associated carnivore teeth will indicate a scavenging/predator-prey dynamic.

The analysis of the three carnivore teeth indicates the presence of two distinct taxa, namely Theropoda and Crocodylomorpha.

**Hypothesis 3** is partially supported. It was anticipated that the two smaller teeth, AM 6147-V (r) and AM 6147-V (s), would belong to the same crocodylomorph taxa. Tooth AM 6147-V (r) has been confirmed as belonging to Crocodylomorpha, however a genus cannot be identified. Tooth AM 6147-V (s) is too degraded to accurately identify to which animal it may belong, but the tooth generally appears to be archosaurian. It was anticipated that the larger tooth, associated with the caudal series, would belong to an archosauromorph. However, analysis of its shape and serrations, suggest that it is likely to have belonged to an unknown theropod dinosaur from the UEF.

The close association of the teeth to the skeleton suggested that the remains may show damage caused by the carnivore teeth, such as tooth marks and puncture marks, however there were no tooth marks or puncture marks visible on the exposed surfaces of the bones of AM 6147.

**Hypothesis 4** is partially supported. There is no clear evidence of the carnivores feasting on the sauropodomorph, however the close association of the teeth to the skeletal remains suggests that there may have been some form of ecological relationship.

### 5.1.3 Synthesis of the findings

The findings of this study confirm the taxonomic validity of AM 6147 as an early diverging sauropodomorph, with phylogenetic analysis recovering it as a member of the Massospondylidae family. Taxonomically AM 6147 presents morphological similarities to other early branching sauropodomorphs of the Early Jurassic. The phylogenetic analysis recovers AM 6147 as a new taxon, *Enkulusaura deklerki*, within Massospondylidae by virtue of five autapomorphic features.

The larger of the 3 teeth (Figure 2.3), associated with the caudal series, is identified as belonging to Theropoda. The two smaller teeth (Figure 2.10 & Figure 2.11), associated with the gastralia of AM 6147-III are identified as belonging to Crocodylomorpha taxa, however AM 6147 – V (s) (Figure 2.11) is too degraded to allow for a confident identification of its genus but appears to be archosaurian. The larger of the 3 teeth is tentatively identified as belonging to an unknown theropod of the UEF, while the two smaller teeth cannot be identified to a species level within this study.

## 5.2 Future work

Revisiting the AM 6147 excavation site may recover more material for further study. The prospecting visit to the site in early 2024 revealed more caudal vertebrae exposed at the surface, as well as other *in situ* fragments of bone. It is possible that further excavations may reveal additional bone elements which would add to the known skeletal material.

Higher resolution scanning and perhaps new comparative specimens may reveal more precise taxonomic identification of the associated teeth of the predators.

In addition, should permission be granted to fully prepare one or more vertebrae, a more complete diagnosis may reveal further anatomical characteristics of *Enkulusaura deklerki*.

## 5.3 Limitations

One of the biggest challenges faced during this study was the lack of permission to fully prepare the elements from the matrix. Of the vertebrae/chevrons available, all 8 are still embedded in the matrix, and an application to remove one or more was denied by the Curator at the Albany Museum. As permission to further prepare the associated teeth was granted on condition they were not removed entirely from the matrix, more of the carinae on AM 6147-V (r) and the larger tooth associated with the caudal series in AM 6147-I was exposed, however as they were still within the matrix describing their full shape was still not possible. We tried to get around the problem of the teeth still within the matrix, by CT scanning, however only two of the teeth were small enough to scan, AM 6147-V (r) and AM 6147-V (s). The largest of the teeth, associated with jacket AM 6147-I, was partially situated underneath a chevron, and the matrix block was too large to scan, this tooth could not be fully described.

Another limitation was the missing bone elements. The associated femur is said to have been stolen during excavation, while the tibia and fibula excavated and found in association with the pes have been lost during transport or mislaid in the museum collection.

Lastly, some preserved elements were uninformative for this study as they were either too small and/or fragmentary.

## REFERENCES

- ALLAIN, R. & AQUESBI, N. 2008. Anatomy and phylogenetic relationships of *Tazoudasaurus naimi* (Dinosauria, Sauropoda) from the late Early Jurassic of Morocco. *Geodiversitas*, 30, 345-424.
- APALDETTI, C., MARTINEZ, R. N., ALCOBER, O. A. & POL, D. 2011. A new basal sauropodomorph (Dinosauria: Saurischia) from Quebrada del Barro Formation (Marayes-El Carrizal Basin), northwestern Argentina. *PLoS One*, 6, e26964.
- APALDETTI, C., POL, D., OTERO, A. & MARTÍNEZ, R. N. 2021. Triassic sauropodomorph dinosaurs from South America: The origin and diversification of dinosaur dominated herbivorous faunas. *Journal of South American Earth Sciences*, 107, 103145.
- APALDETTI, C., POL, D. & YATES, A. 2013. The postcranial anatomy of *Coloradisaurus brevis* (Dinosauria: Sauropodomorpha) from the Late Triassic of Argentina and its phylogenetic implications. *Palaeontology*, 56, 277-301.
- BARRETT, P. M. 2009. A new basal sauropodomorph dinosaur from the upper Elliot Formation (Lower Jurassic) of South Africa. *Journal of Vertebrate Paleontology*, 29, 1032-1045.
- BARRETT, P. M., CHAPELLE, K. E., STAUNTON, C. K., BOTHA, J. & CHOINIÈRE, J. N. 2019. Postcranial osteology of the neotype specimen of *Massospondylus carinatus* Owen, 1854 (Dinosauria: Sauropodomorpha) from the upper Elliot formation of South Africa. *Palaeontologia africana*, 53, 114-178.
- BARRETT, P. M. & CHOINIÈRE, J. N. 2024. *Melanorosaurus readi* Haughton, 1924 (Dinosauria, Sauropodomorpha) from the Late Triassic of South Africa: osteology and designation of a lectotype. *Journal of Vertebrate Paleontology*, e2337802.
- BENTON, M. J. 2004. Origin and relationships of Dinosauria. *The dinosauria*, 2, 7-19.
- BENTON, M. J. & CLARK, J. 1988. Archosaur phylogeny and the relationships of the Crocodylia. *The phylogeny and classification of the tetrapods*, 1, 295-338.
- BODENHAM, E. H. & BARRETT, P. M. 2020. A new specimen of the sauropodomorph dinosaur *Ignavusaurus rachelis* from the Early Jurassic of Lesotho. *Palaeontologia africana*, 54: 2019-2020.
- BORDY, E. & ERIKSSON, P. G. 2015. Lithostratigraphy of the Elliot Formation (Karoo Supergroup), South Africa. *South African Journal of Geology*, 118, 311-316.
- BORDY, E. M., ABRAHAMS, M., SHARMAN, G. R., VIGLIETTI, P. A., BENSON, R. B. J., MCPHEE, B. W., BARRETT, P. M., SCISCIO, L., CONDON, D., MUNDIL, R., RADEMAN, Z., JINNAH, Z., CLARK, J. M., SUAREZ, C. A., CHAPELLE, K. E. J. & CHOINIÈRE, J. N. 2020. A chronostratigraphic framework for the upper Stormberg Group: Implications for the Triassic-Jurassic boundary in southern Africa. *Earth-Science Reviews*, 203, 103120.

- BROOM, R. 1904. II.—On a New Crocodylian Genus (*Notochampsia*) from the Upper Stormberg Beds of South Africa. *Geological Magazine*, 1, 582-584.
- BROOM, R. 1927. On *Sphenosuchus*, and the Origin of the Crocodiles. *Proceedings of the Zoological Society of London*, 97, 359-370.
- BUCKLEY, L. G. 2009. *Individual and ontogenetic variation in theropod dinosaur teeth: a case study of Coelophysis bauri (Theropoda: Coelophysoidea) and implications for identifying isolated theropod teeth*. University of Alberta Edmonton, Alberta, Canada.
- BUSBY III, A. B. & GOW, C. 1984. A new protosuchian crocodile from the Upper Triassic Elliot Formation of South Africa.
- CABREIRA, S. F., SCHULTZ, C. L., BITTENCOURT, J. S., SOARES, M. B., FORTIER, D. C., SILVA, L. R. & LANGER, M. C. 2011. New stem-sauropodomorph (Dinosauria, Saurischia) from the Triassic of Brazil. *Naturwissenschaften*, 98, 1035-1040.
- CATUNEANU, O., WOPFNER, H., ERIKSSON, P. G., CAIRNCROSS, B., RUBIDGE, B. S., SMITH, R. M. H. & HANCOX, P. J. 2005. The Karoo basins of south-central Africa. *Journal of African Earth Sciences*, 43, 211-253.
- CERDA, I. A., CHINSAMY, A., POL, D., APALDETTI, C., OTERO, A., POWELL, J. E. & MARTÍNEZ, R. N. 2017. Novel insight into the origin of the growth dynamics of sauropod dinosaurs. *PloS one*, 12, e0179707.
- CHAPELLE, K. E. J., BARRETT, P. M., BOTHA, J. & CHOINIÈRE, J. N. 2019. Ngwevu intloko: A new early sauropodomorph dinosaur from the Lower Jurassic Elliot Formation of South Africa and comments on cranial ontogeny in *Massospondylus carinatus*. *PeerJ (San Francisco, CA)*, 2019, e7240-e7240.
- CHINSAMY-TURAN, A. 2024. *Megapnosaurus rhodesiensis*. *Nature Ecology & Evolution*, 8, 2151-2151.
- CHOINIÈRE, J. N. 2013. Elliot Sauropodomorph Fieldnotes.
- CLARK, J. M. 1986. *Phylogenetic relationships of the crocodylomorph archosaurs*. The University of Chicago.
- CLARK, J. M. & SUES, H.-D. 2002. Two new basal crocodylomorph archosaurs from the Lower Jurassic and the monophyly of the Sphenosuchia. *Zoological Journal of the Linnean Society*, 136, 77-95.
- COOPER, M. R. 1984. A reassessment of *Vulcanodon karibaensis* Raath (Dinosauria: Saurischia) and the origin of the Sauropoda.
- COPE, E. D. Synopsis of the extinct Batrachia, Reptilia and Aves of North America: read September 18, 1868, and April 2, 1869. 1871. American Philosophical Soc.
- CURRIE, P. J. 1997. Theropoda. In: PADIAN, P. J. C. A. K. (ed.) *Encyclopedia of dinosaurs*.
- DOLLMAN, K. N., CLARK, J. M., VIGLIETTI, P. A., BROWNING, C. & CHOINIÈRE, J. N. 2021. Revised anatomy, taxonomy and biostratigraphy of *Notochampsia istedana* Broom, 1904, a Lower Jurassic crocodyliform from the Clarens Formation (Stormberg Group), and its implications for early crocodyliform phylogeny. *Journal of Systematic Palaeontology*, 19, 651-675.
- DOLLMAN, K. N., VIGLIETTI, P. A. & CHOINIÈRE, J. N. 2019. A new specimen of

- Orthosuchus stormbergi (Nash 1968) and a review of the distribution of Southern African Lower Jurassic crocodylomorphs. *Historical Biology*, 31, 653-664.
- EZCURRA, M. D. 2010. A new early dinosaur (Saurischia: Sauropodomorpha) from the Late Triassic of Argentina: a reassessment of dinosaur origin and phylogeny. *Journal of Systematic Palaeontology*, 8, 371-425.
- EZCURRA, M. D., MÜLLER, R. T., NOVAS, F. E. & CHATTERJEE, S. 2024. Osteology of the sauropodomorph dinosaur Jaklapallisaurus asymmetricus from the Late Triassic of central India. *The Anatomical Record*, 307, 1093-1112.
- GALTON, P. M. & VAN HEERDEN, J. 1985. Partial hindlimb of Blikanasaurus cromptoni n. gen. and n. sp., representing a new family of prosauropod dinosaurs from the Upper Triassic of South Africa. *Geobios*, 18, 509-516.
- GALTON, P. M. & VAN HEERDEN, J. 1998. Anatomy of the prosauropod dinosaur Blikanasaurus cromptoni (Upper Triassic, South Africa), with notes on the other tetrapods from the lower Elliot Formation. *Paläontologische Zeitschrift*, 72, 163-177.
- GOLOBOFF, P. A., FARRIS, J. S. & NIXON, K. C. 2008. TNT, a free program for phylogenetic analysis. *Cladistics*, 24, 774-786.
- GOLOBOFF, P. A. & MORALES, M. E. 2023. TNT version 1.6, with a graphical interface for MacOS and Linux, including new routines in parallel. *Cladistics*, 39, 144-153.
- GOW, C. E. 2000. The skull of Protosuchus haughtoni, an early Jurassic crocodyliform from southern Africa. *Journal of Vertebrate Paleontology*, 20, 49-56.
- GOWER, D. J. 2000. Raurisuchian archosaurs (Reptilia, Diapsida): an overview. *Neues Jahrbuch für Geologie und Paläontologie, Abhandlungen*, 218, 447-488.
- HARRIS, J. D. & DODSON, P. 2004. A new diplodocoid sauropod dinosaur from the Upper Jurassic Morrison Formation of Montana, USA. *Acta Palaeontologica Polonica*, 49, 197.
- HAUGHTON, S. 1915. A new thecodont from the Stormberg beds. *Annals of the South African Museum*, 12, 98-105.
- HAUGHTON, S. H. 1924. *The fauna and stratigraphy of the Stormberg Series*, South African Museum.
- HENDRICKX, C., MATEUS, O. & ARAÚJO, R. 2015. A proposed terminology of theropod teeth (Dinosauria, Saurischia). *Journal of Vertebrate Paleontology*, 35, e982797.
- HUXLEY, T. H. 1870. On the classification of the Dinosauria, with observations on the Dinosauria of the Trias. *Quarterly Journal of the Geological Society*, 26, 32-51.
- JASINSKI, S. E. 2011. Biomechanical modeling of Coelophysis bauri: possible feeding methods and behavior of a Late Triassic theropod. *New Mexico Museum of Natural History and Science Bulletin*, 53, 195-201.
- KITCHING, J. W. & RAATH, M. A. 1984. Fossils from the Elliot and Clarens Formations (Karoo Sequence) of the northeastern Cape, Orange Free State

- and Lesotho, and a suggested biozonation based on tetrapods. *Palaeontologia africana*, 25.
- KNOLL, F. 2010. A primitive sauropodomorph from the upper Elliot Formation of Lesotho. *Geological magazine*, 147, 814-829.
- LANGER, M. C. 2003. The pelvic and hind limb anatomy of the stem-sauropodomorph *Saturnalia tupiniquim* (Late Triassic, Brazil). *PaleoBios*, 23.
- LANGER, M. C., ABDALA, F., RICHTER, M. & BENTON, M. J. 1999. A sauropodomorph dinosaur from the Upper Triassic (Carman) of southern Brazil. *Comptes Rendus de l'Académie des Sciences-Series IIA-Earth and Planetary Science*, 329, 511-517.
- LANGER, M. C., MCPHEE, B. W., MARSOLA, J. C. D. A., ROBERTO-DA-SILVA, L. & CABREIRA, S. F. 2019. Anatomy of the dinosaur *Pampadromaeus barberenai* (Saurischia—Sauropodomorpha) from the Late Triassic Santa Maria Formation of southern Brazil. *PloS one*, 14, e0212543.
- LÜ, J. 2007. New yunnanosaurid dinosaur (Dinosauria, Prosauropoda) from the Middle Jurassic Zhanghe Formation of Yuanmou, Yunnan Province of China. *Memoir of the Fukui Prefectural Dinosaur Museum*, 6, 1.
- MADDISON, W. P. & MADDISON, D. R. 2018. *Mesquite: A modular system for evolutionary analysis* [Online]. Available: <https://www.mesquiteproject.org/> [Accessed].
- MANNION, P. D. & UPCHURCH, P. 2010. Completeness metrics and the quality of the sauropodomorph fossil record through geological and historical time. *Paleobiology*, 36, 283-302.
- MANNION, P. D., UPCHURCH, P., CARRANO, M. T. & BARRETT, P. M. 2011. Testing the effect of the rock record on diversity: a multidisciplinary approach to elucidating the generic richness of sauropodomorph dinosaurs through time. *Biological Reviews*, 86, 157-181.
- MAO, L., XING, L., ZHANG, J., WANG, T. & WANG, D. 2020. Revisiting the world famous Lufeng Formation dinosaur fauna: new approaches to old problems. *Historical biology*, 32, 1062-1070.
- MARSH, A. D. & ROWE, T. B. 2018. Anatomy and systematics of the sauropodomorph *Sarhsaurus aurifontalis* from the Early Jurassic Kayenta Formation. *PLOS ONE*, 13, e0204007.
- MARTÍNEZ, R. N. 2009. *Adeopapposaurus mognai*, gen. et sp. nov. (Dinosauria: Sauropodomorpha), with comments on adaptations of basal Sauropodomorpha. *Journal of Vertebrate Paleontology*, 29, 142-164.
- MARTINEZ, R. N. & ALCOBER, O. A. 2009. A basal sauropodomorph (Dinosauria: Saurischia) from the Ischigualasto Formation (Triassic, Carnian) and the early evolution of Sauropodomorpha. *PLoS One*, 4, e4397.
- MARTÍNEZ, R. N., APALDETTI, C. & ABELIN, D. 2012. Basal sauropodomorphs from the Ischigualasto Formation. *Journal of Vertebrate Paleontology*, 32, 51-69.
- MARTINEZ, R. N., SERENO, P. C., ALCOBER, O. A., COLOMBI, C. E., RENNE, P. R., MONTAÑEZ, I. P. & CURRIE, B. S. 2011. A basal dinosaur from the dawn of

- the dinosaur era in southwestern Pangaea. *science*, 331, 206-210.
- MCPHEE, B., CHOINIÈRE, J., YATES, A. & VIGLIETTI, P. 2015a. A second species of *Eucnemesaurus* Van Hoepen, 1920 (Dinosauria, Sauropodomorpha): New information on the diversity and evolution of the sauropodomorph fauna of South Africa's lower Elliot Formation (latest Triassic). *Journal of Vertebrate Paleontology*, 35, e980504.
- MCPHEE, B. W., BENSON, R. B., BOTHA-BRINK, J., BORDY, E. M. & CHOINIÈRE, J. N. 2018. A giant dinosaur from the earliest Jurassic of South Africa and the transition to quadrupedality in early sauropodomorphs. *Current Biology*, 28, 3143-3151. e7.
- MCPHEE, B. W., BONNAN, M. F., YATES, A. M., NEVELING, J. & CHOINIÈRE, J. N. 2015b. A new basal sauropod from the pre-Toarcian Jurassic of South Africa: evidence of niche-partitioning at the sauropodomorph–sauropod boundary? *Scientific Reports*, 5, 1-12.
- MCPHEE, B. W., BORDY, E. M., SCISCIO, L. & CHOINIÈRE, J. N. 2017. The sauropodomorph biostratigraphy of the Elliot Formation of southern Africa: Tracking the evolution of Sauropodomorpha across the Triassic–Jurassic boundary. *Acta Palaeontologica Polonica*, 62, 441-465.
- MCPHEE, B. W. & CHOINIÈRE, J. N. 2017. The osteology of *Pulanesaura eocollum*: implications for the inclusivity of Sauropoda (Dinosauria). *Zoological Journal of the Linnean Society*, 182, 830-861.
- MCPHEE, B. W., YATES, A. M., CHOINIÈRE, J. N. & ABDALA, F. 2014. The complete anatomy and phylogenetic relationships of *Antetonitrus ingenipes* (Sauropodiformes, Dinosauria): implications for the origins of Sauropoda. *Zoological Journal of the Linnean Society*, 171, 151-205.
- MOOPEN, A., MATIWANE, A., VIGLIETTI, P. A. & CHOINIÈRE, J. N. 2023. Anatomy and phylogenetic relationships of a possible lessemsaurid with associated plant fossils from the lower part of the Elliot Formation. *Palaeontologia africana*, 56, 190-212.
- MUKADDAM, R., BORDY, E. M., LOCKLEY, M. G. & CHAPPELLE, K. E. J. 2021. Reviving *Kalosauropus*, an Early Jurassic sauropodomorph track from southern Africa (Lesotho). *Historical Biology*, 33, 2908-2930.
- MÜLLER, R. T. & GARCIA, M. S. 2020. Rise of an empire: analyzing the high diversity of the earliest sauropodomorph dinosaurs through distinct hypotheses. *Historical Biology*, 32, 1334-1339.
- MUNYIKWA, D. & RAATH, M. A. 1999. Further material of the ceratosaurian dinosaur *Syntarsus* from the Elliot Formation (Early Jurassic) of South Africa. *Palaeontologia africana*, 35, 55-59.
- NASH, D. S. 1975. The morphology and relationships of a crocodylian, *Orthosuchus stormbergi*, from the Upper Triassic of Lesotho. *Annals of the South African Museum*, 67, 227-329.
- NESBITT, S. J. 2011. The Early Evolution of Archosaurs: Relationships and the Origin of Major Clades. *Bulletin of the American Museum of Natural History*, 2011, 1-292, 292.
- NESBITT, S. J., BARRETT, P. M., WERNING, S., SIDOR, C. A. & CHARIG, A. J. 2013a.

- The oldest dinosaur? A Middle Triassic dinosauriform from Tanzania. *Biology Letters*, 9, 20120949.
- NESBITT, S. J., BRUSATTE, S. L., DESOJO, J. B., LIPARINI, A., FRANÇA, M. A. G. D., WEINBAUM, J. C. & GOWER, D. J. 2013b. Rausuchia. *Geological Society, London, Special Publications*, 379, 241-274.
- NESBITT, S. J., IRMIS, R. B., LUCAS, S. G. & HUNT, A. P. 2005. A giant crocodylomorph from the Upper Triassic of New Mexico. *Paläontologische Zeitschrift*, 79, 471-478.
- OTERO, A., APALDETTI, G. C. & POL, D. 2016. Basal Sauropodomorpha (Dinosauria, Saurischia) of Gondwana. *Contribuciones Científicas del Museo Argentino de Ciencias Naturales "Bernardino Rivadavia"*, 6, 119-128.
- OTERO, A., CARBALLIDO, J. L. & MORENO, A. P. 2020. The appendicular osteology of Patagotitan mayorum (Dinosauria, Sauropoda). *Journal of Vertebrate Paleontology*, 40, e1793158.
- OTERO, A., GALLINA, P., CANALE, J. & HALUZA, A. 2012. Sauropod haemal arches: Morphotypes, new classification and phylogenetic aspects. *Historical Biology*, 24, 243-256.
- OTERO, A., KRUPANDAN, E., POL, D., CHINSAMY, A. & CHOINIERE, J. 2015. A new basal sauropodiform from South Africa and the phylogenetic relationships of basal sauropodomorphs. *Zoological Journal of the Linnean Society*, 174, 589-634.
- OTERO, A. & POL, D. 2013. Postcranial anatomy and phylogenetic relationships of Mussaurus patagonicus (Dinosauria, Sauropodomorpha). *Journal of Vertebrate Paleontology*, 33, 1138-1168.
- OWEN, R. 1854. *Descriptive Catalogue of the Fossil Organic Remains of Reptilia and Pisces Contained in the Museum of the Royal College of Surgeons of England*, Taylor & Francis.
- PEYRE DE FABRÈGUES, C. & ALLAIN, R. 2016. New material and revision of Melanorosaurus thabanensis, a basal sauropodomorph from the Upper Triassic of Lesotho. *PeerJ*, 4, e1639.
- PEYRE DE FABRÈGUES, C. & ALLAIN, R. 2019. Kholumolumo ellenbergerorum, gen. et sp. nov., a new early sauropodomorph from the lower Elliot Formation (Upper Triassic) of Maphutseng, Lesotho. *Journal of Vertebrate Paleontology*, 39, e1732996.
- PEYRE DE FABRÈGUES, C., BI, S., AI, T. & XU, X. 2021. A Juvenile Specimen of Sauropodomorpha from the Lower Jurassic of China and a Brief Review of the Lufeng Sauropodomorph Fauna. *Acta geologica Sinica (Beijing)*, 95, 319-332.
- POL, D. & ESCAPA, I. H. 2009. Unstable taxa in cladistic analysis: identification and the assessment of relevant characters. *Cladistics*, 25, 515-527.
- POL, D., GARRIDO, A. & CERDA, I. A. 2011. A New Sauropodomorph Dinosaur from the Early Jurassic of Patagonia and the Origin and Evolution of the Sauropod-type Sacrum. *PLOS ONE*, 6, e14572.
- POL, D. & POWELL, J. E. 2007. New information on Lessemsaurus sauropoides (Dinosauria: Sauropodomorpha) from the upper Triassic of Argentina.

- Special Papers in Palaeontology*, 77, 223.
- RAATH, M. A. 1969. *A new coelurosaurian dinosaur from the Forest Sandstone of Rhodesia*, National Museums of Rhodesia.
- RAATH, M. A., CARPENTER, K. & CURRIE, P. 1990. Morphological variation in small theropods and its meaning in systematics: evidence from Syntarsus. In: CARPENTER, K., AND & CURRIE, P. J. (eds.) *Dinosaur Systematics Approaches and Perspectives*. Cambridge University Press.
- RAMBAUT, A. 2006. *FigTree* [Online]. [Accessed].
- RAUHUT, O., HOLWERDA, F. & FURRER, H. 2020. A derived sauropodiform dinosaur and other sauropodomorph material from the Late Triassic of Canton Schaffhausen, Switzerland. *Swiss Journal of Geosciences*, 113.
- RAY, S. & CHINSAMY, A. 2002. A theropod tooth from the Late Triassic of southern Africa. *Journal of Biosciences*, 27, 295-298.
- SANDER, P. M. & LALLENSACK, J. N. 2018. Dinosaurs: four legs good, two legs bad. *Current Biology*, 28, R1160-R1163.
- SCISCIO, L., BORDY, E. M., ABRAHAMS, M., KNOLL, F. & MCPHEE, B. W. 2017a. The first megatheropod tracks from the lower jurassic upper Elliot formation, Karoo Basin, Lesotho. *PloS one*, 12, e0185941.
- SCISCIO, L., DE KOCK, M., BORDY, E. & KNOLL, F. 2017b. Magnetostratigraphy across the Triassic-Jurassic boundary in the main Karoo Basin. *Gondwana Research*, 51, 177-192.
- SEELEY, H. G. 1888. I. On the classification of the fossil animals commonly named Dinosauria. *Proceedings of the Royal Society of London*, 43, 165-171.
- SERENO, P. 1998. A rational for phylogenetic definitions, with application to the higher level taxonomy of Dinosauria. *Neues Jahrbuch fur Geologie und Palaontologie - Abhandlungen*, 210, 41-83.
- SERENO, P. C. 1999. The evolution of dinosaurs. *Science*, 284, 2137-2147.
- SERENO, P. C. 2007. Basal Sauropodomorpha: historical and recent phylogenetic hypotheses, with comments on Ammosaurus major (Marsh, 1889). *Special Papers in Palaeontology*, 77, 261.
- SERENO, P. C., MARTÍNEZ, R. N. & ALCOBER, O. A. 2012. Osteology of Eoraptor lunensis (Dinosauria, sauropodomorpha). *Journal of Vertebrate Paleontology*, 32, 83-179.
- SERENO, P. C., SIDOR, C. A., LARSSON, H. C. E. & GADO, B. 2003. A new notosuchian from the Early Cretaceous of Niger. *Journal of Vertebrate Paleontology*, 23, 477-482.
- SERRANO-MARTÍNEZ, A., VIDAL, D., SCISCIO, L., ORTEGA, F. & KNOLL, F. 2015. Isolated Theropod Teeth from the Middle Jurassic of Niger and the Early Dental Evolution of Spinosauridae. *Acta Palaeontologica Polonica*, 61, 403-415, 13.
- SMITH, N. D., MAKOVICKY, P., POL, D., HAMMER, W. & CURRIE, P. 2007. The dinosaurs of the Early Jurassic Hanson Formation of the central Transantarctic Mountains: phylogenetic review and synthesis. *US Geological Survey and the National Academies, Short Research Paper*, 3.
- SMITH, N. D. & POL, D. 2007. Anatomy of a basal sauropodomorph dinosaur from

- the Early Jurassic Hanson Formation of Antarctica. *Acta Palaeontologica Polonica*, 52, 657.
- TOLCHARD, F., NESBITT, S. J., DESOJO, J. B., VIGLIETTI, P., BUTLER, R. J. & CHOINIÈRE, J. N. 2019. 'Rauisuchian' material from the lower Elliot Formation of South Africa and Lesotho: Implications for Late Triassic biogeography and biostratigraphy. *Journal of African Earth Sciences*, 160, 103610.
- TOLCHARD, F. B., BORDY, E. M. & CHOINIÈRE, J. N. 2023. New 'rauisuchian' fossil material from the lower Elliot Formation of South Africa. *Palaeontologia africana*, 56.
- VIGLIETTI, P. A., MCPHEE, B. W., BORDY, E. M., SCISCIO, L., BARRETT, P. M., BENSON, R. B. J., WILLS, S., CHAPPELLE, K. E. J., DOLLMAN, K. N., MDEKAZI, C. & CHOINIÈRE, J. N. 2020. Biostratigraphy of the *Massospondylus* Assemblage Zone (Stormberg Group, Karoo Supergroup), South Africa. *South African Journal of Geology*, 123, 249-262.
- VON HUENE, F. 1925. Die Bedeutung der Sphenosuchus-Gruppe für den Ursprung der Krokodile. *Zeitschrift für Induktive Abstammungs- und Vererbungslehre*, 38, 307-320.
- W.D.L. RIDE, C., COGGER, H. G., DUPUIS, C., KRAUS, O., MINELLI, A., THOMPSON, F. C. & TUBBS, P. K. 2000. *INTERNATIONAL CODE OF ZOOLOGICAL NOMENCLATURE* [Online]. The International Trust for Zoological Nomenclature Available: <https://www.iczn.org/the-code/the-code-online/> [Accessed 2024].
- WALKER, A. D. 1990. A Revision of *Sphenosuchus acutus* Haughton, a Crocodylomorph Reptile from the Elliot Formation (Late Triassic or Early Jurassic) of South Africa. *Philosophical Transactions: Biological Sciences*, 330, 1-120.
- WANG, Y.-M., YOU, H.-L. & WANG, T. 2017. A new basal sauropodiform dinosaur from the Lower Jurassic of Yunnan Province, China. *Scientific Reports*, 7, 41881.
- WEISHAMPEL, D. B., BARRETT, P. M., CORIA, R. A., LE LOEUFF, J., XU, X., ZHAO, X., SAHNI, A., GOMANI, E. M. & NOTO, C. R. 2004. Dinosaur distribution. *The dinosauria*, 2, 517-606.
- WILSON, J. 2006. Anatomical nomenclature of fossil vertebrates: standardized terms or 'lingua franca'? *Journal of Vertebrate Paleontology*, 26, 511-518.
- YATES, A. 2004. The death of a dinosaur: dismembering *Euskelosaurus*. *Geoscience Africa*, 715.
- YATES, A. M. 2003. A definite prosauropod dinosaur from the lower Elliot Formation (Norian: Upper Triassic) of South Africa. *Palaeontologia africana*, 39.
- YATES, A. M. 2005. A new theropod dinosaur from the Early Jurassic of South Africa and its implications for the early evolution of theropods. *Palaeontologia africana*, 41, 105-122.
- YATES, A. M. 2007a. The first complete skull of the Triassic dinosaur *Melanorosaurus* Haughton (Sauropodomorpha: Anchisauria). *Evolution*

- and palaeobiology of early sauropodomorph dinosaurs*, 9-55.
- YATES, A. M. 2007b. Solving a dinosaurian puzzle: the identity of Aliwalia rex Galton. *Historical Biology*, 19, 93-123.
- YATES, A. M. 2008. A second specimen of Blikanasaurus (Dinosauria: Sauropoda) and the biostratigraphy of the lower Elliot Formation. *Palaeontologia africana*, 43, 39-43.
- YATES, A. M. & BARRETT, P. 2010. Massospondylus carinatus owen 1854 (Dinosauria: Sauropodomorpha) from the lower jurassic of South Africa: Proposed conservation of usage by designation of a neotype. 45, 7-10.
- YATES, A. M., BONNAN, M. F. & NEVELING, J. 2011. A new basal sauropodomorph dinosaur from the Early Jurassic of South Africa. *Journal of Vertebrate Paleontology*, 31, 610-625.
- YATES, A. M., BONNAN, M. F., NEVELING, J., CHINSAMY, A. & BLACKBEARD, M. G. 2010. A new transitional sauropodomorph dinosaur from the Early Jurassic of South Africa and the evolution of sauropod feeding and quadrupedalism. *Proceedings of the Royal Society B: Biological Sciences*, 277, 787-794.
- YATES, A. M., HANCOX, P. J. & RUBIDGE, B. S. 2004. First record of a sauropod dinosaur from the upper Elliot Formation (Early Jurassic) of South Africa : research letter. *South African Journal of Science*, 100, 504-506.
- YATES, A. M. & KITCHING, J. W. 2003. The earliest known sauropod dinosaur and the first steps towards sauropod locomotion. *Proceedings of the Royal Society of London. Series B: Biological Sciences*, 270, 1753-1758.
- YOUNG, C.-C. 1940. Preliminary notes on the Lufeng vertebrate fossils. *Bulletin of the Geological Society of China*, 20, 235-240.
- YOUNG, C.-C. 1941. *A complete osteology of Lufengosaurus Heunei Young (gen. et sp. nov.) from Lufeng, Yunnan, China*, Geol. Survey of China.

---

## APPENDIX A

### Expanded specimen comparison

Table A.1: Complete list of Late Triassic - Early Jurassic sauropodomorph pes elements available for study at the ESI collection.

ESI COLLECTION		
Specimen #	Taxon	Element
BP/1/6234	<i>Eucnemesaurus</i>	pes
BP/1/4377	<i>Massospondylus</i>	pes
BP/1/6619	Referred <i>Aardonyx</i>	M1
BP/1/6893	Referred <i>Aardonyx</i>	M1
BP/1/6607	Referred <i>Aardonyx</i>	M2
BP/1/6253	Referred <i>Aardonyx</i>	M2
BP/1/6509	Referred <i>Aardonyx</i>	M3

BP/1/6626	Referred <i>Aardonyx</i>	M4
BP/1/6623	Referred <i>Aardonyx</i>	M4
BP/1/6680	Referred <i>Aardonyx</i>	M4
BP/1/7120	<i>Ledumahadi</i>	Ungual 1
BP/1/5271a	<i>Blikanasaurus</i>	M1
BP/1/5271	<i>Blikanasaurus</i>	phalange
BP/1/5091	<i>Antetonitrus</i>	Ungual
BP/1/5091	<i>Antetonitrus</i>	Ungual
BP/1/3215	<i>Blikanasaurus</i> ?	M1
BP/1/4928	<i>Massospondylus</i>	3x Phalange
BP/1/4928	<i>Massospondylus</i>	Ungual
BP/1/5004	Indet. Sauropodomorpha	M1
BP/1/5004	Indet. Sauropodomorpha	M3?
BP/1/5004	Indet. Sauropodomorpha	phalange
BP/1/6191	<i>Pulanesaura</i> ?	M1
BP/1/4952	<i>Antetonitrus</i> (holotype)	M1
BP/1/4952	<i>Antetonitrus</i> (holotype)	M2
BP/1/4952	<i>Antetonitrus</i> (holotype)	M3
BP/1/4952	<i>Antetonitrus</i> (holotype)	ungual
BP/1/4952	<i>Antetonitrus</i> (holotype)	proximal phalanx
BP/1/386	<i>Massospondylus</i>	pes
BP/1/5241	<i>Massospondylus</i>	hindlimb
BP/1/6592	Referred <i>Aardonyx</i>	ungual
BP/1/6650	Referred <i>Aardonyx</i>	phalanx
BP/1/6595	Referred <i>Aardonyx</i>	phalanx
BP/1/6319	Referred <i>Aardonyx</i>	phalanx
BP/1/8398	Referred <i>Aardonyx</i>	phalanx
BP/1/6314	Referred <i>Aardonyx</i>	phalanx
BP/1/6593	Referred <i>Aardonyx</i>	ungual
BP/1/8447	Referred <i>Aardonyx</i>	ungual
BP/1/7044	Referred <i>Aardonyx</i>	ungual
BP/1/6512	Referred <i>Aardonyx</i>	phalanx
BP/1/6250	Referred <i>Aardonyx</i>	ungual
BP/1/8412	Referred <i>Aardonyx</i>	phalanx
BP/1/8237	Sauropodomorph	M3

Table A.2: Complete list of Late Triassic - Early Jurassic sauropodomorph pes elements available for study at the IZIKO collection

IZIKO COLLECTION		
Specimen #	Taxon	Element
SAM-PK-K403	<i>Blikanasaurus</i>	Left pes
SAM-PK-003449	<i>Melanorosaurus</i>	Partial M4

SAM-PK-K5134	<i>Massospondylus</i>	Partial right pes
--------------	-----------------------	-------------------

Table A.3: Complete list of Late Triassic - Early Jurassic sauropodomorph vertebrae elements available for study at the ESI collection

ESI COLLECTION	
Specimen #	Taxon
BP/1/7120	<i>Ledumahadi</i>
BP/1/3177	Indet. Sauropodomorpha
BP/1/3178	Indet. Sauropodomorpha
BP/1/3185	Indet. Sauropodomorpha
BP/1/3191	Indet. Sauropodomorpha
BP/1/3193	Indet. Sauropodomorpha
BP/1/3195	Indet. Sauropodomorpha
BP/1/3203	Indet. Sauropodomorpha
BP/1/3208	Indet. Sauropodomorpha
BP/1/3211	Indet. Sauropodomorpha
BP/1/3215	Indet. Sauropodomorpha
BP/1/4911	Indet. Sauropodomorpha
BP/1/5130	<i>Massospondylus</i> sp.
BP/1/6192	Indet. New Sauropod
BP/1/6201	Indet. New Sauropod
BP/1/6211	Indet. New Sauropod

Table A.4: Complete list of Late Triassic - Early Jurassic sauropodomorph vertebrae elements available for study at the IZIKO collection

IZIKO COLLECTION	
Specimen #	Taxon
SAM-PK-003449	<i>Melanorosaurus</i>

Table A.5: Complete list of Late Triassic - Early Jurassic predator teeth available for study at the ESI collection

ESI COLLECTION	
Specimen #	Taxon
BP/1/6062	<i>Rauisuchid</i>
BP/1/6894	Theropoda – <i>rauisuchid</i>
BP/1/6598	Theropoda – <i>rauisuchid</i>
BP/1/6508	Theropoda – <i>rauisuchid</i>
BP/1/5730	<i>Rauisuchid</i>
BP/1/6504	Large theropod
BP/1/4693	Theropod tooth
BP/1/5243	<i>Dracovenator regenti</i>
BP/1/8235	Theropod tooth

Table A.6: Complete list of Late Triassic - Early Jurassic predator teeth available for study at the IZIKO collection

IZIKO COLLECTION	
Specimen #	Taxon
SAM-PK-K383	3x <i>Rausuchid</i> sp
SAM-PK-003014	<i>Sphenosuchus acutus</i>
SAM-PK-K01321	<i>Protosuchus haughtoni</i>
SAM-PK-K01323	<i>Protosuchus haughtoni</i>
SAM-PK-K08026	<i>Protosuchus haughtoni</i>
SAM-PK-004013	<i>Notochampsia istedana</i>
SAM-PK-011894	<i>Notochampsia istedana</i>
SAM-PK-00428	<i>Notochampsia istedana</i>
SAM-PK-00429	<i>Notochampsia istedana</i>
SAM-PK-K00409	<i>Orthosuchus stormbergi</i>
SAM-PK-K04639	<i>Orthosuchus stormbergi</i>

## APPENDIX B

### Expanded measurements

Table B.1: Pes measurements of AM 6147. Table modified from Yates (2008). Asterisks indicates incomplete measurements.

Element and measurement area	Measurement in mm
<b>Mt. 1</b> (* = approx)	
The midshaft width is % of the total length of the bone	36%
Total Length (mm)	165,1
Minimum anterior-posterior depth of shaft	28,14
Minimum mediolateral shaft width	58,11
Maximum mediolateral width of proximal articular surface	80,92
Maximum depth of proximal surface anterior-posterior	*35,63
Mediolateral width of distal articular surface	83,78
Anterior-posterior depth of distal articular surface	x
<b>Mt.2</b>	
The midshaft width is % of the total length of the bone	32%
Total Length (mm)	173,08
Minimum anterior-posterior depth of shaft	38,08
Minimum mediolateral shaft width	52,39
Maximum mediolateral width of proximal articular surface	105,09
Maximum depth of proximal surface anterior-posterior	90,93
Mediolateral width of distal articular surface	93,42
Anterior-posterior depth of distal articular surface	50,54
<b>Mt.3</b>	
The midshaft width is % of the total length of the bone	20%
Total Length (mm)	300,48
Minimum anterior-posterior depth of shaft	35,81
Minimum mediolateral shaft width	59,85
Maximum mediolateral width of proximal articular surface	*82,70
Maximum depth of proximal surface anterior-posterior	*71,06
Mediolateral width of distal articular surface	95,73
Anterior-posterior depth of distal articular surface	54,57
<b>Mt.4</b>	
The midshaft width is % of the total length of the bone	24%
Total Length (mm)	271,14
Minimum anterior-posterior depth of shaft	23,38

Minimum mediolateral shaft width	54,05
Maximum mediolateral width of proximal articular surface	132,61
Maximum depth of proximal surface anterior-posterior	43,5
Mediolateral width of distal articular surface	88,06
Anterior-posterior depth of distal articular surface	52,23
<b>Mt.5</b>	
The midshaft width is % of the total length of the bone	x
Total Length (mm)	135,64
Minimum anterior-posterior depth of shaft	x
Minimum mediolateral shaft width	x
Maximum mediolateral width of proximal articular surface	113,24
Maximum depth of proximal surface anterior-posterior	45,78
Mediolateral width of distal articular surface	22,13
Anterior-posterior depth of distal articular surface	31,4
<b>Mt.1 phalanges</b>	
PH1	
Total Length (mm)	101,46
Midpoint mediolateral width of the shaft	54,05
Midpoint anterior-posterior width of the shaft	46,11
Maximum mediolateral width of proximal articular surface	72,39
Maximum depth of proximal surface anterior-posterior	65,83
Mediolateral width of distal articular surface	67,53
Anterior-posterior depth of distal articular surface	50,49
Ungual	
Total Length (mm)	173,82
Midpoint mediolateral width of the shaft	*44,86
Midpoint anterior-posterior width of the shaft	*55,25
Width of proximal articular surface mediolateral	55,75
Depth of proximal surface anterior-posterior	60,53
<b>Mt.2 phalanges</b>	
PH1	
ssTotal Length (mm)	109,3
Midpoint mediolateral width of the shaft	59,48
Midpoint anterior-posterior width of the shaft	40,13
Maximum mediolateral width of proximal articular surface	79,81
Maximum depth of proximal surface anterior-posterior	56,28
Mediolateral width of distal articular surface	83,84

Anterior-posterior depth of distal articular surface	x
PH2	
Total Length (mm)	83,27
Midpoint mediolateral width of the shaft	56,75
Midpoint anterior-posterior width of the shaft	36,6
Maximum mediolateral width of proximal articular surface	71
Maximum depth of proximal surface anterior-posterior	55,02
Mediolateral width of distal articular surface	61,49
Anterior-posterior depth of distal articular surface	40,53
Ungual	
Total Length (mm)	*116,60 (distal tip missing, probably *138)
Midpoint mediolateral width of the shaft	*47,25
Midpoint anterior-posterior width of the shaft	*45,64
Width of proximal articular surface mediolateral	55,53
Depth of proximal surface anterior-posterior	51,14
<b>Mt.3 phalanges</b>	
PH1	
Total Length (mm)	*116
Midpoint mediolateral width of the shaft	57,36
Midpoint anterior-posterior width of the shaft	36,93
Maximum mediolateral width of proximal articular surface	91,66
Maximum depth of proximal surface anterior-posterior	67,26
Mediolateral width of distal articular surface	76,12
Anterior-posterior depth of distal articular surface	37,7
PH2	
Total Length (mm)	91,39
Midpoint mediolateral width of the shaft	54,07
Midpoint anterior-posterior width of the shaft	36,92
Maximum mediolateral width of proximal articular surface	71,04
Maximum depth of proximal surface anterior-posterior	54,58
Mediolateral width of distal articular surface	67,55
Anterior-posterior depth of distal articular surface	37,82
PH3	
Total Length (mm)	68,89
Midpoint mediolateral width of the shaft	47,67
Midpoint anterior-posterior width of the shaft	31,47
Maximum mediolateral width of proximal articular surface	63,01
Maximum depth of proximal surface anterior-posterior	46,44
Mediolateral width of distal articular surface	61,04

Anterior-posterior depth of distal articular surface	37,24
Ungual	
Total Length (mm)	*122,10 (tip missing, *134)
Midpoint mediolateral width of the shaft	*44,85
Midpoint anterior-posterior width of the shaft	*39,34
Width of proximal articular surface mediolateral	54,51
Depth of proximal surface anterior-posterior	44,38
<b>Mt.4 phalanges</b>	
PH1	
Total Length (mm)	90,69
Midpoint mediolateral width of the shaft	54,7
Midpoint anterior-posterior width of the shaft	32,69
Maximum mediolateral width of proximal articular surface	80,97
Maximum depth of proximal surface anterior-posterior	60,23
Mediolateral width of distal articular surface	66,72
Anterior-posterior depth of distal articular surface	38,47
PH2	
Total Length (mm)	*60,74
Midpoint mediolateral width of the shaft	55,05
Midpoint anterior-posterior width of the shaft	34,49
Maximum mediolateral width of proximal articular surface	63,25
Maximum depth of proximal surface anterior-posterior	47,85
Mediolateral width of distal articular surface	60,69
Anterior-posterior depth of distal articular surface	40,39
PH3	
Total Length (mm)	62,03
Midpoint mediolateral width of the shaft	47,68
Midpoint anterior-posterior width of the shaft	35,44
Maximum mediolateral width of proximal articular surface	66,03
Maximum depth of proximal surface anterior-posterior	52,6
Mediolateral width of distal articular surface	55,27
Anterior-posterior depth of distal articular surface	31,59
PH4	
Total Length (mm)	57,56
Midpoint mediolateral width of the shaft	39,01
Midpoint anterior-posterior width of the shaft	24,97
Maximum mediolateral width of proximal articular surface	49,29
Maximum depth of proximal surface anterior-posterior	*36,57
Mediolateral width of distal articular surface	46,21
Anterior-posterior depth of distal articular surface	32,5

Ungual	
Total Length (mm)	112,17
Midpoint mediolateral width of the shaft	33,88
Midpoint anterior-posterior width of the shaft	31,77
Width of proximal articular surface mediolateral	42,46
Depth of proximal surface anterior-posterior	41,05
<b>Mt.5 phalange</b>	
Vestigial	
Total Length (mm)	37,28
Midpoint mediolateral width of the shaft	20,17
Midpoint anterior-posterior width of the shaft	23,36

\*PH (1-4) – Phalange (1-4)

Table B.2: Vertebrae and chevrons measurements (mm) for AM 6147.

AM 6147	Caudal vertebrae							
	CV 1	CV 2	CV 3	CV 4	CV 5	CV 6	CV 7	CV 8
<b>Centrum</b>								
Dorsoventral height of the proximal face	94.26	83.04	X	X	X	X	X	X
Dorsoventral height of the distal face	X	X	X	X	X	X	X	X
Mediolateral width of the proximal face	84.53	X	X	X	X	X	X	X
Mediolateral width of the distal face	X	X	X	X	X	X	X	X
Anteroposterior length of the centrum	103.99	102.26	102.15	101.98	98.2	97.95	94.82	X
<b>Neural Spine</b>								
Length of the neural spine	X	X	X	65.63	62.6	59.87	53.92	X
Maximum anteroposterior width of the top of the neural spine	X	X	X	30.44	23.71	31.97	29.26	X
Maximum anteroposterior width of the base of the neural spine	X	X	41.22	37.55	34.13	33.77	32.37	30.18
<b>Zygapophyses</b>								
Length of the prezygapophyses	X	X	X	57.71	38.85	49.63	45.44	50.56

Dorsoventral height of the head of the prezygapophyses	X	X	X	22.19	20.45	20.15	23.65	22.37
Length of the postzygapophyses	X	X	27.4	31.43	27.96	31.49	31.04	X
<b>Transverse process</b>								
Length of the base	62.56	60.01	57.09	50.97	49.56	48.01	47.25	41.22
Length of the transverse flange	X	X	X	*78,84	76.74	74.05	X	X
Width of the base	23.78	26.65	26.43	20.96	21.48	19.64	18.28	17.94
Width of the transverse flange	X	X	X	40.71	30.44	28.97	39.01	X
<b>Chevron</b>								
Length of the shaft	302.88	278.77	257.08	224.8	225.81	80.07	X	X
Maximum width of the shaft	38.13	37.87	34.12	32.57	37.7	37.42	X	X
Minimum width of the shaft	28.12	25.75	24.36	24.23	22.3	21.8	20.82	X
Anteroposterior length of the proximal head	45.56	41.92	38.12	37.46	33.35	32.3	31.28	X
Anteroposterior length of the distal end	46.91	44.03	37.52	40.64	X	X	X	X
Length of the Y shape	X	178.33	149.32	130.66	122.25	X	X	X

Specimen	QG1159	BP/1/ 5241	BP/1/ 4779	SAMPK 1304	SAMPK 388	SAMPK 388
Foot	R	R	R	R	R	L
mT <sub>I</sub>	75.77	84.4	73.3	56.3	64	58
mT <sub>II</sub>	115.32	135.55	128.6	90.3	101	97
mT <sub>III</sub>	113.14	150.12	133.9	110.5	107	112
mT <sub>IV</sub>	117.56	143.57	131.2	93	103	104
mT <sub>V</sub>	64.34	72.09	64.6	-	48	43

Figure B.1: Measurements (mm) of mt. 1 through mt. 5 of *M. carinatus* taken from Mukaddam et al (2021).

# APPENDIX C

## Expanded phylogenetic analysis data and OTU scores



Figure C.1: Bremer support values on the reduced Strict Consensus tree.

Group freqs., 100 replicates, cut=50 (tree 0) - Standard Bootstrap

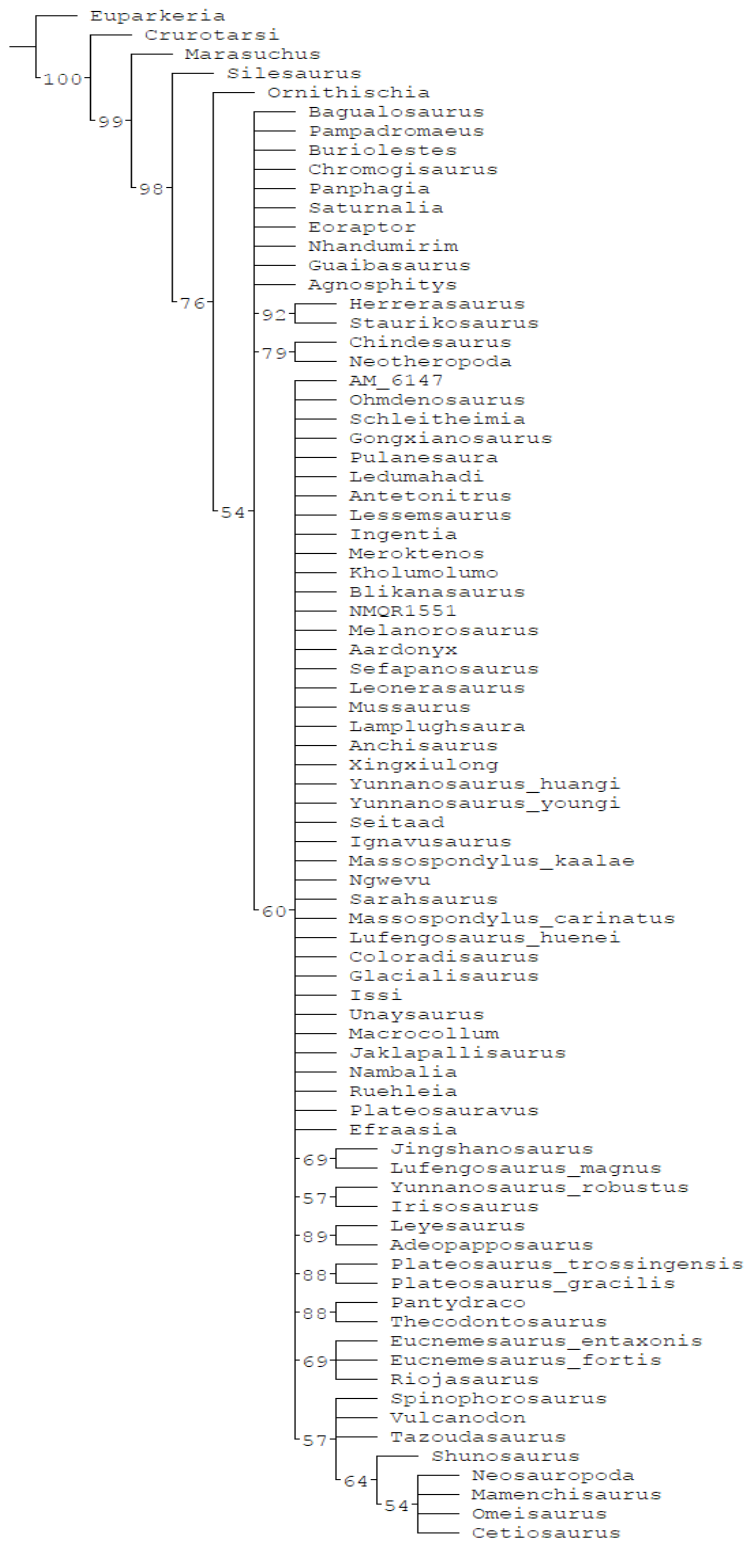


Figure C.2: Bootstrap values on the reduced Strict Consensus tree.

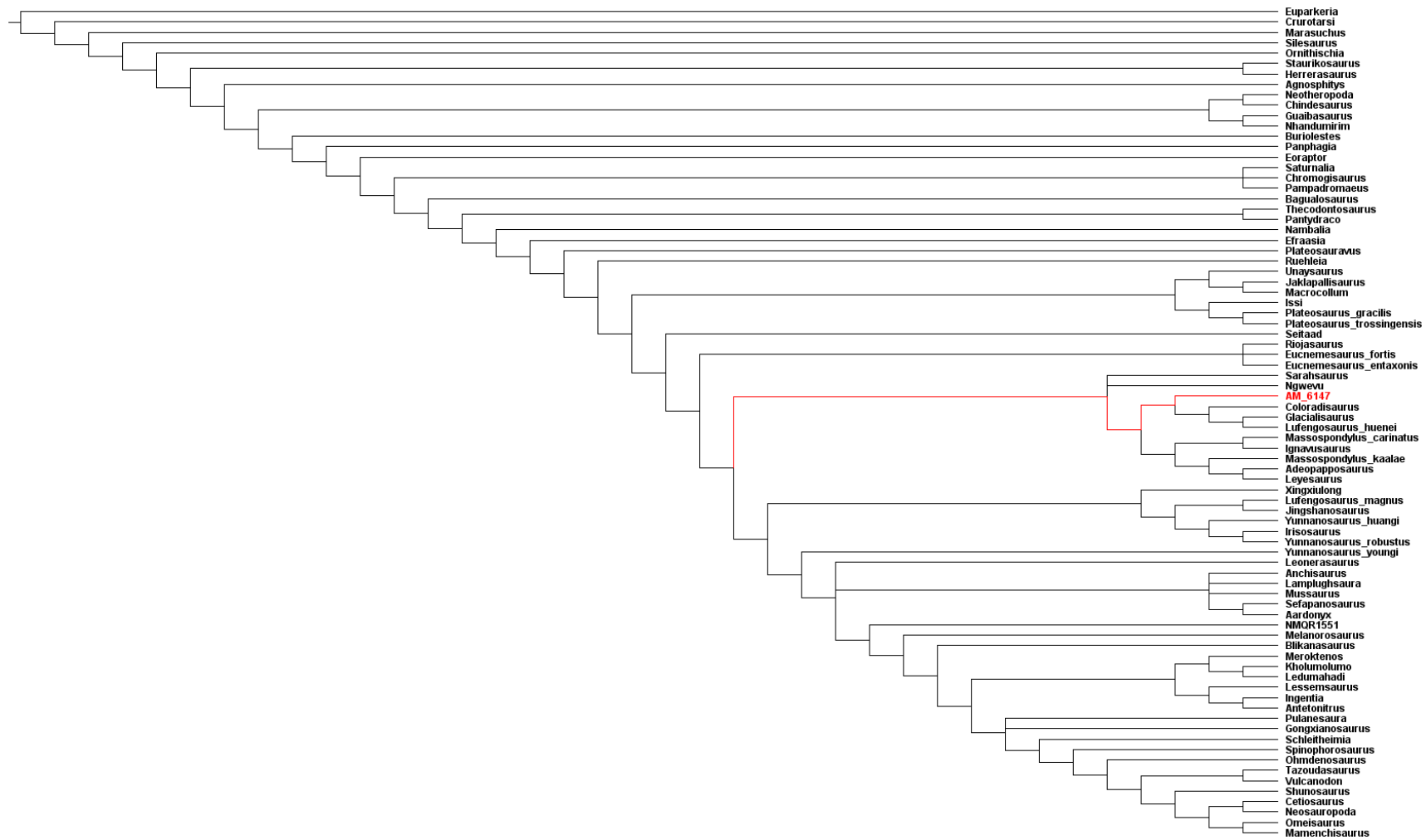


Figure C.3: AM 6147 is recovered among Massospondylidae in a reduced strict consensus summary. 21842 MPTs with a tree length of 1697 steps tree (CI of 0,29 and a RI of 0,67), after ten unstable taxa; Arcusaurus, Pradhania, Xixipiosaurus, Yizhousaurus, Camelotia, Isanosaurus, Amygdalodon, Volkheimeria, Barapasaurus and Patagosaurus were excluded from the consensus. Bremer support = 1, Bootstrap support = 60.

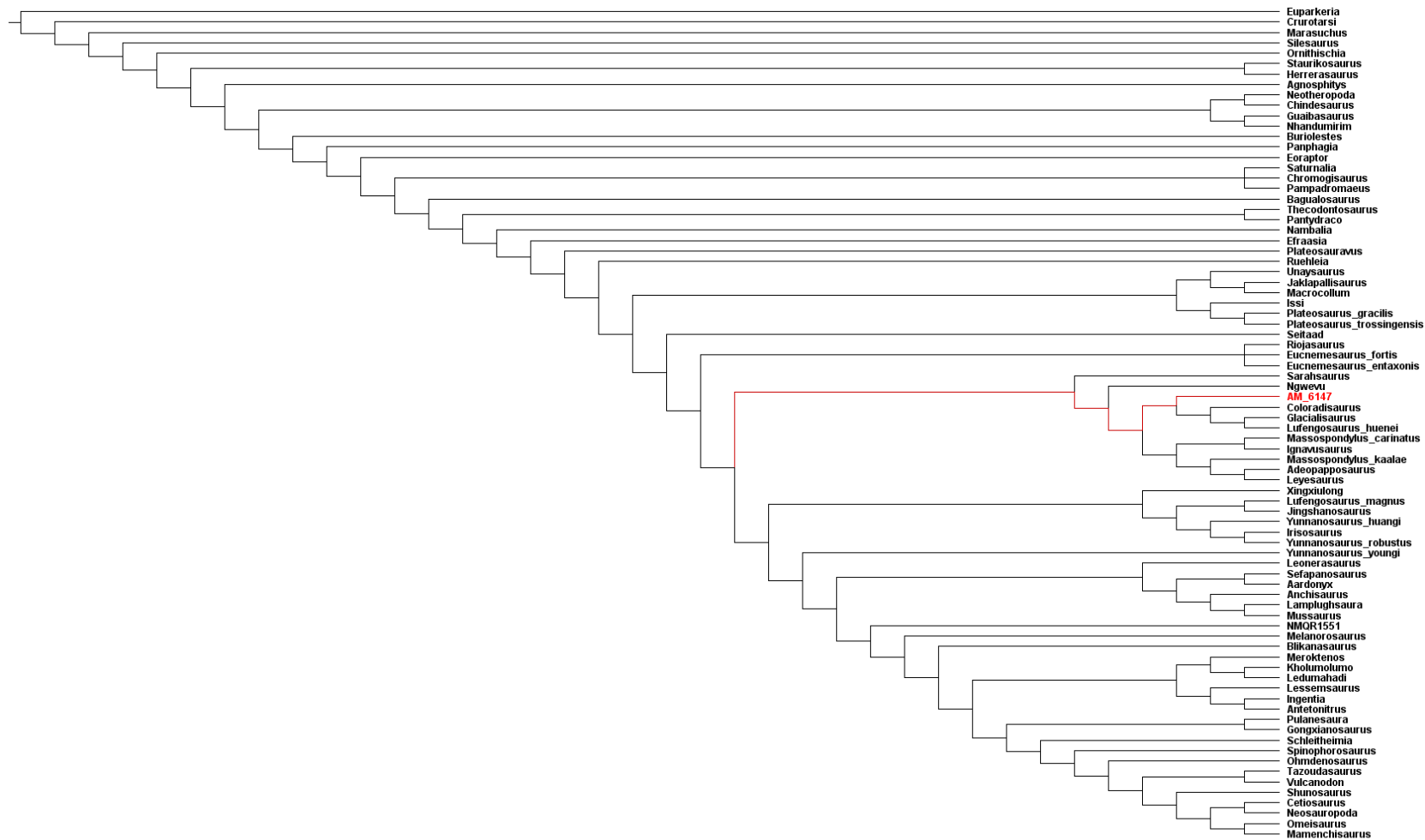


Figure C.4: AM 6147 is recovered among Massospondylidae in a reduced majority rule (50). 21842 MPTs with a tree length of 1697 steps tree (CI of 0,29 and a RI of 0,67), after ten unstable taxa; Arcusaurus, Pradhania, Xixipiosaurus, Yizhousaurus, Camelotia, Isanosaurus, Amygdalodon, Volkheimeria, Barapasaurus and Patagosaurus were excluded from the consensus. Bremer support = 1, Bootstrap support = 60.

## Character List

The complete list of characters used in the phylogenetic analysis is provided here. The following multistate characters were treated as ordered, summing to a total of 37: 8, 13, 19, 23, 40, 57, 69, 92, 102, 108, 117, 121, 134, 144, 147, 149, 150, 157, 167, 170, 171, 177, 205, 207, 222, 227, 242, 251, 254, 277, 294, 299, 336, 342, 349, 353, and 370.

This character list includes the characters listed by Yates (2007a), the characters added by Smith & Pol (2007), those added by Apaldetti *et al.* (2012), Otero & Pol (2013), Otero *et al.* (2015) and Cerda *et al.* (2017).

### Skull

1. Skull to femur ratio: greater than (0), or less than (1), 0.6 (modified from Gauthier, 1986).
2. Lateral plates appressed to the labial side of the premaxillary, maxillary, and dentary teeth: absent (0) or present (1) (Upchurch, 1995).
3. Relative height of the rostrum at the posterior margin of the naris: more than (0), or less than (1), 0.6 times the height of the skull at the middle of the orbit (Langer, 2004).
4. Foramen on the lateral surface of the premaxillary body: absent (0) or present (1) Yates (2007a).
5. Distal end of the dorsal premaxillary process: tapered (0) or transversely expanded (1) (Serenio, 1999).
6. Profile of premaxilla: convex (0) or with an inflection at the base of the dorsal process (1) (Upchurch, 1995).
7. Size and position of the posterolateral process of premaxilla: large and lateral to the anterior process of the maxilla (0) or small and medial to the anterior process of the maxilla (1) Yates (2007a).
8. Relationship between posterolateral process of the premaxilla and the anteroventral process of the nasal: broad sutured contact (0), point contact (1), or separated by maxilla (2) (modified from Gauthier, 1986). Ordered.
9. Posteromedial process of the premaxilla: absent (0) or present (1) (Rauhut, 2003).
10. Shape of the anteromedial process of the maxilla: narrow, elongated, and projecting anterior to lateral premaxilla–maxilla suture (0) or short, broad, and level with lateral premaxilla–maxilla suture (1) Yates (2007a).
11. Development of external narial fossa: absent to weak (0) or well developed with sharp posterior and anteroventral rims (1) Yates (2007a).

12. Development of narial fossa on the anterior ramus of the maxilla: weak and orientated laterally to dorsolaterally (0) or well developed and forming a horizontal shelf (1) (modified from Upchurch, 1995)
13. Size and position of subnarial foramen: absent (0), small (no larger than adjacent maxillary neurovascular foramina) and positioned outside of narial fossa (1), or large and on the rim of, or inside, the narial fossa (2) (modified from Sereno *et al.*, 1993). Ordered.
14. Shape of subnarial foramen: rounded (0) or slot shaped (1) Yates (2007a).
15. Maxillary contribution to the margin of the narial fossa: absent (0) or present (1) Yates (2007a).
16. Diameter of external naris: less than (0), or greater than (1), 0.5 times the orbital diameter (Wilson & Sereno, 1998).
17. Shape of the external naris (in adults): rounded (0) or subtriangular with an acute posteroventral corner (1) (Galton & Upchurch, 2004).
18. Level of the anterior margin of the external naris: anterior to (0) or posterior to (1) the midlength of the premaxillary body (Rauhut, 2003).
19. Level of the posterior margin of external naris: anterior to, or level with, the premaxilla–maxilla suture (0), posterior to the first maxillary alveolus (1), or posterior to the midlength of the maxillary tooth row and the anterior margin of the antorbital fenestra (2) (modified from Wilson & Sereno, 1998). Ordered.
20. Dorsal profile of the snout: straight to gently convex (0) or with a depression behind the naris (1) Yates (2007a).
21. Elongate median nasal depression: absent (0) or present (1) (Sereno, 1999).
22. Width of anteroventral process of nasal at its base: less than (0) or greater than (1) width of anterodorsal process at its base (modified from Sereno, 1999).
23. Nasal relationship with dorsal margin of antorbital fossa: not contributing to the margin of the antorbital fossa (0), lateral margin overhangs the antorbital fossa and forms its dorsal margin (1), overhang extensive, obscuring the dorsal lachrymal–maxilla contact in lateral view (2) (modified from Sereno, 1999).
24. Pointed caudolateral process of the nasal overlapping the lachrymal: absent (0) or present (1) (Sereno, 1999).
25. Anterior profile of the maxilla: slopes continuously towards the rostral tip (0) or with a strong inflection at the base of the ascending ramus, creating a rostral ramus with parallel dorsal and ventral margins (1) (Sereno *et al.*, 1996).

26. Length of rostral ramus of the maxilla: less than (0), or greater than (1), its dorsoventral depth (Serenio *et al.*, 1996).
27. Shape of the main body of the maxilla: tapering posteriorly (0) or dorsal and ventral margins parallel for most of their length (1) Yates (2007a).
28. Shape of the ascending ramus of the maxilla in lateral view: tapering dorsally (0) or with an anteroposterior expansion at the dorsal end (1) Yates (2007a).
29. Rostrocaudal length of the antorbital fossa: greater (0), or less (1), than that of the orbit (Yates, 2003a).
30. Posteroventral extent of medial wall of antorbital fossa: reaching (0), or terminating anterior to (1), the anterior tip of the jugal (modified from Galton & Upchurch, 2004).
31. Development of the antorbital fossa on the ascending ramus of the maxilla: deeply impressed and delimited by a sharp, scarp-like rim (0) or weakly impressed and delimited by a rounded rim or a change in slope (1) Yates (2007a).
32. Shape of the antorbital fossa: crescentic with a strongly concave posterior margin that is roughly parallel to the rostral margin of the antorbital fossa (0), subtriangular with a straight to gently concave posterior margin (1), or antorbital fossa absent (2) (modified from Galton, 1985).
33. Size of the neurovascular foramen at the caudal end of the lateral maxillary row: not larger than the others (0) or distinctly larger than the others in the row (1) (Yates, 2003a).
34. Direction that the neurovascular foramen at the caudal end of the lateral maxillary row opens: caudally (0) or rostrally, ventrally, or laterally (1) (modified from Sereno, 1999).
35. Arrangement of lateral maxillary neurovascular foramina: linear (0) or irregular (1) (modified from Sereno, 1999).
36. Longitudinal ridge on the posterior lateral surface of the maxilla: absent (0) or present (1) (Barrett, Upchurch & Wang, 2005).
37. Dorsal exposure of the lachrymal: present (0) or absent (1) (Gauthier, 1986).
38. Shape of the lachrymal: dorsoventrally short and block-shaped (0) or dorsoventrally elongate and shaped like an inverted L (1) (Rauhut, 2003).
39. Orientation of the lachrymal orbital margin: strongly sloping anterodorsally (0) or erect and close to vertical (1) Yates (2007a).
40. Length of the anterior ramus of the lachrymal: greater than (0), or less than (1), half the length of the ventral ramus, or absent altogether (2) (modified from Galton, 1990). Ordered.

41. Web of bone spanning junction between anterior and ventral rami of lachrymal: absent and antorbital fossa laterally exposed (0) or present, obscuring posterodorsal corner of antorbital fossa (1) Yates (2007a).
42. Extension of the antorbital fossa onto the ventral end of the lachrymal: present (0) or absent (1) (modified from Wilson & Sereno, 1998).
43. Length of the caudal process of the prefrontal: short (0), or elongated (1), so that total prefrontal length is equal to the rostrocaudal diameter of the orbit (Galton, 1985).
44. Ventral process of prefrontal extending down the posteromedial side of the lachrymal: present (0) or absent (1) (Wilson & Sereno, 1998).
45. Maximum transverse width of the prefrontal: less than (0), or more than (1), 0.25 times the skull width at that level (modified from Galton, 1990).
46. Shape of the orbit: subcircular (0) or ventrally constricted, making the orbit subtriangular (1) (Wilson & Sereno, 1998).
47. Slender anterior process of the frontal intruding between the prefrontal and the nasal: absent (0) or present (1) (modified from Sereno, 1999).
48. Jugal–lachrymal relationship: lachrymal overlapping lateral surface of jugal or abutting it dorsally (0), or jugal overlapping lachrymal laterally (1) (Sereno *et al.*, 1993).
49. Shape of the suborbital region of the jugal: an anteroposteriorly elongate bar (0) or an anteroposteriorly shortened plate (1) Yates (2007a).
50. Jugal contribution to the antorbital fenestra: absent (0) or present (1) (Holtz, 1994).
51. Dorsal process of the anterior jugal: present (0) or absent (1) (modified from Rauhut, 2003).
52. Ratio of the minimum depth of the jugal below the orbit to the distance between the rostral end of the jugal and the rostroventral corner of the infratemporal fenestra: less than (0), or greater than (1), 0.2 (modified from Galton, 1985).
53. Transverse width of the ventral ramus of the postorbital: less than (0), or greater than (1), its rostrocaudal width at midshaft (Wilson & Sereno, 1998).
54. Shape of the dorsal margin of postorbital in lateral view: straight to gently curved (0) or with a distinct embayment between the anterior and posterior dorsal processes (1) Yates (2007a).
55. Height of the postorbital rim of the orbit: flush with the posterior lateral process of the

postorbital (0) or raised so that it projects laterally to the posterior dorsal process (1) Yates (2007a).

56. Postfrontal bone: present (0) or absent (1) (Serenio *et al.*, 1993).

57. Position of the rostral margin of the infratemporal fenestra: behind the orbit (0), extends under the rear half of the orbit (1), or extends as far forward as the midlength of the orbit (2) (modified from Upchurch, 1995). Ordered.

58. Frontal contribution to the supratemporal fenestra: present (0) or absent (1) (modified from Gauthier, 1986).

59. Orientation of the long axis of the supratemporal fenestra: longitudinal (0) or transverse (1) (Wilson & Serenio, 1998).

60. Medial margin of supratemporal fossa: simple smooth curve (0) or with a projection at the frontal/postorbital–parietal suture producing a scalloped margin (1) (Leal *et al.*, 2004).

61. Length of the quadratojugal ramus of the squamosal relative to the width at its base: less than (0), or greater than (1), four times its width (Serenio, 1999).

62. Proportion of infratemporal fenestra bordered by squamosal: more than (0), or less than (1), 0.5 times the depth of the infratemporal fenestra.

63. Squamosal–quadratojugal contact: present (0) or absent (1) (Gauthier, 1986).

64. Angle of divergence between jugal and squamosal rami of quadratojugal: close to 90° (0) or close to parallel (1) Yates (2007a).

65. Length of jugal ramus of quadratojugal: no longer than (0), or longer than (1), the squamosal ramus (Wilson & Serenio, 1998).

66. Shape of the rostral end of the jugal ramus of the quadratojugal: tapered (0) or dorsoventrally expanded (1) (Wilson & Serenio, 1998).

67. Relationship of quadratojugal to jugal: jugal overlaps the lateral surface of the quadratojugal (0), quadratojugal overlaps the lateral surface of the jugal (1), or quadratojugal sutures along the ventrolateral margin of the jugal (2). Unordered.

68. Position of the quadrate foramen: on the quadrate–quadratojugal suture (0), deeply incised into, and partly encircled by, the quadrate (1), or on the quadrate–squamosal suture, just below the quadrate head (2) (modified from Rauhut, 2003). Unordered.

69. Shape of posterolateral margin of quadrate: sloping anterolaterally from posteromedial ridge (0), everted posteriorly creating a posteriorly facing fossa (1), posterior fossa deeply excavated, invading quadrate body (2) (Wilson & Serenio, 1998). Ordered.

70. Exposure of the lateral surface of the quadrate head: absent, covered by lateral sheet of the squamosal (0) or present (1) (Sereno *et al.*, 1993).
71. Percentage of the length of the quadrate that is occupied by the pterygoid wing: at least 70% (0) or greater than 70% (1) (Yates, 2003a).
72. Depth of the occipital wing of the parietal: less than (0), or more than (1), 1.5 times the depth of the foramen magnum (Wilson & Sereno, 1998).
73. Position of foramina for midcerebral vein on occiput: between supraoccipital and parietal (0) or on the supraoccipital (1) (modified from Yates, 2003a).
74. Postparietal fenestra between supraoccipital and parietals: absent (0) or present (1) Yates (2007a).
75. Shape of the supraoccipital: diamond-shaped, at least as high as wide (0), or semilunate and wider than high (1) (Yates, 2003b).
76. Orientation of the supraoccipital plate: erect to gently sloping (0) or strongly sloping forward so that the dorsal tip lies level with the basiptyergoid processes (1) (Galton & Upchurch, 2004).
77. Orientation of the paroccipital processes in occipital view: slightly dorsolaterally directed to horizontal (0) or ventrolaterally directed (1) (Rauhut, 2003).
78. Orientation of the paroccipital processes in dorsal view: posterolateral forming a V-shaped occiput (0) or lateral forming a flat occiput (1) (Wilson, 2002).
79. Size of the post-temporal fenestra: large fenestra (0) or a small hole that is much less than half the depth of the paroccipital process (1) Yates (2007a).
80. Exit of the midcerebral vein: through trigeminal foramen (0) or through a separate foramen anterodorsal to trigeminal foramen (1) (Rauhut, 2003).
81. Shape of the floor of the braincase in lateral view: relatively straight with the basal tuberae, basiptyergoid processes, and parasphenoid rostrum roughly aligned (0), bent with the basiptyergoid processes and the parasphenoid rostrum below the level of the basioccipital condyle and the basal tuberae (1), or bent with the basal tuberae lowered below the level of the basioccipital and the parasphenoid rostrum raised above it (2) (modified from Galton, 1990). Unordered.
82. Shape of basal tuberae: knob-like, with basisphenoidal component rostral to basioccipital component (0), or forming a transverse ridge with the basisphenoidal component lateral to the basioccipital component (1) Yates (2007a).

83. Length of the basiptyergoid processes (from the top of the parasphenoid to the tip of the process): less than (0), or greater than (1), the height of the braincase (from the top of the parasphenoid to the top of the supraoccipital) (Benton *et al.*, 2000).
84. Ridge formed along the junction of the parabasisphenoid and the basioccipital, between the basal tuberae: present with a smooth rostral face (0), present with a median fossa on the rostral face (1), or absent with the basal tuberae being separated by a deep, caudally opening U-shaped fossa (2) Yates (2007a). Unordered.
85. Deep septum spanning the interbasiptyergoid space: absent (0) or present (1) (Galton, 1990).
86. Dorsoventral depth of the parasphenoid rostrum: much less than (0), or about equal to (1), the transverse width (Yates, 2003a).
87. Shape of jugal process of ectoptyergoid: gently curved (0) or strongly recurved and hook-like (1) (Yates, 2003a).
88. Pneumatic fossa on the ventral surface of the ectoptyergoid: present (0) or absent (1) (Sereno *et al.*, 1996).
89. Relationship of the ectoptyergoid to the ptyergoid: ectoptyergoid overlapping the ventral (0), or dorsal (1), surface of the ptyergoid (Sereno *et al.*, 1993).
90. Position of the maxillary articular surface of the palatine: along the lateral margin of the bone (0) or at the end of a narrow anterolateral process owing to the absence of the posterolateral process (1) (Wilson & Sereno, 1998).
91. Centrally located tubercle on the ventral surface of palatine: absent (0) or present (1) Yates (2007a).
92. Medial process of the ptyergoid forming a hook around the basiptyergoid process: absent (0), flat and blunt-ended (1), or bent upward and pointed (2) (modified from Wilson & Sereno, 1998). Ordered.
93. Length of the vomers: less than (0), or more than (1), 0.25 times the total skull length Yates (2007a).
94. Position of jaw joint: no lower than the level of the dorsal margin of the dentary (0) or depressed well below this level (1) (Sereno, 1999).
95. Shape of upper jaws in ventral view: narrow with an acute rostral apex (0) or broad and U-shaped (1) (Wilson & Sereno, 1998).
96. Length of the external mandibular fenestra: more than (0), or less than (1), 0.1 times the length of the mandible (modified from Upchurch, 1995).

97. Caudal end of dentary tooth row medially inset with a thick lateral ridge on the dentary forming a buccal emargination: absent (0) or present (1) (Gauthier, 1986).
98. Height: length ratio of the dentary: less than (0), or greater than (1), 0.2 modified from Benton *et al.*, 2000).
99. Orientation of the symphyseal end of the dentary: in line with the long axis of the dentary (0) or strongly curved ventrally (1) (Sereno, 1999).
100. Position of first dentary tooth: adjacent to symphysis (0) or inset one tooth's width from the symphysis (1) (Sereno, 1999).
101. Dorsoventral expansion at the symphyseal end of the dentary: absent (0) or present (1) (Wilson & Sereno, 1998).
102. Splenial foramen: absent (0), present and enclosed (1), or present and open anteriorly (2) (Rauhut, 2003). Ordered.
103. Splenial-angular joint: flattened sutured contact (0), synovial joint surface between tongue-like processes of angular, fitting in groove of the splenial (1) (Sereno *et al.*, 1993).
104. A stout, triangular, medial process of the articular, behind the glenoid: present (0) or absent (1) (Yates, 2003a).
105. Length of the retroarticular process: less than (0), or greater than (1), than the depth of the mandible below the glenoid (Yates, 2003a).
106. Strong medial embayment behind glenoid of the articular in dorsal view: absent (0), or present (1) (Yates & Kitching, 2003).
107. Number of premaxillary teeth: four (0) or more than four (1) (Galton, 1990).
108. Number of dentary teeth (in adults): fewer than 18 (0) or 18 or more (1) (modified from Wilson & Sereno, 1998).
109. Arrangement of teeth within the jaws: linearly placed, crowns not overlapping (0) or imbricated with distal side of tooth overlapping mesial side of the succeeding tooth (1) Yates (2007a).
110. Orientation of the maxillary tooth crowns: erect (0) or procumbent (1) (modified from Gauthier, 1986).
111. Orientation of the dentary tooth crowns: erect (0) or procumbent (1) (modified from Gauthier, 1986).
112. Teeth with basally constricted crowns: absent (0) or present (1) (Gauthier, 1986).

113. Tooth–tooth occlusal wear facets: absent (0) or present (1) (Wilson & Sereno, 1998).

114. Mesial and distal serrations of the teeth: fine and set at right angles to the margin of the tooth (0) or coarse and angled upwards at an angle of 45° to the margin of the tooth (1) (Benton *et al.*, 2000).

115. Distribution of serrations on the maxillary and dentary teeth: present on both the mesial and distal carinae (0), absent on the posterior carinae (1), or absent on both carinae (2) (Wilson, 2002). Unordered.

116. Long axis of the tooth crowns distally recurved: present (0) or absent (1) (Gauthier, 1986).

117. Texture of the enamel surface: entirely smooth (0), finely wrinkled in some patches (1), or extensively and coarsely wrinkled (2) (modified from Wilson & Sereno, 1998).

118. Lingual concavities of the teeth: absent (0) or present (1) (Upchurch, 1995).

119. Longitudinal labial grooves on the teeth: absent (0) or present (1) (Upchurch, 1998).

120. Distribution of the serrations along the mesial and distal carinae of the tooth: extend along most of the length of the crown (0) or are restricted to the upper half of the crown (1) (Yates, 2003a).

#### Vertebrae

121. Number of cervical vertebrae: eight or fewer (0), nine to ten (1), 12–13 (2), or more than 13 (3) (modified from Wilson & Sereno, 1998). Ordered.

122. Shallow, dorsally facing fossa on the atlantal neurapophysis bordered by a dorsally everted lateral margin: absent (0) or present (1) (Yates & Kitching, 2003).

123. Width of axial intercentrum: less than (0), or greater than (1), width of axial centrum (Sereno, 1999).

124. Position of axial prezygapophyses: on the anterolateral surface of the neural arch (0) or mounted on anteriorly projecting pedicels (1) Yates (2007a).

125. Posterior margins of the axial postzygapophyses: overhang the axial centrum (0) or are flush with the caudal face of the axial centrum (1) (Sereno, 1999).

126. Length of the axial centrum: less than (0), or at least (1), three times the height of the centrum Yates (2007a).

127. Length of the anterior cervical centra (cervicals 3–5): no more than (0), or greater than (1), the length of the axial centrum Yates (2007a).

128. Length of middle to posterior cervical centra (cervicals 6–8): no more than (0), or greater than (1), the length of the axial centrum Yates (2007a).
129. Dorsal excavation of the cervical parapophyses: absent (0) or present (1) (Upchurch, 1998).
130. Lateral compression of the anterior cervical vertebrae: centra are no higher than they are wide (0) or are approximately 1.25 times higher than wide (1) (Upchurch, 1998).
131. Relative elongation of the anterior cervical centra (cervicals 3–5): lengths of the centra are less than 2.5 times the height of their anterior faces (0), lengths are 2.5–4 times the height of their anterior faces (1) or the length of at least cervicals 4 or 5 exceeds four times the anterior centrum height (2) (modified from Sereno, 1999). Ordered.
132. Ventral keels on cranial cervical centra: present (0) or absent (1) (modified from Upchurch, 1998).
133. Height of the midcervical neural arches: no more than (0), or greater than (1), height of the posterior centrum face Yates (2007a).
134. Cervical epipophyses on the dorsal surface of the postzygapophyses: absent (0), or present on at least some cervical vertebrae (1).
135. Caudal ends of cranial, postaxial epipophyses: with a free pointed tip (0) or joined to the postzygapophysis along their entire length (1) Yates (2007a).
136. Shape of the epipophyses: tall ridges (0) or flattened, horizontal plates (1) (Yates, 2003a).
137. Epipophyses overhanging the rear margin of the postzygapophyses: absent (0), or present in at least some postaxial cervical vertebrae (1) (Sereno *et al.*, 1993).
138. Anterior spur-like projections on midcervical neural spines: absent (0) or present (1) Yates (2007a).
139. Shape of midcervical neural spines: less than (0), or at least (1), twice as long as high Yates (2007a).
140. Shape of cervical rib shafts: short and posteroventrally directed (0) or longer than the length of their centra and extending parallel to cervical column (1) (Sereno, 1999).
141. Position of the base of the cervical rib shaft: level with, or higher than, the ventral margin of the cervical centrum (0) or located below the ventral margin because of a ventrally extended parapophysis (1) (Wilson & Sereno, 1998).

142. Postzygodiapophyseal lamina in cervical neural arches 4–8: present (0) or absent (1) (Yates, 2003a).

143. Laminae of the cervical neural arches 4–8: well, developed tall laminae (0) or weakly developed low ridges (1) (Wilson & Sereno, 1998).

144. Shape of anterior centrum face in cervical centra: concave (0), flat (1), or convex (2) (modified from Gauthier, 1986). Ordered.

145. Ventral surface of the centra in the cervicodorsal transition: transversely rounded (0) or with longitudinal keels (1) (Rauhut, 2003).

146. Number of vertebrae between cervicodorsal transition and primordial sacral vertebrae: 15–16 (0) or no more than 14 (1) (modified from Wilson & Sereno, 1998).

147. Lateral surfaces of the dorsal centra: with at most vague, shallow depressions (0), with deep fossae that approach the midline (1), or with invasive, sharp-rimmed pleurocoels (2) (Gauthier, 1986). Ordered.

148. Oblique ridge dividing pleural fossa of cervical vertebrae: absent (0) or present (1) (Wilson & Sereno, 1998).

149. Laterally expanded tables at the midlength of the dorsal surface of the neural spines: absent in all vertebrae (0), present on the pectoral vertebrae (1) or present on the pectoral and cervical vertebrae (2) (Yates & Kitching, 2003). Ordered.

150. Dorsal centra: entirely amphicoelous to amphiplatyan (0), first two dorsals are opisthocoelous (1), or cranial half of dorsal column is opisthocoelous (2) (Wilson & Sereno, 1998). Ordered.

151. Shape of the posterior dorsal centra: relatively elongated for their size (0) strongly axially compressed for their size (1) (modified from Novas, 1993).

152. Laminae bounding triangular infradiapophyseal fossae (chonae) on dorsal neural arches: absent (0) or present (1) (Wilson, 1999).

153. Location of parapophysis in first two dorsals: at the anterior end of the centrum (0), or located at the midlength of the centrum, within the middle chonos (1) Yates (2007a).

154. Parapophyses of the dorsal column completely shift from the centrum to the neural arch: anterior (0), or posterior (1), to the thirteenth presacral vertebra (Langer, 2004).

155. Orientation of the transverse processes of the dorsal vertebrae: most horizontally directed (0) or all upwardly directed (1) (Upchurch, 1998).

156. Contribution of the paradiapophyseal lamina to the margin of the anterior chonos in

mid-dorsal vertebrae: present (0) or prevented by high placement of parapophysis (1) Yates (2007a).

157. Hyposphenes in the dorsal vertebrae: absent (0), present but less than the height of the neural canal (1), or present and equal to the height of the neural canal (2) (modified from Gauthier, 1986). Ordered.

158. Prezygodiapophyseal lamina and associated anterior triangular fossa (chonos): present on all dorsals (0) or absent in mid-dorsals (1) (Yates, 2003a).

159. Anterior centroparapophyseal lamina in dorsal vertebrae: absent (0) or present (1) (Wilson, 2002).

160. Prezygoparapophyseal lamina in dorsal vertebrae: absent (0) or present (1) Yates (2007a).

161. Accessory lamina dividing posterior chonos from postzygapophysis: absent (0) or present (1) Yates (2007a).

162. Lateral pneumatic fenestra in middle chonos of middle and posterior dorsal vertebrae opening into neural cavity: absent (0) or present (1) (Wilson & Sereno, 1998).

163. Separation of lateral surfaces of anterior dorsal neural arches under transverse processes: widely spaced (0) or only separated by a thin midline septum (1) (Upchurch *et al.* 2004).

164. Height of dorsal neural arches, from neurocentral suture to level of zygapophyseal facets: much less than (0), or subequal to or greater than (1), height of centrum Yates (2007a).

165. Form of anterior surface of neural arch: simple centroprezygapophyseal ridge (0) or broad anteriorly facing surface bounded laterally by centroprezygapophyseal lamina (1) (Bonaparte, 1999).

166. Shape of posterior dorsal neural canal: subcircular (0) or slit-shaped (1) (Wilson & Sereno, 1998).

167. Height of middle dorsal neural spines: less than the length of the base (0), higher than the length of the base but less than 1.5 times the length of the base (1) or greater than 1.5 times the length of the base (2) (modified from Bonaparte, 1986). Ordered.

168. Shape of anterior dorsal neural spines: lateral margins parallel in anterior view (0) or transversely expanding towards dorsal end (1) Yates (2007a).

169. Cross-sectional shape of dorsal neural spines: transversely compressed (0), broad and triangular (1), or square-shaped in posterior vertebrae (2) (modified from Bonaparte, 1986).

170. Spinodiapophyseal lamina on dorsal vertebrae: absent (0), present and separated from spinopostzygapophyseal lamina (1) or present and joining spinopostzygapophyseal lamina to create a composite posterolateral spinal lamina (Wilson & Sereno, 1998).
171. Well-developed, sheet-like suprapostzygapophyseal laminae: absent (0), present on at least the caudal dorsal vertebrae (1) (Bonaparte, 1986).
172. Shape of the spinopostzygapophyseal lamina in middle and posterior dorsal vertebrae: singular (0) or bifurcated at its distal end (1) (Wilson, 2002).
173. Shape of posterior margin of middle dorsal neural spines in lateral view: approximately straight (0) or concave with a projecting posterodorsal corner (1) (Yates, 2003b).
174. Transversely expanded plate-like summits of posterior dorsal neural spines: absent (0) or present (1) (Novas, 1993).
175. Last presacral rib: free (0) or fused to vertebra (1) Yates (2007a).
176. Sacral rib much narrower than the transverse process of the first primordial sacral vertebra (and dorsosacral if present) in dorsal view: absent (0) or present (1) (Yates & Kitching, 2003).
177. Number of dorsosacral vertebrae: none (0), one (1), or two (2) (modified from Gauthier, 1986). Ordered.
178. Caudosacral vertebra: absent (0) or present (1) (Galton & Upchurch, 2004).
179. Shape of the iliac articular facets of the first primordial sacral rib: singular (0) or divided into dorsal and ventral facets separated by a non-articulating gap (1) Yates (2007a).
180. Depth of the iliac articular surface of the primordial sacra: less than (0), or greater than (1), 0.75 times the depth of the ilium (modified from Novas, 1992).
181. Sacral ribs contributing to the rim of the acetabulum: absent (0) or present (1) (Wilson, 2002).
182. Posterior and anterior expansion of the transverse processes of the first and second primordial sacral vertebrae, respectively, partly roofing the intercostal space: absent (0) or present (1) (Langer, 2004).
183. Length of first caudal centrum: greater than (0), or less than (1), its height (Yates, 2003a).
184. Length of base of the proximal caudal neural spines: less than (0), or greater than (1), half the length of the neural arch (Gauthier, 1986).

185. Position of postzygapophyses in proximal caudal vertebrae: protruding with an interpostzygapophyseal notch visible in dorsal view (0) or placed on either side of the caudal end of the base of the neural spine without any interpostzygapophyseal notch (1) (Yates, 2003a).

186. A hyposphenal ridge on caudal vertebrae: absent (0) or present (1) (Upchurch, 1995).

187. Depth of the bases of the proximal caudal transverse processes: shallow, restricted to the neural arches (0), deep, extending from the centrum to the neural arch (1) (Upchurch, 1998).

188. Position of last caudal vertebra with a protruding transverse process: distal (0), or proximal (1), to caudal 16 (Wilson, 2002).

189. Orientation of posterior margin of proximal caudal neural spines: sloping posterodorsally (0) or vertical (1) (Novas, 1992).

190. Longitudinal ventral sulcus on proximal and middle caudal vertebrae: present (0) or absent (1) (modified from Upchurch, 1995).

191. Length of midcaudal centra: greater than (0), or less than (1), twice the height of their anterior faces (Yates, 2003a).

192. Cross-sectional shape of the distal caudal centra: oval with rounded lateral and ventral sides (0) or square-shaped with flattened lateral and ventral sides (1) Yates (2007a).

193. Length of distal caudal prezygapophyses: short, not overlapping the preceding centrum by more than a quarter (0) or long and overlapping the preceding centrum by more than a quarter (Gauthier, 1986).

194. Shape of the terminal caudal vertebrae: unfused, size decreasing toward tip (0) or expanded and fused to form a club-shaped tail (1) (Upchurch, 1995).

195. Length of the longest chevron: is less than (0), or greater than (1), twice the length of the preceding centrum (modified from Yates, 2003a).

196. Anteroventral process on distal chevrons: absent (0) or present (1) (Upchurch, 1995).

197. Midcaudal chevrons with a ventral slit: absent (0) or present (1) (Upchurch, 1995).

#### Appendicular skeleton

198. Longitudinal ridge on the dorsal surface of the sternal plate: absent (0) or present (1) (Upchurch, 1998).

199. Craniocaudal length of the acromion process of the scapula: less than (0), or greater than (1), 1.5 times the minimum width of the scapula blade

(Wilson & Sereno, 1998).

200. Minimum width of the scapula: less than (0), or greater than (1), 20% of its length (Gauthier, 1986).

201. Caudal margin of the acromion process of the scapula: rises from the blade at angle that is less than (0), or greater than (1), 65° from the long axis of the scapula at its steepest point (modified from Novas, 1992).

202. Width of dorsal expansion of the scapula: less than (0), or equal to (1), the width of the ventral end of the scapula (Pol & Powell, 2007b).

203. Flat, caudoventrally facing surface on the coracoid between glenoid and coracoid tubercle: absent (0) or present (1) (Yates & Kitching, 2003).

204. Coracoid tubercle: present (0) or absent (1) (modified from Pérez-Moreno *et al.* 1994).

205. Length of the humerus: less than 55% (0), 55–65% (1), 65–70% (2), or more than 70% (3), of the length of the femur (modified from Gauthier, 1986). Ordered.

206. Shape of the deltopectoral crest: subtriangular (0) or sub-rectangular (1) (Gauthier, 1986).

207. Length of the deltopectoral crest of the humerus: less than 30% (0), 30–50% (1), or greater than 50% (2), of the length of the humerus (modified from Sereno *et al.*, 1993). Ordered.

208. Shape of the anterolateral margin of the deltopectoral crest of the humerus: straight (0) or strongly sinuous (1) (Yates, 2003a).

209. Rugose pit centrally located on the lateral surface of the deltopectoral crest: absent (0) or present (1) Yates (2007a).

210. Well-defined fossa on the distal flexor surface of the humerus: present (0) or absent (1) (Yates & Kitching, 2003).

211. Transverse width of the distal humerus: is less than (0), or greater than (1), 33% of the length of the humerus (Langer, 2004).

212. Shape of the entepicondyle of the distal humerus: rounded process (0) or with a flat, distomedially facing surface bounded by a sharp proximal margin (1) Yates (2007a).

213. Length of the radius: greater than (0), or less than (1), 80% of the length of the humerus (Langer, 2004).

214. Deep radial fossa, bounded by an anterolateral process, on proximal ulna: absent (0) or present (1) (Wilson & Sereno, 1998).

215. Olecranon process on proximal ulna: present (0) or absent (1) (Wilson & Sereno, 1998).
216. Maximum linear dimensions of the ulnare and radiale: exceed that of at least one of the first three distal carpals (0) or are less than any of the distal carpals (1) (Yates, 2003a).
217. Transverse width of the first distal carpal: less than (0), or greater than (1), 120% of the transverse width of the second distal carpal (Sereno, 1999).
218. Sulcus across the medial end of the first distal carpal: absent (0) or present (1) Yates (2007a). 219. Lateral end of first distal carpal: abuts (0), or overlaps (1), second distal carpal (Yates, 2003a).
220. Second distal carpal: does (0), or does not (1), completely cover the proximal end of the second metacarpal (Yates & Kitching, 2003).
221. Ossification of the fifth distal carpal: present (0) or absent (1) Yates (2007a).
222. Length of the manus: less than 38% (0), 38–45% (1), or greater than 45% (2), of the humerus + radius (modified from Sereno *et al.*, 1993). Ordered.
223. Shape of metacarpus: flattened to gently curved and spreading (0) or a colonnade of subparallel metacarpals tightly curved into a U-shape (1) (Wilson & Sereno, 1998).
224. Proximal width of first metacarpal: less than (0), or greater than (1), the proximal width of the second metacarpal (modified from Gauthier, 1986).
225. Minimum transverse shaft width of first metacarpal: less than (0), or greater than (1), twice the minimum transverse shaft width of second metacarpal Yates (2007a).
226. Proximal end of first metacarpal: flush with other metacarpals (0) or inset into the carpus (1) (Sereno, 1999).
227. Shape of the first metacarpal: proximal width less than 65% (0), 65–80% (1), 80–100% (2), or greater than 100% (3), of its length (modified from Sereno, 1999). Ordered.
228. Strong asymmetry in the lateral and medial distal condyles of the first metacarpal: absent (0) or present (1) (Gauthier, 1986).
229. Deep distal extensor pits on the second and third metacarpals: absent (0) or present (1) (Novas, 1993).
230. Shape of the distal ends of second and third metacarpals: sub-rectangular in distal view (0) or trapezoidal with flexor rims of distal collateral ligament pits flaring beyond extensor rims (1) Yates (2007a).

231. Shape of the fifth metacarpal: longer than wide at the proximal end with a flat proximal surface (0) or close to as wide as it is long with a strongly convex proximal articulation surface (1) (Yates, 2003a).

232. Length of the fifth metacarpal: less than (0), or greater than (1), 75% of the length of the third metacarpal (Upchurch, 1998).

233. Length of manual digit one: less than (0), or greater than (1), the length of manual digit two (Yates, 2003a).

234. Ventrolateral twisting of the transverse axis of the distal end of the first phalanx of manual digit one relative to its proximal end: absent (0), present but much less than 60° (1), or 60° (2) (Sereno, 1999). Ordered.

235. Length of the first phalanx of manual digit one: less than (0), or greater than (1), the length of the first metacarpal (Gauthier, 1986).

236. Shape of the proximal articular surface of the first phalanx of manual digit one: rounded (0) or with an embayment on the medial side (1) (modified from Sereno, 1999).

237. Shape of the first phalanx of manual digit one: elongate and subcylindrical (0) or strongly proximodistally compressed and wedge-shaped (1) (Wilson, 2002).

238. Length of the penultimate phalanx of manual digit two: less than (0), or greater than (1), the length of the second metacarpal (Rauhut, 2003).

239. Length of the penultimate phalanx of manual digit three: less than (0), or greater than (1), the length of the third metacarpal (Rauhut, 2003).

240. Shape of nonterminal phalanges of manual digits two and three: longer than wide (0) or as long as wide (1) (Yates, 2003a).

241. Shape of the unguals of manual digits two and three: straight (0), or strongly curved with tips projecting well below flexor margin of proximal articular surface (1) (Sereno *et al.*, 1993).

242. Length of the ungual of manual digit two: greater than the length of the ungual of manual digit one (0), 75–100% of the ungual of manual digit one (1), less than 75% of the ungual of manual digit one (2), or the ungual of manual digit two is absent (3) (modified from Gauthier, 1986). Ordered.

243. Phalangeal formula of manual digits two and three: three and four, respectively (0), or with at least one phalanx missing from each digit (1) (modified from Wilson & Sereno, 1998).

244. Phalangeal formula of manual digits four and five: greater than (0), or less than (1), 2–0, respectively (Gauthier, 1986).

245. Strongly convex dorsal margin of the ilium: absent (0) or present (1) (Gauthier, 1986).
246. Cranial extent of preacetabular process of ilium: does not (0), or does (1), project further forward than cranial end of the pubic peduncle (Yates, 2003a).
247. Shape of the preacetabular process: blunt and rectangular (0) or with a pointed, projecting cranioventral corner and a rounded dorsum (1) (modified from Sereno, 1999).
248. Depth of the preacetabular process of the ilium: much less than (0), or subequal to (1), the depth of the ilium above the acetabulum (modified from Gauthier, 1986).
249. Length of preacetabular process of the ilium: less than (0), or greater than (1), twice its depth.
250. Buttress between preacetabular process and the supra-acetabular crest of the ilium: present (0) or absent (1) (Gauthier, 1986).
251. Medial wall of acetabulum: fully closing acetabulum with a triangular ventral process between the pubic and ischial peduncles (0), partially open acetabulum with a straight ventral margin between the peduncles (1), partially open acetabulum with a concave ventral margin between the peduncles (2), or fully open acetabulum with medial ventral margin closely approximating lateral rim of acetabulum (3) (modified from Gauthier, 1986). Ordered.
252. Length of the pubic peduncle of the ilium: less than (0), or greater than (1), twice the craniocaudal width of its distal end (Sereno, 1999).
253. Caudally projecting 'heel' at the distal end of the ischial peduncle: absent (0) or present (1) (Yates, 2003b).
254. Length of the ischial peduncle of the ilium: similar to pubic peduncle (0), much shorter than pubic peduncle (1), or virtually absent so that the chord connecting the distal end of the pubic peduncle with the ischial articular surface contacts the postacetabular process (2) (Upchurch *et al.* 2004). Ordered.
255. Length of the postacetabular process of the ilium: between 40 and 100% of the distance between the pubic and ischial peduncles (0), less than 40% of this distance (1), or more than 100% of this distance (2) Yates (2007a). Unordered.
256. Well-developed brevis fossa with sharp margins on the ventral surface of the postacetabular process of the ilium: absent (0) or present (1) (Gauthier, 1986).
257. Anterior end of ventrolateral ridge bounding brevis fossa: not connected to (0), or joining (1), supraacetabular crest (1) Yates (2007a).

258. Shape of the caudal margin of the postacetabular process of the ilium: rounded to bluntly pointed (0), square-ended (1), or with a pointed ventral corner and a rounded caudodorsal margin (2) (Yates, 2003b). Unordered.
259. Width of the conjoined pubes: less than (0), or greater than (1), 75% of their length (Cooper, 1984).
260. Pubic tubercle on the lateral surface of the proximal pubis: present (0) or absent (1) (Yates, 2003a).
261. Proximal anterior profile of pubis: anterior margin of pubic apron smoothly confluent with anterior margin of iliac pedicel (0) or iliac pedicel set anterior to the pubic apron, creating a prominent inflection in the proximal anterior profile of the pubis (1) Yates (2007a).
262. Minimum transverse width of the pubic apron: much more than (0), or less than (1), 40% of the width across the iliac peduncles of the ilium.
263. Position of the obturator foramen of the pubis: at least partially occluded by the iliac pedicel (0), or completely visible (1), in anterior view (Galton & Upchurch, 2004).
264. Lateral margins of the pubic apron in anterior view: straight (0) or concave (1) (Yates & Kitching, 2003).
265. Orientation of distal third of the blades of the pubic apron: confluent with the proximal part of the pubic apron (0) or twisted posterolaterally relative to proximal section so that the anterior surface turns to face laterally (1) (Langer, 2004).
266. Orientation of the entire blades of the pubic apron: transverse (0) or twisted posteromedially (1) (Wilson & Sereno, 1998).
267. Craniocaudal expansion of the distal pubis: absent (0), less than (1), or greater than (2), 15% of the length of the pubis (modified from Gauthier, 1986). Ordered.
268. Notch separating posteroventral end of the ischial obturator plate from the ischial shaft: present (0) or absent (1) (Rauhut, 2003).
269. Elongate interischial fenestra: absent (0) or present (1) (Yates, 2003b).
270. Longitudinal dorsolateral sulcus on proximal ischium: absent (0) or present (1) (Yates, 2003a).
271. Shape of distal ischium: broad and plate-like, not distinct from obturator region (0) or with a discrete, rod-like distal shaft (1) Yates (2007a).
272. Length of ischium: less than (0), or greater than (1), that of the pubis (Salgado, Coria &

Calvo, 1997).

273. Ischial component of acetabular rim: larger than (0), or equal to (1), the pubic component (Galton & Upchurch, 2004).

274. Shape of the transverse section of the ischial shaft: ovoid to sub-rectangular (0) or triangular (1) (Serenio, 1999).

275. Orientation of the long axes of the transverse section of the distal ischia: meet at an angle (0) or are coplanar (1) (Wilson & Sereno, 1998).

276. Depth of the transverse section of the ischial shaft: much less than (0), or at least as great as (1), the transverse width of the section (Wilson & Sereno, 1998).

277. Distal ischial expansion: absent (0) or present (1) (Holtz, 1994).

278. Transverse width of the conjoined distal ischial expansions: greater than (0), or less than (1), their sagittal depth (Yates, 2003a).

279. Length of the hindlimb: greater than (0), or less than (1), the length of the trunk (Gauthier, 1986).

280. Longitudinal axis of the femur in lateral view: strongly bent with an offset between the proximal and distal axes greater than  $15^\circ$  (0), weakly bent with an offset of less than  $10^\circ$  (1), or straight (2) (Cooper, 1984). Ordered.

281. Shape of the cross-section of the midshaft of the femur: subcircular (0) or strongly elliptical with the long axis orientated mediolaterally (1) (Wilson & Sereno, 1998).

282. Angle between the long axis of the femoral head and the transverse axis of the distal femur: about  $30^\circ$  (0) or close to  $0^\circ$  (1) (Carrano, 2000).

283. Shape of femoral head: roughly rectangular in profile with a sharp medial distal corner (0) or roughly hemispherical with no sharp medial distal corner (1) Yates (2007a).

284. Posterior proximal tubercle on femur: well developed (0) or indistinct to absent (1) (Novas, 1996).

285. Shape of the lesser trochanter: small rounded tubercle(0), proximodistally orientated, elongate ridge (1), or absent (2) (modified from Gauthier, 1986). Unordered.

286. Position of proximal tip of lesser trochanter: level with (0), or distal to (1), the femoral head (Galton & Upchurch, 2004).

287. Projection of the lesser trochanter: just a scar upon the femoral surface (0) or a raised process (1).

288. Transverse ridge extending laterally from the lesser trochanter: absent (0) or present (1) (Rowe, 1989).
289. Height of the lesser trochanter in cross section: less than (0), or at least as high as (1), basal width (modified from Galton, 1990).
290. Position of the lesser trochanter: near the centre of the anterior face (0), or close to the lateral margin (1), of the femoral shaft in anterior view.
291. Visibility of the lesser trochanter in posterior view: not visible (0) or visible (1) (Galton & Upchurch, 2004).
292. Height of the fourth trochanter: tall crest (0) or a low rugose ridge (1) (Gauthier, 1986).
293. Position of the fourth trochanter along the length of the femur: in the proximal half (0) or straddling the midpoint (1) (Galton, 1990).
294. Symmetry of the profile of the fourth trochanter of the femur: subsymmetrical without a sharp distal corner (0) or asymmetrical with a steeper distal slope than the proximal slope and a distinct distal corner (1) (Langer, 2004).
295. Shape of the profile of the fourth trochanter of the femur: rounded (0) or subrectangular (1).
296. Position of fourth trochanter along the mediolateral axis of the femur: centrally located (0) or on the medial margin (1) (Galton, 1990).
297. Extensor depression on anterior surface of the distal end of the femur: absent (0) or present (1) (Molnar, Kurzanov & Dong, 1990).
298. Size of the medial condyle of the distal femur: subequal to (0), or larger than (1), the fibular + lateral condyles (modified from Wilson, 2002).
299. Tibia: femur length ratio: greater than 1.0 (0), between 0.6 and 1.0 (1) or less than 0.6 (2) (modified from Gauthier, 1986). Ordered.
300. Orientation of cnemial crest: projects anteriorly to anterolaterally (0) or projecting laterally (1) (Wilson & Sereno, 1998).
301. Paramarginal ridge on lateral surface of cnemial crest: absent (0) or present (1) Yates (2007a).
302. Position of the tallest point of the cnemial crest: close to the proximal end of the crest (0) or about half-way along the length of the crest, creating an anterodorsally sloping proximal margin of the crest (1) Yates (2007a).

303. Proximal end of tibia with a flange of bone that contacts the fibula: absent (0) or present (1) (Gauthier, 1986).

304. Position of the posterior end of the fibular condyle on the proximal articular surface tibia: anterior to (0) or level with (1), the posterior margin of the proximal articular surface Yates (2007a).

305. Shape of the proximal articular surface of the tibia: ovoid, anteroposteriorly longer than transversely wide (0) or subcircular and as wide transversely as anteroposteriorly long (1) (Wilson & Sereno, 1998).

306. Transverse width of the distal tibia: subequal to (0), or greater than (1), its craniocaudal length (Gauthier, 1986).

307. Anteroposterior width of the lateral side of the distal articular surface of the tibia: as wide (0), or narrower than (1), the anteroposterior width of the medial side Yates (2007a).

308. Relationship of the posterolateral process of the distal end of the tibia with the fibula: not flaring laterally and not making significant contact with the fibula (0) or flaring laterally and backing the fibula (1) Yates (2007a).

309. Shape of the distal articular end of the tibia in distal view: ovoid (0) or subrectangular (1) Yates (2007a).

310. Shape of the anteromedial corner of the distal articular surface of the tibia: forming a right angle (0) or forming an acute angle (1) (Langer, 2004).

311. Position of the lateral margin of descending caudoventral process of the distal end of the tibia: protrudes laterally at least as far as (0), or set well back from (1), the craniolateral corner of the distal tibia (Wilson & Sereno, 1998).

312. A triangular rugose area on the medial side of the fibula: absent (0) or present (1) (Wilson & Sereno, 1998).

313. Transverse width of the midshaft of the fibula: greater than 0.75 (0), between 0.5 and 0.75 (1), or less than 0.5 (2), times the transverse width of the midshaft of the tibia (Langer, 2004). Ordered.

314. Position of fibula trochanter: on anterior surface of fibula (0), laterally facing (1), or anteriorly facing but with strong lateral bulge (2) (modified from Wilson & Sereno, 1998).

315. Depth of the medial end of the astragalar body in cranial view: roughly equal to the lateral end (0) or much shallower, creating a wedge-shaped astragalar body (1) (Wilson & Sereno, 1998).

316. Shape of the posteromedial margin of the astragalus in dorsal view: forming a moderately sharp corner of a subrectangular astragalus (0) or evenly rounded without

formation of a caudomedial corner (1) (Wilson & Sereno, 1998).

317. Dorsally facing horizontal shelf forming part of the fibular facet of the astragalus: present (0) or absent with a largely vertical fibular facet (1) (Sereno, 1999).

318. Pyramidal dorsal process on the posteromedial corner of the astragalus: absent (0) or present (1).

319. Shape of the ascending process of the astragalus: anteroposteriorly deeper than transversely wide (0) or transversely wider than anteroposteriorly deep (1) Yates (2007a).

320. Posterior extent of ascending process of the astragalus: well anterior to (0), or close to the posterior margin of (1), the astragalus (Wilson & Sereno, 1998).

321. Sharp medial margin around the depression posterior to the ascending process of the astragalus: absent (0) or present (1) (Novas, 1996).

322. Buttress dividing posterior fossa of astragalus and supporting ascending process: absent (0) or present (1) (Wilson & Sereno, 1998).

323. Vascular foramina set in a fossa at the base of the ascending process of the astragalus: present (0) or absent (1) (Wilson & Sereno, 1998).

324. Transverse width of the calcaneum: greater than (0), or less than (1), 30% of the transverse width of the astragalus (Yates & Kitching, 2003).

325. Lateral surface of calcaneum: simple (0) or with a fossa (1) Yates (2007a).

326. Medial peg of calcaneum fitting into astragalus: present, even if rudimentary (0) or absent (1) (Sereno *et al.*, 1993).

327. Calcaneal tuber: large and well developed (0) or highly reduced to absent (1) Yates (2007a).

328. Shape of posteromedial heel of distal tarsal four (lateral distal tarsal): proximodistally deepest part of the bone (0) or no deeper than the rest of the bone (1) (Sereno *et al.*, 1993).

329. Shape of posteromedial process of distal tarsal four in proximal view: rounded (0) or pointed (1) (Langer, 2004).

330. Ossified distal tarsals: present (0) or absent (1) (Gauthier, 1986).

331. Proximal width of the first metatarsal: less than (0), or at least as great as (1), the proximal width of the second metatarsal (modified from Wilson & Sereno, 1998).

332. Orientation of proximal articular surface of metatarsal one: horizontal (0) or sloping proximolaterally relative to the long axis of the bone (1) (Wilson, 2002).

333. Orientation of the transverse axis of the distal end of metatarsal one: horizontal (0) or angled proximomedially (1) (Wilson, 2002).
334. Shape of the medial margin of the proximal surface of the second metatarsal: straight (0) or concave (1) (modified from Sereno, 1999).
335. Shape of the lateral margin of the proximal surface of the second metatarsal: straight (0) or concave (1) (modified from Sereno, 1999).
336. Length of the third metatarsal: greater than (0), or less than (1), 40% of the length of the tibia (Gauthier, 1986).
337. Minimum transverse shaft diameters of third and fourth metatarsals: greater than (0), or less than (1), 60% of the minimum transverse shaft diameter of the second metatarsal (Wilson & Sereno, 1998).
338. Transverse width of the proximal end of the fourth metatarsal: less than (0), or at least (1), twice the anteroposterior depth of the proximal end (modified from Sereno, 1999).
339. Transverse width of the proximal end of the fifth metatarsal: less than 25% (0), between 30 and 49% (1), or greater than 50% (2), of the length of the fifth metatarsal (modified from Sereno, 1999). Ordered.
340. Transverse width of distal articular surface of metatarsal four in distal view: greater (0), or less than (1), anteroposterior depth (Sereno, 1999).
341. Pedal digit five: reduced, non-weight bearing (0) or large (fifth metatarsal at least 70% of fourth metatarsal), robust and weight bearing (1) (Wilson & Sereno, 1998).
342. Length of nonterminal pedal phalanges: all longer than wide (0), proximal-most phalanges longer than wide whereas more distal phalanges are as wide as long (1), or all nonterminal phalanges are as wide, if not wider, than long (2) modified from Wilson & Sereno, 1998). Ordered.
343. Length of the first phalanx of pedal digit one: greater than (0), or less than (1), the length of the ungual of pedal digit one (Yates & Kitching, 2003).
344. Length of the ungual of pedal digit one: less than at least some nonterminal phalanges (0) or longer than all nonterminal phalanges (1) Yates (2007a).
345. Shape of the ungual of pedal digit one: shallow, pointed, with convex sides and a broad ventral surface (0) or deep, abruptly tapering, with flattened sides and a narrow ventral surface (1) (Wilson & Sereno, 1998).

346. Shape of proximal articular surface of pedal unguals: proximally facing, visible on medial and lateral sides (0) or proximomedially facing and visible only in medial view, causing medial deflection of pedal unguals in articulation (1) (Wilson & Sereno, 1998).
347. Penultimate phalanges of pedal digits two and three: well developed (0) or reduced disc-shaped elements if they are ossified at all (1) (Wilson & Sereno, 1998).
348. Shape of the unguals of pedal digits two and three: dorsoventrally deep with a proximal articulating surface that is at least as deep as it is wide (0) or dorsoventrally flattened with a proximal articulating surface that is wider than deep (1) (Wilson & Sereno, 1998).
349. Length of the unguis of pedal digit two: greater than (0), between 90 and 100% of (1), or less than 90% of (2), the length of the unguis of pedal digit one (modified from Gauthier, 1986). Ordered.
350. Size of the unguis of pedal digit three: greater than (0), or less than (1), 85% of the unguis of pedal digit two in all linear dimensions (Yates, 2003a).
351. Number of phalanges in pedal digit four: four (0) or fewer than four (1) (Gauthier, 1986).
352. Phalanges of pedal digit five: present (0) or absent (1) (Gauthier, 1986).
353. Femoral length: less than 200 mm (0), between 200 and 399 mm (1), between 400 and 599 mm (2), between 600 and 799 mm (3), between 800 and 1000 mm (4), or greater than 1000 mm (modified from Yates, 2004). Ordered.
354. Lateral extent of ventrolateral flange on plantar surface of metatarsal II in proximal aspect: similar in development to ventromedial flange (0) or well developed, extending further laterally than ventromedial flange extends medially (1) (Smith & Pol, 2007).
355. Distal articular surface of astragalus: relatively flat or weakly convex (0) or extremely convex and 'roller-shaped' (1) (Smith & Pol, 2007).
356. Distal surface of tibiofibular crest: as deep anteroposteriorly as wide mediolaterally or deeper (0) or wider mediolaterally than deep interoposteriorly (1) (Smith & Pol, 2007).
357. Well-developed facet on proximolateral corner of plantar ventrolateral flange of metatarsal II for articulation with medial distal tarsal: absent (0) or present (1) (Smith & Pol, 2007).
358. Proximal outline of metatarsal III: subtriangular with acute or rounded posterior border (0) or subtrapezoidal, with posterior border broadly exposed in plantar view (1) Yates (2007a).
359. Angle formed by the anterior and anteromedial borders of metatarsal IV: obtuse (0), right angle or acute (1) (Smith & Pol, 2007).

360. Well-developed tibiofibular crest on distal femur: absent (0) or present (1) (Smith & Pol, 2007).
361. Shaft of metatarsal I: closely appressed to metatarsal II throughout its length (0) or only closely appressed proximally, with a space between metatarsals I and II distally (1) (Smith & Pol, 2007).
362. Posterior margin of astragalus: straight (0) or convex (1) (Otero & Pol, 2013).
363. Ventromedial ridge of scapula: absent (0) or present (1) (Otero & Pol, 2013).
364. Mediolateral surface of distal astragalus straight (0), concave (1), or convex (0). (Otero & Pol, 2013). Unordered.
365. Anterior fossa on the proximal region of the pubic apron: absent (0) or present (1). (Apaldetti *et al.*, 2012).
366. Proximal end of the tibia with a transverse/anteroposterior length ratio: narrow (ratio less than 0.7) (0) or broad (more than 0.7) (1) (Apaldetti *et al.*, 2012).
367. Caudodistal tubercle of the radius: absent (0) or present (1). (Otero *et al.*, 2015).
368. Biceps tubercle of the radius: absent (0) or present (1). (Otero *et al.*, 2015).
369. Ventromedial margin of first metacarpal: poorly concave (0) or deeply concave (1). (Otero *et al.*, 2015).
370. Length of first phalanx of manual digit 1: much greater than (0), subequal or equal to (1), or much less than (2), its mediolateral width at proximal end. (Otero *et al.*, 2015).
371. Presence of growth marks (LAGs and/or annuli) in the cortical bone: growth marks in the whole cortex (0) or growth marks absent or only formed in the outer cortex (1). (Cerda *et al.*, 2017)
372. Relative abundance of woven fibered (WFB) or parallel fibered bone (PFB) in the primary compact bone: PFB>WFB (0), WFB>PFB: (1). (Cerda *et al.*, 2017)



Neotheropoda00[0 1]0[0 1]002[0 1]000201001100001[0 1]000000[0  
 1]00000110000000010[0 1]100[0 1]01000001[0 1]0001[0 1  
 2]0100000010110000101110001000000001?0000000000000000101100110000010000[0  
 1]1000010200001010110010000001000000000[1  
 2]10001100000000010100001000101100000100010001200000010?0001001101[1  
 2]010101013000211101010000111110000110100001?011000100000000[0  
 1]011011111002001011000011111000?0?000001000000000001200000?1?00?0001000111  
 111[0 1]120111[0 1]0000?0??[0 1]?01000000????????????0[0 1][0 1]10

Staurikosaurus

00??  
 ?????????????????????0000000001000?00?0000000000????????00010????00?01001?00001  
 1?000?00000000020000001??010101110000110010????1?1????????????????????????  
 ?????????????????000000200110000110?010?00010?00000100001??000?0101?000000001  
 000000001????01??1????????????00????01??????1?11  
 0?010?00??

Chindesaurus

??  
 ???100????????????01?0?0?1??  
 0?1??????000?00????????????1?0?0??1?00????????????????????????????????????  
 ?????????????????0??101?1????0????????????00?0101110001000100?00?01111100?  
 ??011110100??1????????????????????????????1????????????00????1??????10?10??00??  
 ?????????????????????????????

Herrerasaurus

00000000?0001000000000000?000100000000001000000100010101000001000011  
 01000000101?0001000?1000?00000000?1000000000000000001010001100000100100?00  
 0010000011??0010[0  
 1]10000002000000100000101110000110010100?1010??011000000000000012000001100  
 00011011010010000002000000000000010??01?010100100001011100010110001000010  
 00010001001001010000001100010000100000000000?0200000000?0000100010000011  
 1011[0 1]011000000??0??0?0000101?20?1???101100

Guaibasaurus

??  
 ???  
 011001000000??000000?000000?00000?01?0??[0  
 1]00??0?????110????1?0??????0????110??0?1?00??0?0?000?00[1  
 2]100210100010000000010?1011000000100100001011000100?0?01111100100?01101?00  
 1011100000000101000000000001100?00?0?0?00010102????????111?1111??00?0??????  
 ?????????????????????

Nhandumirim

??  
 ???  
 0??????0?0?0??????????????0??[0 1]?000??1[0  
 1]00??000000[1  
 2]1?0210????????????????????0000[0 1]01100001011000[0  
 1]?????10?110?0????????????????????0000??1?0??0?0????00????????????????12????  
 ???1??1[0 1]????????????????????????????????????

Eoraptor

0001?001?0001000011000111010000010000110100000?101100??100?011000011  
 01???11?1?????????????????10000010??0?0100?10[0  
 1]0000001?????110000000010?1011??0000?00?00??00?000?00000011??10???101??00  
 1?00??000?0000??1?10??00101??????20?00011?00010?00000101101000[1  
 2]0002101??0?00?0??10?1011?10??0?011100010110000011?00[0  
 1]1010??1?0?0?0??01????000??00?0000000000?010????????????0010002101111011  
 1100110??10?0?????0?00?0?0?1?1???101100

Saturnalia

10????????????????????????????????1????????00?100?0????????????????????10?????????0?  
 ??0?0?0101?0????????????0?000??????1000100000000????????0010010010?01101?0000  
 010000110000000000000000000000001000101??0??1000?0??11101111100010100??????????  
 ?????????????????????00?0001100210000000001001100100100000010111000101100010  
 00000010100010010010100000001000000001010000?000?001000000000000000000000?12??  
 000??11111?1100??101?00?0000?0????????????????01??

Panphagia

?0?????????????????????0?1?????????????????????0??1?????????1?0?0?????????10?0?1  
 11????0?????????????????1?0?0?1010000?10?0101000000?????????00000100011?01101?000?  
 01??01?10000?0?0000000?0??00????????????00?0?000?????????????????????????????  
 ??????????????????0?0?0?11002100?00?000?????1??0??10????????????????????????001000[0  
 1]10100??010?1010????????????????0????????????????????????????????????02????????111?  
 1?0????????????00?0??1?211???????????

Chromogisaurus

??  
 ???  
 ??????????????????????01000??1100??1????????????????????????????????0????????????????  
 ??????????0????0[1  
 2]1002100?????????????????????0?????1???10110??1000000010100010?????????????  
 ???????????0?0??000??10????????????0????12??????11?11????0?????????????????  
 ????????????????

Buriolestes

0?01000210101010011000111000000[0  
 1]00000100100000?10110011100001?00001?01100110000??0?0?1?001000000101000  
 00100010000000010100010010001001011?1101000000100011?000000000000000000?010  
 0010?0?000?000??0??1????111010011?0????????????01????????????????000000100021  
 00?0??0?001?011?0001101000000111000101101000?1?000?01?0?1??1?0?????0100??00  
 0??00?010000000??0100?10??10??0?????1?????11?1?????0010?[0  
 1]?????????0?01?[1 2]??1??????00

Pampadromaeus

0001000210101?10?11000?11000?01100001100000????0?1001??0??1?????110?  
 1????????????????????000??000000??00001100101000000??10001?????????????1?????0?  
 ?001??0?1?10??0000000000[0  
 1]0?0?0001?10?0?1000?00??1110??1?101010000????????????????????????????00000  
 01110?10?????????0?1?????????00001011100010110?0?00?00??????01?????????????  
 ???000??0??1?0??0????????0?????0?????????10?100??1??1?????????0??????0?????  
 ??????????????00

Bagualosaurus

10?1?00[1  
 2]??0?10??1?????001?000?1000?10??0??0?10110?????????????0?????????????????  
 ???????010000010?????01?00101000?00????????????????????????????0?001?0?1??10?

0?000000?0??01?001?????01???0??  
??0?00?1100?10[0  
2]?00?00?0?????????????000?0111000101110?1000000?01??010?????????????????0?1?  
?00?0100?????????11?0??110?????????10?0????1?????????0?????????????????  
??0??01

Thecodontosaurus

?0?????????????????????????????1??1??1000?????0?0?0?0??00?????????????????0??0  
?1010?10011?0?????????00?10010??????1100101010000?1?????000101010?1?01101?000  
001??00110000000000000000?1000?0101100?01000?00?0000112110001010011000120  
10001100001010000010100?00121000001??0?000??011??01010?000011100001011000  
10000000101100??011010100????110001110?1?000??00?0????1?????????????0??000100  
00??01?110??000?00?000?10??0??????????????????

Pantyraco ?0??0?????????????[0 1]00?0??1??1????000100100000010?1000[0

1]1?00?????????00?000?1?10??00110011?000?00?00010??0000?1001010100001001??110  
0?10101[0  
1]01101101?00???1????1?????????????????????????????0??11?00010000000?????11?1?00????  
?????????????????????????????????????00100121100001?????????0011??10110?00?????????  
1?1?000?0000000?01?001?????????????????001110011?000000001001?0??00000????0?  
??0100??1??1??0??0??0??1100??00??0??2101?1?00??1

Arcusaurus ?0?1??0[1

2]1?0?????0?010?1?????????????????????????0?????001?????????????????????????????  
??0?????0?01010?????011?0101010000???  
?????????????????????????????00?????????????????0?0?????????????????????????????  
????????0???  
??????????????????[1 2]??0?0????[1  
2]???0?

Efraasia

100?1001?000??1?111?112?1110?101??00100100000??0?10??11?0??1?????10?  
000?1????10001100?????10010010??11?011001010100001??1?1100110100101101101  
000001??001?0000000000000000110000101000?0110000?0?010011212000111001101  
012010?1100000111010001000010013100010100001000000110010110100001111000010  
1100010000001101?001?011010?0?01?1110001??0011?0010000010002??0??000?10001  
000100001??1111??100000011001?00??0????2?11?0?????01

Plateosauravus

???  
??10??0100001?01101?00[1  
2]0011?00110000000001000000??10??0111?0??110?????????0??[2  
3]1110011110?????????????1?????????????????00100131100101?01?????????11??10110?00  
001111000010110001000000110110?????0?????????????????11?0????0?????????4?????  
????1?000?????????????????????0??0?????????????0?????????????????

Ruehleia

???  
??10??0??01??101?002001?  
?0011001000001100000?1100001?10?0?0110?????00001111[1  
2]00011100?0100?01011101000??0?00??001001311000020??11000110110?10110?1  
01011110000102100010?00?011011001?010010100?????????????????????????????3????  
?????0?00010?????????????????????0??0?????????????0?????????????????

Pradhania

????????????????????????????????1????????00????????????????????????????????  
 0????????????????????0????1?1????????????1?1010????????????????20????????????10?????????  
 ???11??????[  
 1  
 2]0?0??  
 ???  
 ???  
 ?????????????????????????????????

Nambalia

??  
 ???  
 ???  
 10??0110??????12?0??10??0??????????1????111?0100111100001011010????????1101?0?  
 ??011010??00101??00101?011100??00??00100000010??????????????????11?10?0?00??  
 ?????????????????????????????????????

Jaklapallisaurus

??  
 ???  
 ???  
 ???  
 11010??0??0??00?01001?1?[0  
 1]????????????00?000??0?0?1????????????????????1??11??0????????????????????????????  
 ?

Macrocollum

100110021000211111111211100100100001001000001100100111010010000011  
 01??????101??????0?100??1001011010?1?0110010101000011?01111002001001111011  
 01000000111011101000000000000100110?0010?0000001000100?0000111120000110011  
 0111201010101000111000001000010012100010200?0?0001?01100101110100000110000  
 101100010000[0  
 1]11011001001101010001011100010100111000000001000100000011001?00000??????  
 ???1??1???110010??????0?00?1??????????????1?

Unaysaurus

?001100?1010??1?111??1??1010??001000????????????0??00?????01??000??0?0  
 ??????????????10????????0?10110?????01100101010000????0?1?????0?1????????????0??  
 0011100110000000000000????????????????????1000?00?000001?1101001100??????10?0  
 ?110????1110??0??  
 110110??01?010?00????????11??????0??0??????0?????????1????????????????????  
 ?????1?01?110??????????1????1????????1?

Plateosaurus\_gracilis

?00??001?0002?110111?1??1110?100??00?10?1010?0??0?10001100??10????????  
 ???????????1?????????????0?0110?????11100101010?001?????1100??01??01101101?0  
 0?001?10011000000000000010?1010001010000001000?00????????1200?11100?1011?1  
 0101010000??10?????0?001001311001020010100011111001011??00001111000010110?  
 010000?0??0110????????????????????0?????????0?0?????????2  
 3]????????0010?0?000?00001101111?1?01?00????????????0????????????0??0?

Plateosaurus\_trossingensis

1001100110002011[0  
 1]111112111100100100001001010101100110011000110010011011001011011100110001



1]110100001001011010101011001010100011100?1100200100011101101100200111001  
1000000000000001011101001[0 1]10000000000100?01[0 1]011112010111[0  
1]011011110111210010021100000200001001310001000110110010011001011100010110  
10000102101010000001101100100111101000111110001110012000100000210020?00?01  
1001000001?10000[0 1]???????1?10002010011100000000[0 1]100001000001

Adeopapposaurus

100110021000211101111011011111100001011010001101111111110010001021  
01[0 1]01100101100011100101000001011[0 1]10101011111110[0  
1]0001110011110020010001110110110020011001100000000000001001101001000000  
000100?0000000101110001110011011110111210110011100000200001001311001000110  
110010?1100101100000011010000102101010000001101100100111101000111010001110  
012000110000110010000001101000000?00000??1?11?11?1000201001?100000?010?11  
100?000001

Leyesaurus

?001?00?1000211??11?????1010?11110000101101?00?1011111111?00100010[0  
2]1010?????????00?11??0?1?00?10110??1010?111101000001?1??11110020010001110  
11????0??0000?001????00????????????????????  
??100????????????????????????????  
????????????????????????????????010????????12000????0???0??????00????????????000?????  
?????????0?0?00?1?0?00?0??11?1?????000?

Sarahsaurus

10?1?00?10?11010?11?1?1?011?111100000101001010010?110001110010?0??10  
1000111001?0?01?1101??1?10?10010?????011001010100011?0011110120011001110110  
11002001110?1?000000000000?10?1100001110001001000000000001010210011110?10  
11110110111110020100000200001001311101000[0 1]101100100110[0 1]101110[0  
1]?00?10100001011[0 1]?010000001101[0 1]0011011[0  
1]101000?11110111110012000?1000011001?[0 1]000011010?[0  
1]000????????????????????[0 1]0021??????????0011?0??1???10??0?

Ngwevu

1?01010??10021111111????111110111000?10110?000?100110111111?000110010  
1001111001??00??111?001011?11010?????011011010100011????111?020?11001110?1?  
?1?00?0??0?????0???0000?0010000????????????????????????0???1121?101??0??????  
????11????2010????????????????????0?1?1100????????????1010?101000010??1??1?  
?????????0????????0????????0001?0??2?00??000????0???0?????1????????0?????????  
????????????????????????011011010100??01

Massospondylus\_kaalae

?????00????0211?101????110110111000010110??0?101110??1????????????1???  
????[0  
1]?0??00??1????????0??0100?????01101101000001????????????????????????????  
??  
??  
??  
?????????0[0 1]?000??????01

Ignavusaurus

??101????????????????  
????????????????????????????????00????????????101010001????????????????????10??0010  
01011000000000?0000100?10000?1???0?0?100?100????????????0?0?0????????????01

10?????000?00001001310001001?1011001000100101?000?0?1101000010??0??1?????0  
10100??01111010?????110??11?012?10??000?0?0??000001?0?????????????????  
??

Riojasaurus

1001?00??0002011?110??00111011?11000?100001000?10010?1111100100000110  
1?0?100101?0001??????1?001000?1??101?100010101000[0  
1]10??111100110100001101101?00100111001100000000000010?1101001[0  
1]10000011000??0?01001031210111100111111?010111011001010001020?001001311001  
0201101000110110010110010110111010110201101000000110110010011010100??011?0  
0011100121011[0 1]00001??13??????0?10[0  
1]00010100000?011110?0011002??0????000????????????00??

Eucnemesaurus\_fortis

??  
??0??01??  
001100[0  
1]10000?00?0????????11000?01100????????10????????????????????????????  
????????????????????110??0????????0110111010?1010110?000000110110?????  
??[2  
3]????????1????????????????????1?0????????????????????????????????

Eucnemesaurus\_entaxonis

??  
??0??01??  
0????0??000?0000?00?101??1110?0?01????????????????????????????????????  
????????????0??13??[0  
1]0100??1?0?0?0?11?010110?101101101001010110?0????110111?1?0??0????0????  
?00111?01[1  
2]?0?11000????20??0????????????????????????????1????1????????????????  
????

Seitaad

??  
??00?[0  
1]?1?00?00?001????0000????????????????????????0000011?11000111[0  
1]011?11100101310?00?2110?0??0????????????0?1000001????????????????  
????????0?00?01101?0??01101010?0??11?00?1??001??11[0  
1]0000010??0??0?10?0??001??

Yunnanosaurus\_youngi

??  
??1??0101100100110[0  
1]00??1101100200111001100?0000?0?000010?01010?1110?0?00[0  
1]0??100??1311000020110?1?020  
0?11?1?11[0  
1]??  
????????????01??????111??10????????????????????????????????????

Yunnanosaurus\_huangi

100?1002??00??10?111?1??111?111????00101011?00??0?110111?001000?01?01  
?0?00010????????????????10[0 1]10010??1??00010?21000????111100110110[0  
1]0??01101?00?0011?0011000000000000010?0101101[0

1]1000?00?0?1?0000?0?01200?11110??01??0011?2101100201000[0  
1]020?0010013100000001101[0 1]00[1 2]0?110010111?0010111100001011[0  
1]10100000011011001?01101010001111?0??11?01????????????2?0??11?0??1??010  
100000?01?11??00100?2??????????0?000????????1????

Irisosaurus

????????000?1??1????10????1????????????????????????????????  
??0?10?21100????????000????????0??1101?002001  
1?0????00000?0?00001????????????????????????01010??2??01?110??????[0 1]01[0  
1]1[2 3]10110[0  
1]2010001020????????????????????????1??10110????????????????????????  
????????????????????????????????????0?0????????????????0??1?01??0????????????0???  
?2????????????????????????????

Yunnanosaurus\_robustus ?1????0[2 3]1?00??1??11?????1[0

1]1?1111??00?11?????0??10?1?0?0???  
????1001??2110[0  
1]1?????????000?????00??101?0020011?00110000001??0000?0??101??1?1?00?00100?  
?????????0120??1?110?????001??[2  
3]?????0?0?0001??0?????131000?02011000001??110????10??0?0?1100001011110100  
00??100110?1?011010??0??????10111[0  
1]0?2?0111000001002000011110?0??1??1??000?10??1101?010??1??????????[0  
1]????????????????

Lufengosaurus\_magnus

??  
??0????????????00200111  
0?11000000??1?0?0??????????11??0?0?1??10?00[0  
1]101011201011110?????0011?310?10?1[0 1]??001??0000100131[0  
1]00?02011101002??1?0?????00[0  
1]01110000101111010?00?0110110?10011010??0??????10?110012?0111000021003[0  
1]00?0?110?0011?0101?????0111101?010??21????????????????????????

Jingshanosaurus 1001?102100021111111?1?11111[0

1]111000?11?001??1?1111011111001000??101100000101?2?00?10?0??1?10111010?00  
1101100101011001????111??010?????1??10110?0011100?1??0000000000?0??10??  
01110000001000100?0[0 1]10??11201011110??00??0011?3100100?[0  
1]10001020000100131000002011101002??110010110?000011[0  
1]10000101111010?0000110110?10011010?00?????0101110012001120000[0  
1]1004?????????0?1??1??00000????11?1?0?002[1 2]????????????????1????1??0?

Xingxiulong

????????????????????????1??1?1111??0?10?00??0110?11001100001000101?01?  
00100101????1?1?????0?????????0[0  
1]1??00?????0??1100111100100110001?0110110020011100110000000010000110011  
??1111000001??100?0[0 1][0 1]0??[1 2]120?011110????1??????[1  
2]101????????????001001311000020?1011002??11??0?1000010111100001011110?00  
000[0 1]10?110010011010?0??011?001011000121011100002100[2  
3]00000?11??011??1?0?????1?1101?0??0??1?0?0?????0?0????????????0?

Yizhousaurus

1101100210002111110111111111111000011100100011011111111100??00??1  
0?100?00101?2?????0?1001010110010??0000110[0

1]1010110011?10111100100110001?011011[0 1]0[1 2]0011100[1  
2]10000000001000010?010100111000?01??????000101[0 1]01[1  
2]00011110?????0010?21011001010001020000100?311000001101100[1  
2]?0110010110?1110111100001011110????????????????????????????????  
????????4??1???1????0?1?010100000??1??1??0?0?2???0???00?0??1??????????01  
Anchisaurus 10?1?00?10002?1??11?????111010[0 1]110?0010101100011001111[0  
1]121[0  
1]010?????011001101011200111000001110?10?00?01000000101?11?0111?0011???10  
0100?111011?1000??010?001100?000??0000000?0100?0???01?00?10?????10[0  
1]0??21100101110??0??1101011100100201000002000[0 1]10113100000?01111[0  
1]0010011?001010000101101000010[0  
1]11101000000110111?1?01?010???10111?0?01?0011?0010000010011?0?????10??00??  
010200000?01?11?110100?21?10????000??01????1??????0?  
Lamplughsaura 100100?????????????0????????????[0  
1]????????????0????????1?0??????????10?1???11????1001?????0?1?10?01111??11?01?  
001010110011??000110000011?100??1101?0020?1??0?1??000000?[0  
1]0000010????????1?0????????0?0?0?0[0  
1]0??3110?10?110??????0010?110?10??0?000[0  
1]?200??????3100????01?1?1?0100?????01?00[0  
1]00011??????101111?1?0?0??11???101?011010?1?00?1???1?11110?????111000?210?3?0  
??01?????1?????1????0??????1??1??1???2?????????????????????????????1????  
Mussaurus 10011002?000??111111?1?111011111000010100?000?10011?1?11100[0  
1]0?0?01?0?1????????????????????????10101111???1?0??0?1?1111001????????00100????  
0?10110?0000?10000100000000?00000010??111?011?1?0001110?????0010?0[1  
2]11001[0 1]1110?1?11?00101210110[0 1]201000[0 1]0200???0113100010?011[0 1]?[0  
1]001?011??10110?1010111100001011110100000011011101101101000[0  
1]?????01011100120011100001100300?00111111?011010[1 2]???????111??11?????2[0  
1]?????????00?01?????????1[0 1][0 1]01  
Leonerasaurus  
??  
?????????????????????????????0?0?????????1?11010110011???001??010?1???????1100?00?0?1  
0000110000000?00000100?111001?????????????????0000???1100000????????????????  
????????????????????1101?3100?????????0?????11??1?1????????????????????????????  
?????????????????????????10111?????????0??????0?0??1?0?????????1?????????1????????  
?????????????????0 1]?????????????100??  
Sefapanosaurus  
??  
?????????????????????????????1????????????????????????????????00??0110?????0?10??00?001?  
???1?00000001?0000?????1?????11?00??011????0?0?0010?1?00?????10?1011??01013101  
0??1010???0?111110000??11[0  
1]???000000?????0?00110101010001??0???11?0?2?0?????????????00?0????011?01111?  
??  
Aardonyx  
1101?00210002?11?11?????1110?1001000?????1010??0?11011??10?1?????????1  
?0?????????????????????1?0?0?1?0?????11?00101011001?1?????0010?110100101101?0  
000011?00110000000020000010?1100?0110000?01110?00?????11?????????10??00????  
??13101???1?10??10?????????????????????110100010011??10110?101?111100001111000?

?????1101110?0??01?????????010111?01?0?2??00?0??0[3  
4]??00011??0?111?????????????????0??2?????????0?????????????0?

Melanorosaurus

1001?1031000211111101?1110101110??1010101101011011101111?0000001022  
0110110010??0??10011011001?00101?1000110?10021100110?01011001?01100001011  
[0 1]10000001??0??100??0?0?10000000??111001??010?0?1??0?????1????[2  
3]1100?0?110?????0010?2100101[1 2]0?0001020000100?31000[0 1]0[1  
2]??????????1??10110?????????????1??11010000001?011?01?0??0?0??0011100101  
111012?011[1 2]00001100301100?11?????????????0??11????????0002?[0  
1]0?????0000?????1??????01

NMQR1551

??  
??11??00?001??  
00210000000010000000??2?100121000?0[0  
1]1100????0100??2??000110??????????21????????????????00100?3100000[0  
1]011010001????????????11101111001110[0  
1]111010000001101100100?10101000?????1011100????1120000????3001?0?11????0??  
??????????11?1?????0001????????????????????????????????????

Blikanasaurus

??  
??  
??  
??0000?0110111?1?0  
10010100101110010111112102120000100?211?0?1?1?0?0????????????????????0??  
?2????????????????????????????????

Kholumolumo

??01????????????????  
??0101?1?1????0?01?00?0011  
??2??0000101????????????0111?0?1111001??010??311000[0  
1]??00??????????2101??1?10??????10000131110000010?10001????0?????0001111  
0000011110?1?0010000001100?1?????????????????0111??1200??????????31?000011?0  
?0[0 1]1010?1??????11?1????????????????????????????????01??

Meroktenos

??  
??  
??  
?????????0?0?131?00001011?00001????????????11111100?00111110????????????  
????????????????????01????????????????????1?0??????0????????????????????  
????????????????????????????

Ingentia

??  
??111????01011?0?0?????  
??11[0  
1]0010110?1?10?00111310110?????????0????????????????????????????????  
??  
111??01??

Lessemsaurus

??  
 ???  
 100[1 2]10000010121001000??0101???11[0  
 1]0010110?????????0?1?310?????0?0??1????0010013100000?011110001???1??10110?1110  
 11?10???11111?0?0000001001[0 1]1???01101[0  
 1]101??????????11??12101??00??0???311?????10?201??1001?????1?1111??1010??2????  
 ?????????????????????????????01??

Antetonitrus

?1??  
 ???  
 1]0?????????????00?000001??00[1  
 2]10001010121001000???1????110?0?01100???0?0111??311000[0  
 1]0110??????0011?3101???1010?????????00100?3???0002011010001?????????????1110111  
 1001111111101000000100111010?????????????????????111110?????[1  
 2]1200?0????31?100??1?0?00111?????????????110??0???2?????????????????????????????  
 ??

Ledumahadi

??  
 ???  
 ??[1 2]?0000010121001000?????1???1??00?01????????????????????????????????10?????????????[2  
 3]1??  
 ???0????????????????????????????  
 ???0?????????[4  
 5]??0???1??0????????????????0????????????????????

Camelotia

??  
 ???  
 002100000000??00?0????????????1???0??011??  
 ?????????????????????????????????1????????????1??00111?111011110111?1??110?000000?????  
 ???[1  
 2]???000????5??1????????????????????????????????  
 ?

Pulanesaura

??  
 ???  
 ?00?0010?01?00[0  
 1]0000?????????112?11011???0?????????????????10??1????????????????????????????????  
 ??????????????????????????0?11?1?11????????????????????????????????00000000101????????????  
 ??????????????????????1?????????????????????????0?????????????????????????????1????????????  
 ?????????????????????

Gongxianosaurus

1?????0????????????12??  
 ?????????????????????????????????????00???1??2121????????????????0????????????????1??0??001?  
 ?0?????0?0?0?000?????????????1??0?0?1?0?100?011??2110?????1?1????????????????  
 ??????????????????0?100????0????????????????????????????????????[1  
 2]111?2??????1???1101??????1?0??1???0?1?1?????1?11??010???10?2?1112000020005??  
 ???22????????????????????????????????????

Schleithemia





